20th International Workshop on

Radiative Properties of Hot Dense Matter

BOOK OF ABSTRACTS

RPHDM2024
PARIS

SORBONNE UNIVERSITE

Pierre et Marie Curie Campus

November 18-22, 2024
Paris

The RPHDM bi-annual meeting series began in 1980 and, since 2000, has alternated between locations in Europe and the United States. The last three editions were held in Santa Barbara, United States (2016), Hamburg, Germany (2018), and Santa Fe, United States (2022).

The purpose of the meeting is to bring together an international community of researchers focused on interactions between radiation and hot dense matter, along with related topics.

Past meetings have covered a broad range of subjects, including hot-plasma absorption and emission spectroscopy, radiation transport, opacity, spectral line shapes, non-LTE population kinetics, dense plasma effects, and their role in the breakdown of the isolated atom model.

Experiments using high-intensity short-pulse lasers and z-pinch type discharges to generate and diagnose hot dense matter are central. XUV, VUV and X-FEL sources, warm-dense matter studies, and high-energy laser-related experiments, are particularly timely.

SCIENTIFIC COMMITTEE

Jim BAILEY, Sandia National Laboratories, USA

Serena BASTIANI, LULI, Polytechnique, France

Djamel BENREDJEM, LAC, Université Paris-Saclay, France

James COLGAN, Los Alamos National Laboratory, USA

Marta FAJARDO, Instituto Superior Técnico, Lisboa, Portugal

Chris FONTES, Los Alamos National Laboratory, USA

Carlos IGLESIAS, Lawrence Livermore National Laboratory, USA

Roberto MANCINI, University of Nevada, Reno, USA

Jean-Christophe PAIN, CEA, France

Yuri RALCHENKO, NIST, Gaithersburg, USA

Evgeny STAMBULCHIK, Weizmann Institute of Science, Israel

Pedro VELARDE, Instituto de Fusion Nuclear GV, Spain

Feilu WANG, National Astronomical Observatories, China

Justin WARK, University of Oxford, UK

Hitoki YONEDA, Institute for Laser Science, Japan

Beata ZIAJA-MOYKA, CFEL, DESY, Germany

LOCAL ORGANIZING COMMITTEE

Djamel BENREDJEM, LAC, Université Paris-Saclay (Chair)

Jean-Christophe PAIN, CEA (co-Chair)

Serena BASTIANI, LULI, Polytechnique

Christopher BOWEN, CEA

Olivier GUILBAUD, IJCLab, Université Paris-Sacaly

Sylvie JACQUEMOT, LULI, Polytechnique

Patrick RENAUDIN, CEA

Caterina RICONDA, LULI, Sorbonne Université

Stéphane SEBBAN, LOA, Polytechnique

PROUD SPONSORS
OF RPHDM2024

TOPICS

- ASTROPHYSICAL PLASMAS: ASTRO
- FREE-ELECTRON LASERS: XFEL
- INERTIAL CONFINEMENT FUSION: ICF
- MAGNETIZED PLASMAS: MAG
- OPACITY: OPA
- PLASMA SPECTROSCOPY: SPECTRO
- SPECTRAL LINE SHAPES: SLS
- X-RAY SOURCES: XRS

The scientific program includes both oral and poster sessions.

Table of contents

OPACITY-I **1**

OPA-I.1: The Opacity Project: R-Matrix opacities for laboratory and astrophysical plasma sources
A. Pradhan 2

OPA-I.2: Thoughts about the Iron Opacity Controversy
C. J. Fontes 3

OPA-I.3: Opacity model with self-consistent plasma effect
C. E. Starrett 4

SPECTRAL LINE SHAPES-I **5**

SLS-I.1: Review of the 7th Spectral Line Shapes in Plasmas code comparison workshop
A. Calisti 6

SLS-I.2: SALSAA: Statistically Averaged Line Shapes from Average Atom
S. B. Hansen 7

SLS-I.3: Detailed line-shape modeling for diagnostics of high-energy-density plasmas
E. Stambulchik 8

OPACITY-II **9**

OPA-II.1: Time-resolved spectroscopy for Z stellar opacity research
G. P. Loisel 10

OPA-II.2: Oxygen opacity experiments for stellar interiors at Z and NIF
D. C. Mayes 11

OPA-II.3: Progress on opacity measurements at stellar interior conditions using the National Ignition Facility
R. F. Heeter 12

PLASMA SPECTROSCOPY-I **13**

SPECTRO-I.1: Review of the use of machine-learning methods with spectroscopy in fusion plasmas
M. Koubiti 14

SPECTRO-I.2: A comparison of plasma conditions inferred from optical Thomson scattering measurements and X-ray spectroscopy
E. V. Marley 15

SPECTRO-I.3: Radiative cooling of an Al plasma in an AlTi or AlAu mixtures heated by an ultraintense laser pulse
L. Lecherbourg 16

SPECTRAL LINE SHAPES-II **17**

SLS-II.1: Zeeman splitting observed and simulated in laser-produced magnetized blast waves
A. Triantafyllidis 18

SLS-II.2: Zeeman Stark line shapes affected by periodic electric fields
I. Hannachi 19

OPACITY-III **20**

OPA-III.1: Towards opacity measurements at the LMJ facility: preliminary experiments with the atomic physics platform
C. Bowen 21

OPA-III.2: Photon scattering contribution in plasma transmission experiments
C. A. Iglesias 22

OPA-III.3: Laboratory measurement of L-shell opacity at GEKKO XII/LFEX High Power Laser Facility
J. Dun 23

XFEL-I **24**

XFEL-I.1: Distinct transient structural rearrangement of ionized water revealed by XFEL X-ray pump X-ray probe experiment
B. Ziaja 25

XFEL-I.2: XFEL induced K-shell fuorescence in the solid to plasma regime
G. O. Williams 26

XFEL-I.3: Ultrahigh Resolution X-ray Thomson Scattering Measurements at the European XFEL
T. R. Preston 27

PLASMA SPECTROSCOPY-II **28**

SPECTRO-II.1: High resolution, sub-picosecond x-ray spectroscopy of buried layers heated with high intensity, short pulse lasers
R. Shepherd 29

SPECTRO-II.2: Temperature determination of shock-compressed foams using x-ray fluorescence spectroscopy
M. J. MacDonald 30

SPECTRO-II.3: Unveiling preplasma dynamics via collisional processes with nanosecond and sub-picosecond laser pulses
D. Khaghani 31

OPACITY-IV **32**

OPA-IV.1: Production of an opacity table for air
J. Colgan 33

OPA-IV.2: Implementation of a super-shell refinement algorithm for plasma opacities
D. P. Aberg 34

OPA-IV.3: Full-potential treatment for multiple-scattering calculation of hot dense plasma opacity
H. B. Tran Tan 35

INERTIAL CONFINEMENT FUSION **36**

ICF.1: Evaluation of Au L-shell spectroscopy as a Te diagnostic for NIF hohlraum plasmas
N. Aybar 37

ICF.2: Evidence of gold NLTE model in the deficiency of NIF ICF hohlraum x-ray drive prediction
H. Chen 38

ICF.3: Understanding the effects of preheat from the Au M-band and L-band hohlraum radiation on EOS experiments
J. Nilsen 39

XFEL-II **40**

XFEL-II.1: Probing dense plasmas with high harmonics
P. Velarde 41

XFEL-II.2: Modelling non-thermal XFEL heating of iron
L. Ansia 42

XFEL-II.3: X-ray imaging and ionization dynamics in ultra-relativistic laser plasmas revelaled with an X-ray Free Electron Laser
U. Zastrau 43

XFEL-II.4: Simulation of K-shell emission spectra of Mg in the interaction of XFEL
C. Gao 44

X-RAY SOURCES **45**

XRS.1: Recent advances on laser-plasma based soft x-ray lasers
S. Sebban 46

XRS.2: Laser-irradiated X-ray sources for X-ray diffraction of dynamically compressed matter on Sandia's Z-machine
T. Ao 47

XRS.3: Quantum coherence and inner-shell x-ray lasing in XFEL generated NLTE hot and dense plasmas
J. Yuan 48

XRS.4: Diagnosing surface heating in relativistic laser plasma using GISAXS
S. V. Rahul 49

NLTE **50**

NLTE.1: NLTE-12, Benford's law for atomic databases and all that
Yu. Ralchenko 51

NLTE.2: Testing high density XSTAR models with Fe photoionized plasma experiments on Z
P. Cho 52

ASTROPHYSICS **53**

ASTRO.1: Structure of high velocity radiative shocks from optically thin to thick
M. Koenig 54

ASTRO.2: Helioseismic inference of the solar radiative opacity
G. Buldgen 55

DENSE PLASMAS-I **56**

DENSE-I.1: Interrogating the population kinetics in dense plasmas using X-ray Free Electron Laser resonant photopumping
E. Galtier 57

DENSE-I.2: Population kinetics for laser plasma interactions
B. E. Marré 58

DENSE-I.3: Ionization and temperature measurements in warm dense copper using x-ray absorption spectroscopy
T. Cordova 59

DENSE-I.4: Influence of two-temperature effect on the ionization potential depression in hot dense plasma
Y. Hou 60

MAGNETIZED PLASMAS **61**

MAG.1: Tungsten VUV spectroscopy in WEST tokamak 1-4 keV plasmas
R. Guirlet 62

MAG.2: Spectroscopic characterization of compressed core conditions in directly-driven magnetized cylindrical implosions
R. Florido 63

DENSE PLASMAS-II **64**

DENSE-II.1: Scattering of ultrashort X-ray pulses in optically dense plasma: account for pulse duration and propagation effects
V. A. Astapenkpo 65

DENSE-II.2: Toward electron temperature profiles in hot-dense plasmas from x-ray spectral ensembles
B. F. Kraus 66

DENSE-II.3: Line shifts induced by plasma screening in x-ray heated matter
M. Smid 67

DENSE-II.4: Ionisation equilibrium in dense carbon and beryllium plasmas
D. O. Gericke 68

POSTERS/ASTRO **69**

ASTRO.1: Photoionized plasma experiments at NIF driven by a long-duration x-ray drive
R. C. Mancini 70

ASTRO.2: Magnetized radiative shocks: their role in global evolution of the interstellar medium
D. Oportus 71

ASTRO.3: Radiative decay parameters for spectral lines in lanthanide ions of interest for the study of kilonovae in their nebular phase
P. Quinet 72

POSTERS/DENSE PLASMAS **73**

DENSE.1: Thomas-Fermi version of the VAMPIRES model
T. Blenski 74

DENSE.2: Consistent treatment of dense plasma effects on atomic structures, collisions, and spectral signatures
I. E. Golovkin 75

DENSE.3: Radiation-Hydrodynamics code HELIOS-CR: improved models for dense plasma effects and IFE simulations
V. N. Golovkina 76

DENSE.4: An explicit numerical scheme for Milne's phase-amplitude equations
R. Piron 77

POSTERS/ICF **78**

ICF.1: NIF x-ray crystal calibration via mulptiple throughput measurement techniques
M. Dozieres-Aybar 79

ICF.2: Electron heat transport in plasmas through Molecular Dynamics and Particle-In-Cell simulations
D. Guerroudj 80

POSTERS/MAG **81**

MAG.1: Transition energy measurements of highly-charged Xe and W in support of ITER's XRCS and SPARC's XRS
A. J. Fairchild 82

POSTERS/NLTE **83**

NLTE.1: Effects of super-Gaussian electron velocity distribution functions on atomic kinetics and radiative emission of hot under-dense Gold plasmas
C. Blancard 84

NLTE.2: The role of collisions and radiation transport on the emision signature from x-ray driven plasma
S. Cardoch 85

NLTE.3: Alignment-transfer rate coefficients for collisional excitation of O V ion in an anisotropic two-temperature plasma
M. K. Inal 86

NLTE.4: Electron-impact ionization cross sections and rates for Si IV-VIII
J. C. Pain 87

POSTERS/OPACITY **88**

OPA.1: Two decades of stellar interior opacity research at Z
J. E. Bailey 89

OPA.2: Opacity determination of photospheric-phase kilonova ejecta based on detailed atomic data calculations
J. Deprince 90

OPA.3: Opacity measurements of hot expanded metallic plasma wires
F. Gilleron 91

OPA.4: Effect of interatomic interactions on opacity in hot dense plasmas
J. M. Kasper 92

OPA.5: Comparison between ab initio and semi-empirical calculated bound-bound opacities of Tm ions
A Meftah 93

OPA.6: Platform-dependent advantages and challenges of laboratory stellar-opacity measurements
T. Nagayama 94

OPA.7: HRXS – a new High Resolution X-ray Spectrometer of LMJ
F. Reverdin 95

OPA.8: Efficient computation of low frequency opacity in WDM regime
M. Tacu 96

POSTERS/SLS **97**

SLS.1: Stark line shapes in a constant magnetic field and a periodic electric field
R. Stamm 98

SLS.2: Pseudoatom Molecular Dynamics Plasma Microfields
J. R. White 99

POSTERS/SPECTRO **100**

SPECTRO.1: Generation of high-energy-density plasma using Compound Parabolic Concentrator and high-contrast laser
Y. Karaki 101

POSTERS/XFEL **102**

XFEL.1: Hybrid Collisional-Radiative/Molecular-Dynamics studies of anisotropic melting of ice induced by ultrafast Non-thermal heating
C. Caleman 103

POSTERS/XRS **104**

XRS.1: Characterization of high brightness and multi-keV x-ray sources at the LMJ facility
C. Baccou 105

XRS.2: Toward a realistic modeling of the heating and ionization of a solid target irradiated by an ultra-intense laser
X. Davoine 106

Author Index **107**

OPACITY-I

The Opacity Project: R-Matrix Opacities for Laboratory and Astrophysical Plasma Sources

Anil Pradhan[1] *

[1]The Ohio State University, Columbus, Ohio, USA 32210

The Opacity Project (OP) was initiated in 1983 and aimed to employ the state-of-the-art atomic physics based on the powerful R-matrix method to compute stellar opacities[1, 2]. However, hitherto computational and theoretical issues related to its implementation have proved to be intractable. Simpler approximations based on atomic structure and distorted wave methods were used in the OP work, akin to other existing opacity models. The primary difference is that the R-matrix method accounts more precisely for electron correlation, configuration interaction, and channel coupling effects. That, for example, gives rise to autoionization resonances in bound-free photoionization cross sections in an *ab initio* manner [2, 3]. This presentation describes recent developments reported in a series of papers on R-matrix calculations for opacities (RMOP I-IV: [4, 5, 6, 7]), including (i) large-scale atomic calculations for iron ions of heretofore unprecedented complexity, and (ii) a new treatment of plasma effects on resonances in photoionization cross sections with collisional electron impact, Stark ion microfield, and thermal Doppler broadening mechanisms. Generally, these physical effects are likely to manifest themselves for atomic processes in high-energy-density (HED) environments such as stellar interiors. In addition to atomic-plasma issues, the OP-RMOP works employ the Mihalas-Hummer-Däppen equation-of-state (EOS), and it is important to ascertain its precise behavior which may also affect opacities via atomic ionization states and level populations as function of temperature and density [8]. An exemplar of astrophysical applications is the "solar problem" which depends on an accurate determination of opacities. Similarly, laboratory measurements of opacities (viz. [9]) are also addressed. The interface of EOS, atomic data, and opacities is important for HED plasmas [8], and might constitute a topic of detailed discussion for the RPHDM workshop.

References

[1] M.J. Seaton, Y. Yu, D. Mihalas and A.K. Pradhan, MNRAS, **266**, 805 (1994).

[2] The Opacity Project Team, *The Opacity Project*, Vol.1 IOP Publishing Bristol (1995).

[3] A.K. Pradhan and S.N. Nahar, *Atomic Astrophysics and Spectroscopy* Cambridge University Press (2011).

[4] RMOP-I: A.K. Pradhan, S.N. Nahar and W. Eissner, J.Phys.B, 57, 125001 (2024),

[5] RMOP-II: S.N. Nahar, W. Eissner, L. Zhao and A.K. Pradhan, J.Phys.B, 57, 125002 (2024)

[6] RMOP-III: A.K. Pradhan, J.Phys.B, 57, 125003 (2024).

[7] RMOP-IV: L. Zhao, S.N. Nahar and A.K. Pradhan, J.Phys.B, 57, 125004 (2024).

[8] A.K. Pradhan, MNRAS **527**, L179 (2024).

[9] J. Bailey, et al.: Nature, **517**, 56 (2015).

*E-mail: pradhan.1@osu.edu

Thoughts about the Iron Opacity Controversy

C.J. Fontes[1]*, C.P. Ballance[2], C.E. Starrett[1], J. Colgan[1], T. Nagayama[3], J.E. Bailey[3]

[1]Los Alamos National Laboratory, Los Alamos, NM 87545, USA
[2]Queen's University of Belfast, Belfast BT7 1NN, Northern Ireland, UK
[3]Sandia National Laboratories, Albuquerque, New Mexico 87185, USA

The controversy concerning the opacity of iron, arising from a discrepancy between helioseismology [1] and revised solar elemental abundances [2], continues to defy explanation. Experiments at the Sandia Z-facility have produced iron, nickel and chromium spectra [3, 4, 5] that have yielded both good and poor agreement with theoretical calculations, adding to the mystery. For example, the bound-free contribution to the opacity agrees well between theory and experiment for nickel and chromium at all measured conditions, while the iron comparisons display good agreement at lower temperatures/densities, but not at higher temperatures/densities. Continuing with a previous study that was presented at the 2023 Atomic Processes in Plasma (APiP) Conference in Vienna, we compare photoionization cross sections generated with the distorted-wave (DW) and R-matrix (RM) methods. At the APiP Conference, good agreement was demonstrated between the DW and RM methods for the case of He-like iron, Fe^{24+}. In this talk, we focus on the Ne-like ion stage, Fe^{16+}, which is predicted to dominate the charge state distribution for iron under the conditions that are present in the Sandia experiments. The DW results are calculated with the Los Alamos Suite of Atomic Physics Codes [6] and the RM results are calculated with the Dirac Atomic R-matrix Codes (DARC) [7]. We consider both the background and resonance contributions to various photoionization cross sections produced with each method, highlighting similarities, differences, and consequences for the corresponding opacities.

LANL is operated by Triad National Security, LLC, for the National Nuclear Security Administration of the U.S. Department of Energy under Contract No. 89233218NCA000001.

References

[1] S. Basu and H.M. Antia, Phys. Rep. **457**, 217 (2008).

[2] M. Asplund, N. Grevesse, J.A. Sauval and P. Scott, Annu. Rev. Astron. Astrophys. **47**, 481 (2009).

[3] J.E. Bailey et al, Phys. Rev. Lett. **99**, 265002 (2007).

[4] J.E. Bailey et al, Nature **517**, 56 (2015).

[5] T. Nagayama et al, Phys. Rev. Lett. **122**, 235001 (2019).

[6] C.J. Fontes, H.L. Zhang, J. Abdallah, Jr., R.E.H. Clark, D.P. Kilcrease, J. Colgan, R.T. Cunningham, P. Hakel, N.H. Magee and M.E. Sherrill, J. Phys. B **48**, 144014 (2015).

[7] C.P. Ballance, *DARC R-matrix codes*, http://connorb.freeshell.org, (2020).

*E-mail: cjf@lanl.gov

Opacity Model with Self-Consistent Plasma Effect

C. E. Starrett[1] and C. J. Fontes[1]

[1]Los Alamos National Laboratory, U.S.A

In warm and hot dense matter, the high density and elevated temperature introduce non-perturbative plasma effects into the electronic structure. These effects influence the measured opacity in complicated ways, and are hard to model. Techniques, like diagnosis of plasma conditions from line shapes, and the modeling of physical systems like stars, require an ability to accurately predict the opacity of these dense plasmas. We have developed a variational model that includes plasma effects in a self-consistent way. It does this in part by including all electrons, bound and free, and not making a hard distinction between them [1,2]. We present calculations of the opacity in dense conditions relevant to the solar interior. Comparisons with a state-of-the-art traditional approach reveal some important differences.

References

[1] C. E. Starrett, T. Q. Thelen, C. J. Fontes and D. A. Rehn, Phys. Rev. E **109**, 035201 (2024).

[1] T. Q. Thelen, D. A. Rehn, C. J. Fontes and C. E. Starrett, Phys. Rev. E **110**, 015207 (2024).

* E-mail: starrett@lanl.gov

SPECTRAL LINE SHAPES-I

Review of the 7th Spectral Line Shapes in Plasmas code comparison workshop.

A. Calisti[1] *

[1]Aix-Marseille University, CNRS, PIIM laboratory, Marseille, France.

Spectroscopy is one of the richest sources of plasma diagnostics [1]. Since diagnostics are based on the comparison of observed and modeled data, accurate theoretical models of atomic physics and radiation are required to be reliable.

The modeling of spectral lines in plasmas, which involves a complex combination of atomic physics, statistical physics and plasma physics, plays a crucial role in the interpretation of spectroscopic observations. Except for a few special cases, the calculation of line profiles in plasmas requires the use of numerical codes. There are a number of such codes, more or less complex, which necessarily differ in their scope and accuracy. To verify the accuracy and validity of models and codes, it is necessary to compare them to well-characterized reference experiments, when these exist, or to test them by comparing them to other models.

The SLSP (Spectral Line Shapes in Plasmas) Code Comparison Workshop was established in 2012 to encourage and facilitate such comparisons, which were almost non-existent [2]. Six editions of this workshop, organized in cooperation with the International Atomic Energy Agency (IAEA), have been held to date, during which a large number of diverse problems have been analyzed. The result has been a better understanding of the underlying phenomena and more accurate models [3, 4, 5, 6]. However, despite the progress made, several problems remain open, such as the interpretation of white dwarf spectra [7, 8] or those of WDM experiments [9].

In this talk, a report of the 7th SLSP, held in Gran Canaria, Spain, from 30 September to 4 October 2024, will be presented. A variety of topics were covered, ranging from standard cases that are highly demanding for codes and models to modeling experimental data and studying effects first addressed at SLSP such as Van der Waals broadening, the motional Stark effect (MSE), and periodic electric fields in the presence of a constant magnetic field.

References

[1] H. R. Griem. Principles of Plasma Spectroscopy. Cambridge University Press, Cambridge, England, (1997).

[2] https://plasma-gate.weizmann.ac.il/slsp/.

[3] E. Stambulchik, Review of the 1st Spectral Line Shapes in Plasmas code comparison workshop, HEDP, 9(3):528–534, (2013). doi:10.1016/j.hedp.2013.05.003.

[4] E. Stambulchik, A. Calisti, H.-K. Chung, and M. A González. Special issue on Spectral Line Shapes in Plasmas. Atoms, 2(3):378–381, (2014). doi:10.3390/atoms2030378.

[5] J. Rosato, Report on the third SLSP code comparison workshop, HEDP 22, 60–63 (2017).

[6] E.Stambulchik, A.Calisti, H.-K.Chung, and M.A.González, Spectral Line Shapes in Plasmas II. Atoms, 7(1):20, (2019). doi:10.3390/atoms7010020.

[7] J. Rosato, Effect of collisions on motional Stark broadening of spectral lines. J. Quant. Spectrosc. Radiat. Transfer, 306:108628, (2023). doi:10.1016/j.jqsrt.2023.108628.

[8] T. A. Gomez, M. C. Zammit, C. J. Fontes, and J. R. White, A quantum-mechanical treatment of electron broadening in strong magnetic fields. Astrophys. J., 951(2):143, (2023). doi:10.3847/1538-4357/acda28.

[9] S.X.Hu, et al., Probing atomic physics at ultrahigh pressure using laser-driven implosions. Nat. Commun., 13(1):6780, (2022). doi:10.1038/s41467-022-34618-6.

*E-mail: annette.calisti@univ-amu.fr

SALSAA: Statistically Averaged Line Shapes from Average Atom

S. Hansen[1 *], K. Adler[1] and T. Gomez[2]

[1]Sandia National Laboratories, Albuquerque, NM, USA
[2]University of Colorado, CO, USA

We report on an approach to computing ion-Stark contributions to line shapes based on self-consistent data from an average-atom model. The average-atom model uses density functional theory (DFT) to generate Kohn-Sham orbitals for electrons in a self-consistent electron-ion potential within a neutral ion sphere. The free-electron part of the electron distribution is used along with a response function to produce an ion-ion potential that defines a self-consistent radial distribution function and nearest-neighbor distribution for the ions. In traditional approaches to line-broadening, the ion distribution would be used to generate an electric field distribution which, coupled with perturbation theory for the response of bound states to electric microfields, provides the ion-Stark contribution to emission and absorption line broadening. In SALSAA, perturbations in electron binding energies are computed due to changes in the nearest-neighber location and convolved with the self-consistent nearest-neighbor distribution function to generate the ion-Stark contribution to line broadening. This presentation will compare each part of the new method to traditional calculations, showing that the statistical approach can reproduce many of the features of traditional methods with high computational efficiency, enabling self-consistent estimates of ion-Stark line broadening in multi-electron ions.

This work was supported by SNL's LDRD program, project number 218456. SNL is managed and operated by NTESS under DOE NNSA contract DE-NA0003525.

[*] E-mail: sbhanse@sandia.gov

Detailed line-shape modeling for diagnostics of high-energy-density plasmas

E. Stambulchik*, **R. Doron, and Y. Maron**

Weizmann Institute of Science, Rehovot 7610001, Israel

Radiation of mid-Z tracer species is widely used for diagnosing high-energy-density plasmas. In particular, the Stark broadening of K-shell transitions is a ubiquitous tool for inferring the electron density. Almost universally, it is a single quantity – the line width – that is used for the analysis. Here, however, we explore finer details of line profiles, including the shift, that may allow for determining the plasma density alternatively and for probing the atomic composition of the tracer ion environment. The calculations were carried out using computer simulations [1], recently extended [2] to treat the radiator–plasma interaction beyond the standard multipole approximation.

References

[1] E. Stambulchik and Y. Maron, J. Quant. Rad. Trans. **99**, 730–749 (2006).

[2] E. Stambulchik and C. A. Iglesias, Phys. Rev. E **105**, 055210 (2022).

*E-mail: evgeny.stambulchik@weizmann.ac.il

OPACITY-II

Time-resolved spectroscopy for Z stellar opacity research

G. P. Loisel[1], J. E. Bailey[1], T. Nagayama[1], S. B. Hansen[1], G. S. Dunham[1], P. D. Gard[1], A. P. Colombo[1], A. D. Edens[1], R. Speas[1], Q. Looker[1], M. Kimmel[1], J. Stahoviak[1], J. L. Porter[1], E. C. Harding[1], G. A. Rochau[1], C. J. Fontes[2], C. Blancard[3], Ph. Cossé[3], G. Faussurier[3], F. Gilleron[3], J.-C. Pain[3], D. Aberg[4]

[1]Sandia National Laboratories, Albuquerque, New Mexico 87185, USA
[2]Los Alamos National Laboratory, Los Alamos, New Mexico 87545, USA
[3]CEA, DAM-DIF, Arpajon, F-91297, France
[4]Lawrence Livermore National Laboratory, Livermore, California 94550, USA

Time-resolved spectroscopy using a novel hCMOS Ultra-fast X-ray Imager (UXI) is transforming stellar interior opacity measurements at the Sandia Z facility. Calculated opacities disagree with measured opacities [Bailey et al. Nature (2015), Nagayama et al. PRL (2019)], which questions the accuracy of calculated opacities used for the solar interior. The novel time-resolved data help to resolve this dilemma in three unprecedented ways. First, time-resolved measurements of the backlighter history, sample evolution, together with calculated opacities at each time step allows us to assess how temporal integration have affected the published, film-based results. These tests show that the temporal integration cannot explain the reported discrepancy. Second, measurements of the sample temperature and density evolution refine our understanding of the Z opacity platform and enable improved experimental design. Third, Sandia's UXI technology enables measurements of iron opacities at multiple conditions from a single experiment. This not only increases the number of opacity measurements per experiment but also allows to study how opacity changes with conditions from a single experiment. In this presentation, I will summarize the results on sample evolution in Fe experiments as well as progress towards the first extraction of absolute *time-resolved* opacity and remaining challenges to obtain that goal.

SNL is managed and operated by NTESS under DOE NNSA contract DE-NA0003525.

* E-mail: gploise@sandia.gov

Oxygen opacity experiments for stellar interiors at Z and NIF

D.C. Mayes[1 *], J.E. Bailey[2], P.A. Bradley[3], G.S. Dunham[2], C.J. Fontes[3], T.A. Gomez[4], S.B. Hansen[2], R.F. Heeter[5], B.A. Hobbs[1], M. Hohenberger[5], H.M. Johns[3], G.P. Loisel[2], T. Nagayama[2], Y.P. Opachich[5], T.S. Perry[3]

[1] University of Texas at Austin, Austin, TX, USA
[2] Sandia National Laboratories, Albuquerque, NM, USA
[3] Los Alamos National Laboratory, Los Alamos, NM, USA
[4] University of Colorado Boulder, Boulder, CO, USA
[5] Lawrence Livermore National Laboratory, Livermore, CA, USA

Much of what we know about the universe is rooted in our understanding of the Sun. However, ongoing disagreement between solar models and helioseismic measurements of the interior structure of the Sun raises concerns about the accuracy of stellar models. One hypothesis that could help resolve this discrepancy is that the opacities of matter at solar interior conditions are higher than models predict. Experiments on the Z Machine and at NIF investigate this by measuring iron and oxygen opacities at conditions near the solar convection zone base (CZB). The published iron measurements [1] are higher than model predictions, supporting this hypothesis. This talk will focus on the progress of the oxygen opacity experiments at each facility. Oxygen is the largest contributor to the opacity at the solar CZB and no experimental benchmark in this regime exists to date. We will discuss our methods for characterizing the opacity and plasma conditions and show preliminary oxygen measurements from both Z and NIF.

This work was supported by the Wootton Center for Astrophysical Plasma Properties under NNSA Stewardship Science Academic Alliances award number DE-NA0004149. Experimental time was provided by the Z Fundamental Science Program of SNL and the NIF Discovery Science Program of LLNL. SNL is managed and operated by NTESS under DOE NNSA contract DE-NA0003525, and LLNL is operated under DOE NNSA contract DE-AC52-07NA27344.

References

[1] Bailey, J., Nagayama, T., Loisel, G. et al. Nature **517**, 56–59 (2015).

* E-mail: dmayes@utexas.edu

Progress on Opacity Measurements at Stellar Interior Conditions Using the National Ignition Facility

R.F. Heeter[1 *], T.S. Perry[2], H.M. Johns[2], Y.P. Opachich[1], M.S. Hohenberger[1], D.P. Aberg[1], P.A. Bradley[2], P.B. Cho[1], J.P. Colgan[2], T.H. Day[2], E.C. Dutra[3], C.J. Fontes[2], E. Gallardo-Diaz[6], J.M. Heinmiller[3], B.A. Hobbs[4], R. Knight[3], D.C. Mayes[4], M.H. Montgomery[4], A.E. Peterson[3,6], R.S. Posadas[1], H.F. Robey[2], E. Smith[2], S. Stoupin[1], T.J. Urbatsch[2], M.S. Wallace[3], L.G. Webster[1], D.E. Winget[4], J.E. Bailey[5], S.B. Hansen[5], G.P. Loisel[5], and T. Nagayama[5]

[1]Lawrence Livermore National Laboratory, Livermore, CA, USA
[2]Los Alamos National Laboratory, Los Alamos, NM, USA
[3]Nevada National Security Sites, Livermore, CA, USA
[4]University of Texas at Austin, Austin, TX, USA
[5]Sandia National Laboratories, Albuquerque, NM, USA
[6]University of Nevada, Reno, NV, USA

There is little spectrally resolved experimental opacity data of plasma at temperatures and densities relevant to the physics of the sun, other stars, and laboratory high-energy-density experiments. Prior and ongoing opacity experiments on the Sandia National Laboratories Z machine have shown up to factor-of-2 discrepancies with theory - a challenging puzzle [1]. Since 2015, an additional set of experiments on the National Ignition Facility (NIF) have begun measuring opacities of iron and other materials at temperatures ~150 eV and density ~7×10^{21} electrons/cm^3 [2], and since 2021 those measurements have been extended to densities above 10^{22} electrons/cm^3. Figure 1 shows preliminary analysis of some NIF iron data, with the higher-density data showing higher opacity than expected theoretically [3]. This presentation summarizes the NIF experiments, efforts to constrain hypotheses for systematic errors, and new capabilities [4]. This data may have implications for modeling the structure of the sun and for determining the age of white dwarf stars.

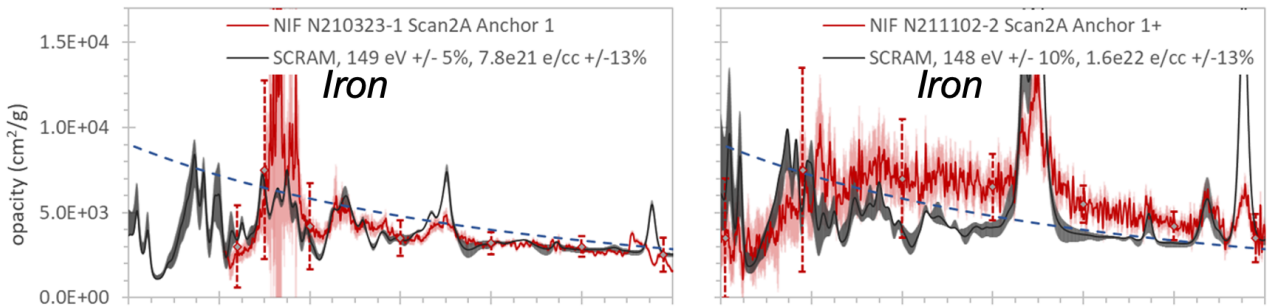

Figure 1. Samples of iron opacity measurements at two different densities, from NIF (Livermore, CA, USA).

This work was performed under the U.S. Department of Energy LANL contract 89233218CNA000001, LLNL Contract No. DE-AC52-07NA27344, Sandia Contract No. DENA0003525, and NNSS Contract No. DE-NA000362.

References

[1] J. E. Bailey *et al.*, Nature **517**, 56-59 (2015); doi:10.1038/nature14048

[2] R. F. Heeter *et al.*, Atoms **6**, 57 (2018); doi:10.3390/atoms6040057

[3] R. F. Heeter, T. Nagayama, H. M. Johns, S.B. Hansen: Tri-Lab Assessment, LLNL-PRES-854225 (2023)

[4] Y. P. Opachich, Rev. Sci. Instrum. **95**, 083513 (2024); https://doi.org/10.1063/5.0218014

* E-mail: heeter1@llnl.gov

PLASMA SPECTROSCOPY-I

Review of the use of machine-learning methods with spectroscopy in fusion plasmas

M. Koubiti*, N. Saura and S. Benkadda

Aix-Marseille Université/CNRS, PIIM Lab., Av. Escadrille Normandie-Niemen, F-13397 Marseille Cedex 20, France

Artificial Intelligence (AI) tools are taking an important place in plasma science [1] and particularly in plasma physics [2-4]. In this context, there is an incrasing actitivity related to the use of Machine Learning in the field of plasma spectroscopy. Combining machine or deep learning methods with plasma spectroscopy have various purposes including real-time inference of plasma dynamics in magnetic fusion devices [5] or the prediction of the plasma parameters [6]. In this paper, we review the various applications of machine-learning and deep-learning algorithms to spectroscopic data in plasmas with a focus on magnetic fusion plasmas without excluding other types of plasmas. We also present our own work related to the use of neural networks such as Convolutional Neural Network (CNN) to theoretical Balmer-α line spectra emitted by hydrogen isotopes for the hydrogen isotopic ratio prediction for Tokamak plasmas [7-8]. The paper will also be an opportunity to discuss the advantages and the drawbacks of the introduction of AI in plasma physics.

References

[1] R. Anirudh *et al*., IEEE Transactions on Plasma Science, **51**, 1750-1838 (2023).

[2] C. M. Samuell et al, Rev. Sci. Instrum., **92**, 043520 (2021).

[3] B. Dorland, machine learning for plasma physics and fusion energy, Journal of Plasma Physics (2022).

[4] Machine learning methods in plasma physics, Contrib. Plasma. Phys, **63**, Issues 5-6 (2023).

[5] L. Malhotra *et al*, 4th IAEA Techn. Meeting on Fusion Data Processing, Validation and analysis (2021).

[6] D. Nishijima *et al*, Rev. Sci. Instrum., **92** 023505 (2021).

[7] M. Koubiti, EPJD, **77**, 137 (2023).

[8] N. Saura, M. Koubiti, S. Benkadda, Study of line spectra emitted by hydrogen isotopes in tokamaks through Deep-Learning algorithms, submitted to Nuclear Materials and Energy

* E-mail: mohammed.koubiti@univ-amu.fr

A Comparison of Plasma Conditions Inferred from Optical Thomson Scattering Measurements and X-ray Spectroscopy

E.V. Marley[1]*, G. Swadling[1], C.Bruulsema[1], E. R. Toro[2], J. Katz[3], E. Folsom[1]

[1]Lawrence Livermore National Laboratory
[2]Stanford University, Department of Mechanical Engineering
[3]Laboratory For Laser Energetics University of Rochester

The K-shell emission of low- and mid-Z elements are commonly used in HED plasma experiments to infer the plasma conditions. A study has been done utilizing simultaneous x-ray spectroscopy and Optical Thomson Scattering (OTS) measurements to compare the electron temperature inferred from the ion acoustic wave (IAW) feature and from fitting the measured x-ray spectra with atomic kinetics codes. A buried layer platform was used to create uniform non-local thermodynamic equilibrium plasmas (ne $\sim$ few $10^{21}/\mathrm{cm}^3$, Te $\sim$0.8 — 1.2 keV) for this study. The target was a 250 μm diameter, 200 nm thick dot buried between two 1000 μm diameter, 5 μm thick beryllium foils. Lasers heat the target from both sides for 3ns. The density was inferred using both the electron plasma wave EPW feature as well as the size of the emitting volume measured with time resolved x-ray imaging. Two different target materials were used for the study: titanium and copper. The K-shell emission of the titanium and the K- and L-shell emission of the copper were measured time resolved. The comparison of the plasma conditions inferred from fitting the x-ray spectra with different atomic kinetic codes and the OTS measurements will be discussed.

This work was performed under the auspices of the U.S. Department of Energy by Lawrence Livermore National Laboratory under Contract DE-AC52-07NA27344.

*E-mail: marley2@llnl.gov

Radiative cooling of an Al plasma in an AlTi or AlAu mixtures heated by an ultraintense laser pulse

L. Lecherbourg[1,2]*, Ch. Blancard[1,2], S. Baton[3], A. Chaleil[1], P. Cossé[1,2], L. Duthoit[1,3], G. Faussurier[1,2], L. Gremillet[1,2], B. Loupias[1], F. Perez[3], J-.C. Pain[1,2], O. Poujade[1,2], and P. Renaudin[1]

[1]CEA, DAM, DIF, F-91297 Arpajon, France
[2]Univ. Paris-Saclay, CEA, LMCE, 91680 Bruyères-le-Châtel, France
[3]LULI, CNRS, École Polytechnique, CEA, Sorbonne université, 91120 Palaiseau, France

The rapid heating and cooling dynamics of thin solid foils driven by an ultraintense ($\sim 10^{18}$ W/cm^2) picosecond laser pulse has been experimentally studied through time-integrated and time-resolved x-ray emission spectroscopy as well as 2D x-ray imaging. Targets consisted of plastic foils with buried Al, $Al_{42}Ti_{58}$, or $Al_{85}Au_{15}$ layers, with Al as a tracer to infer the plasma conditions. Our measurements indicate that the Al K-shell emission occurs over a shorter duration and from a narrower region in AlTi or AlAu mixtures compared to pure Al samples.

The experimental data are then compared with the 2D hydrodynamic-radiative code TROLL and the atomic physics code SAPHyR. Approximating the heating phase using a simple description of a collisional heating, the simulations reproduced the trends to a good approximation, and pinpoint the importance of radiative cooling in high-Z samples.

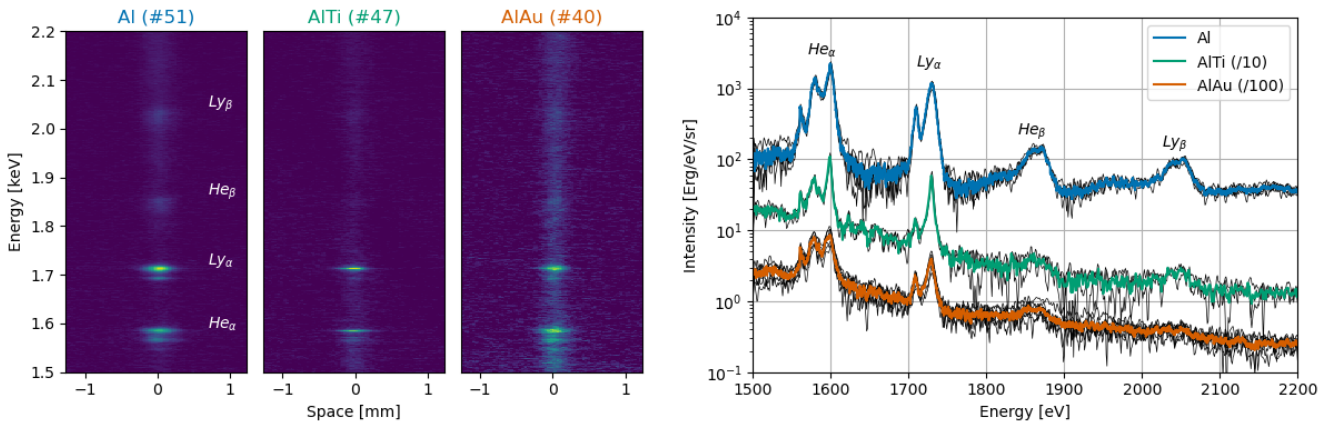

Figure 1. Example of time-integrated and space-integrated high resolution spectra of Al, AlTi and AlAu samples. (left) Raw data, (right) line profiles.

*E-mail: ludovic.lecherbourg@cea.fr

SPECTRAL LINE SHAPES-II

Zeeman Splitting Observed and Simulated in Laser-Produced Magnetized Blast Waves

A. Triantafyllidis[1*], J. -R. Marquès[1], S. Ferri[2], A. Callisti[2], Y. Benkadoum[1], A. Ciardi[3], A. Dearling[4], N. Ozaki[5,6], Y. De León[1], J. Beard[7], P. Renaudin [8], M. Koenig[1], B. Albertazzi[1]

[1]LULI - CNRS, CEA, Sorbonne Universités, Ecole Polytechnique, Institut Polytechnique de Paris, Palaiseau, France
[2]Aix Marseille Université, CNRS, PIIM, F-13013 Marseille, France
[3]Sorbonne Université, Observatoire de Paris, Université PSL, CNRS, LERMA, 75005 Paris, France
[4]York Plasma Institute, Department of Physics, University of York, YO10 5DD
[5]Institute of Laser Engineering, Osaka University, 2-6 Yamada-Oka, Suita, Osaka, 565-0871 Japan
[6]Graduate School of Engineering, Osaka University, Osaka, 565-0871, Japan
[7]Laboratoire National des Champs magnétiques Intenses (LNCMI), UPR 3228, CNRS-Université Joseph Fourier (UJF)-Université Paul Sabatier (UPS)-Institut National des Sciences Appliquées (INSA), F-31400 Toulouse, France
[8]CEA, DAM, DIF, Arpajon 91297, France

Magnetic fields are ubiquitous in the Universe and play a critical role in laboratory experiments, fundamentally influencing plasma behavior. For example, they can smooth out discontinuities in blast waves, alter the geometry of supernova remnants from spherical to barrel-shaped, and inhibit heat transport [1, 2]. Investigating these systems requires accurate determination of the plasma's parameters (density and temperature), the magnetic fields' strength and orientation, as well as whether it has been influenced by the plasma (compression or diffusion).

The recent advent of apparatuses capable of generating strong magnetic fields coupled with high-energy laser facilities [3] necessitates the development of advanced experimental platforms and numerical codes for magnetic field diagnostics. Even though multiple diagnostics already exist, all face significant limitations; B-dot probes disturb the plasma, proton deflectometry requires an extra, high-intensity laser beam, and polarimetry is not sensitive enough for certain systems.

To address this need, we developed an optical, time-resolved, high-dispersion spectrometer (resolution of ~0.1 nm) and performed measurements on laser-produced blast waves at the LULI2000 facility. Utilizing a pulsed-power system, we generated well-characterized magnetic fields of up to 20 T, both perpendicular and parallel to the blast waves' propagation. We collected the emitted spectra of multiple intense radiative transitions of nitrogen (2s22p(2P0)3l - 2s22p(2P0)3l') and used line-shape modeling to extract the parameters of the plasma; from the distinct signatures of the Zeeman and Stark effects on spectral lines, we inferred the average magnitude of the magnetic field inside the plasma and its density while its temperature was calculated from line intensity ratios and Doppler broadening. Our experimental results were extensively compared with spectra simulated using the Stark-Zeeman line-shape code PPPB, developed at PIIM [4], to examine if the magnetic field was compressed by the plasma.

Here, we present the first clear observation of Zeeman splitting in a homogenous, low-temperature, diffuse plasma (5-20 eV, ~10^{18} cm^{-3}) and show an excellent agreement between the experiment and the PPPB simulations for all magnetic field strengths and orientations. These results reveal that the external magnetic field diffuses into the post-shock region and demonstrate the capabilities of PPPB to accurately interpret our data, allowing for the establishment of a novel experimental platform for benchmarking atomic physics codes.

References

[1] Mabey, P., Albertazzi, B., Rigon, G., et al. 2020, ApJ

[2] Triantafyllidis, A., Marquès, J.-R., Benkadoum, Y., et al., under review in PRL

[3] Albertazzi, B., Béard, J., Vinci, T., et al. 2013, Rev. Sci. Instrum.

[4] Ferri, S., Peyrusse, O., & Calisti, A., 2022, MRE

* E-mail: angelos.triantafyllidis@polytechnique.edu

Zeeman Stark line shapes affected by periodic electric fields

I. Hannachi[1,2*], R. Stamm[1], J. Rosato[1] and Y. Marandet[1]

[1]Aix-Marseille Univ. and CNRS, PIIM, 13397 Marseille, France
[2]University of Batna 1, PRIMALAB, Department of Physics, Batna, Algeria

Atoms and ions emitting in a plasma are often subjected to periodic electric fields which can affect the emitted line shapes. Such conditions are typical in non-equilibrium plasmas where ion sound and Langmuir waves are frequently observed. In laboratory settings and magnetic fusion devices, radio frequency waves (rf) are employed for heating and current drive. Spectroscopic measurements of regions heated by the rf field are crucial for enhancing our understanding of wave-plasma coupling [1]. Modeling the effect of periodic electric fields has a long history involving various line shape formalisms, and has often focused on a monochromatic and linearly polarized wave $\vec{E}_w \cos(\omega t + \varphi)$, where φ is a random phase. In this study, we explore the utility of computer simulations in understanding the impact of the particle microfield and a concurrent periodic electric field on line shapes. By solving numerically the Schrödinger equation for a hydrogen emitter, we accurately capture the complex dynamics of our physical system. Several groups employ such computer simulations today, and a recent comparison of the outcomes from their codes has been performed for hydrogen lines in a periodic electric field [2], which will be briefly reviewed and updated here. We will also examine the influence of the magnitude E_w and the frequency ω of the wave, and present the application of the simulation to cases where both the magnetic field and the different electric fields affect the line shape.

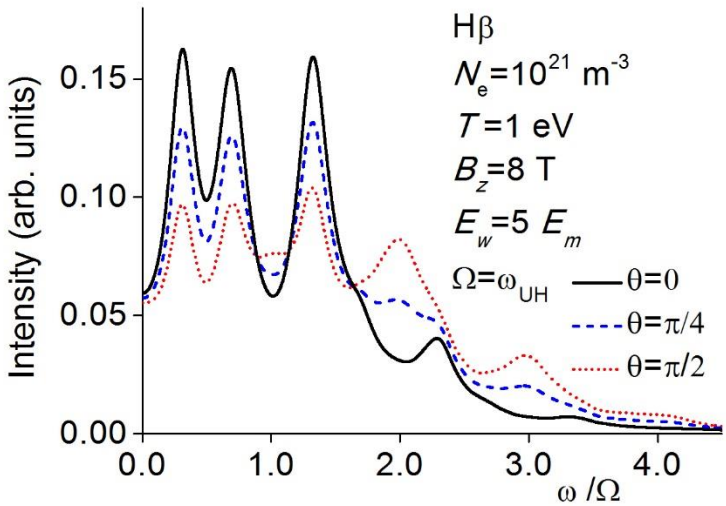

Figure 1. Hβ line observed at different angles with the magnetic field, for a wave magnitude equal to five time the average plasma microfield and an oscillation frequency equal to the upper hybrid frequency.

References

[1] C. Klepper *et al*., Phys. Rev. Lett. **110**, 215005 (2013).
[2] I. Hannachi, S. Alexiou, R. Stamm, Atoms **12(4)**, 19 (2024).

* E-mail: ibtissam.hannachi@univ-batna.dz

OPACITY-III

Towards opacity measurements at the LMJ facility: preliminary experiments with the atomic physics platform

C. Bowen[1*], M. Bonneau[1], Q. Alexandre[1], M. Brochier[3], T. Chirac[1], C. Courtois[1], S. Debesset[3], V. Denis[3], R. du Jeu[3], P. Dupré[3], S. Ferré[1], T. Fonseca[1], I. Geoffray[2], D. Gontier[1], L. Jacquet[1], S. Khieu[2], L. Le-Deroff[3], C. Meyer[1], J.-C. Pain[1], V. Prévot[1], P. Prunet[1], C. Reverdin[1], G. Soullie[1], M. Sozet[1], B. Vauzour[1] and B. Villette[1]

[1] CEA, DAM, DIF, F-91297 Arpajon, France
[2] CEA, CVA, F-21120 Is-sur-tille, France
[3] CEA-CESTA, F-33116, Le Barp, France

The new High Resolution X-ray Spectrometer (HRXS) of the Laser Mega Joule facility (LMJ) was commissioned at the end of 2023. Combined with the broadband X-ray spectrometers DMX and mini-DMX and with X-ray imaging diagnostics [1], it constitutes a platform for atomic physics experiments at LMJ. In particular, we are interested in opacity measurements, for which the control of the sample hydrodynamics and the quality of the transmission measurement are cornerstones [2]. We plan to measure the transmission of a copper plasma, generated in a laser-heated baffle Hohlraum. The center channels of HRXS provide time resolution, and spatial resolution along one axis. The time resolution should suppress the background signal, while we can use the spatial resolution to select the signal transmitted by the Cu plasma on the one hand and the signal that propagated through a witness area on the other hand. Following the HRXS commissioning, we performed preliminary experiments with HRXS, testing separately different backlighters and the Hohlraum, in order to assess the accessible quality of the transmission measurement and the sample preparation.

References

[1] W. Cayzac *et al.*, High Energy Density Phys. **52**, 101125 (2024).

[2] Heeter R. et al, Milestone 7720: National Opacity Program - Tri-Lab Assessment of Measurements and Models. No LLNL-TR-858890, Lawrence Livermore National Laboratory (LLNL), Livermore, CA (United States) (2023).

[*] E-mail: christopher.bowen@cea.fr

Photon scattering contribution in plasma transmission experiments

Veronika A. Kruse, D. Aberg, C. A. Iglesias

Abstract

The photon scattering contribution in recent transmission experiments at the Sandia Z-Facility [1] is examined using several approaches. First, spectral lines from single photon absorption are compared to resonant scattering estimates at line centers where photon scattering makes the largest contribution. Second, the full Waller-Kramers-Heisenberg expression [2] is applied to a few initial levels producing spectral lines prominent in the experimental spectrum. Finally, a dispersion-type relation [3] is used to compute the total plasma photon scattering cross-section. This last method accounts for all initial levels included in the photon absorption calculation. The numerical results show that photon scattering by bound electrons fails to resolve the extant discrepancies between transmission measurements of Fe and plasma radiation models.

[1] J.E. Bailey, T. Nagayama, G.P. Loisel, G.A. Rochau et al., Nature 517 (2015) 56-59, doi:10.1038/nature14048. T. Nagayama, J. E. Bailey et al, PRL 122, 235001 (2019), https://doi.org/10.1103/PhysRevLett.122.235001

[2] J. J. Sakurai, Advanced Quantum Mechanics, Addison-Wesley: Reading, MA, (1967)

[3] W.D. Barfield, W.F. Huebner, J. Quant. Spectrosc. Radiat. Transfer 16 (1976) 27-34.

This work was performed under the auspices of the U.S. Department of Energy by Lawrence Livermore National Laboratory under contract DE-AC52-07NA27344. LLNL-ABS-866212

Laboratory Measurement of L-Shell Opacity at GEKKO XII/LFEX High Power Laser Facility

J. Dun[1,2]*, F. Delahaye[3], H. Matsubara[1,2], Y. Karaki[1,2], T. Pikuz[1], A. Ciardi[3,4], R. Takizawa[1], K. F. F. Law[1], Y. Gong[1], M. Koenig[5], and S. Fujioka[1,6]

[1]Institute of Laser Engineering, Osaka University, Osaka, Japan
[2]Graduate School of Science, Osaka University, Osaka, Japan
[3]LERMA, Observatoire de Paris, Paris, France
[4]Laboratoire LULI, Ecole Polytechnique, CNRS, Paris, France
[5]LULI-CNRS, CEA, Paris, France
[6]National Institute for Fusion Science, Gifu, Japan

Opacity represents a fundamental parameter in high-energy-density (HED) physics, which controls the process of radiation energy transfer in a HED plasma. Understanding the atomic process in stellar interior conditions depends on the opacities of mid-atomic-number elements over a wide range of temperatures, which can also help us to understand the efficiency of inertial confinement fusion. However, some of the details of the radiative transfer process are neglected due to the complexity of the atomic process calculation, which leads to inaccurate predictions. For example, one possible explanation of the disagreement between solar models and helioseismology observation is insufficient theoretical opacities. [1] Experimental validation of the opacity models is crucial for astrophysics and the HED science.

Approximately ten years ago, the first measurement of plasma opacity at temperatures above 150 eV and electron densities above $10^{22}/\mathrm{cm}^3$, was achieved by the Z facility at Sandia National Laboratory (SNL). [2] The experiment revealed discrepancies between data and predictions of iron plasmas from different opacity modeling codes in the temperature-density region equivalent to solar convection-radiative boundary condition. The study proposes a hypothesis that the existing opacity models are missing some important physics processes that become significant at stellar interior conditions. [3]

In this paper, we present the work done toward verifying the hypothesis mentioned above and discuss the prospects for future research. A platform for measuring opacity has been developed with the GEKKO XII high-intensity laser facility. The bespoke laser-driven hohlraum can heat the calcium and titanium sample to a HED state while avoiding direct laser heating. The enhanced platform is equipped with the capacity for high-temporal resolution measurement utilizing the LFEX picosecond laser system. The experimental campaign yielded confirmation that the radiation temperature achieved by the laser-driven hohlraums with disparate geometric designs and driven laser energy combinations could reach 100 to 120 eV radiation energy. For the first time, several sets of high-temporal resolution spectra of transmission, sample emission, and backlight emission have been measured, which could be used for opacity calculation.

References

[1] S. Basu, H. M. Antia, Physics Reports **457**, 217-283 (2008).

[2] J. E. Bailey et al., Nature **517**, 56-59 (2015).

[3] T. Nagayama et al., Phys. Rev. Lett. **122**, 235001 (2019).

*E-mail: u725029c@ecs.osaka-u.ac.jp

XFEL-I

Distinct transient structural rearrangement of ionized water revealed by XFEL X-ray pump X-ray probe experiment.

B. Ziaja[1,2*]

in collaboration with: M. Stransky, T.J. Lane, A. Gorel, S. Boutet, I. Schlichting, A.P. Mancuso, Z. Jurek.

[1] Center for Free-Electron Laser Science CFEL, DESY, Hamburg, Germany
[2] Institute of Nuclear Physics, PAN, Kraków, Poland

Using X-ray free electron laser (XFEL) radiation to conduct an X-ray pump X-ray probe experiment, we studied strongly ionized water as part of our ongoing work on radiation damage [1]. After irradiance with a pump pulse with a nominal fluence of ~5×10^5 J/cm2 , we observed for pump-probe delays of 75 fs and longer an unexpected structural rearrangement, exhibiting a characteristic length scale of ~9 Å. Simulations suggest that the experiment probes a superposition of ionized water in two distinct regimes. In the first, fluences expected at the X-ray focus create nearly completely ionized water, which as a result becomes effectively transparent to the probe [2]. In the second regime, out of focus pump radiation produces O^{1+} and O^{2+} ions, which rearrange due to Coulombic repulsion over 10s of fs. Importantly, structural changes in the low fluence regime have implications for the design of two-pulse X-ray experiments that aim to study unperturbed liquid samples. Our simulations account for two key observations in the experimental data: the decrease in ambient water signal and an increase in low-angle X-ray scattering. They cannot, however, account for the experimentally observed 9 Å feature. A satisfactory account of this feature presents a new challenge for theory.

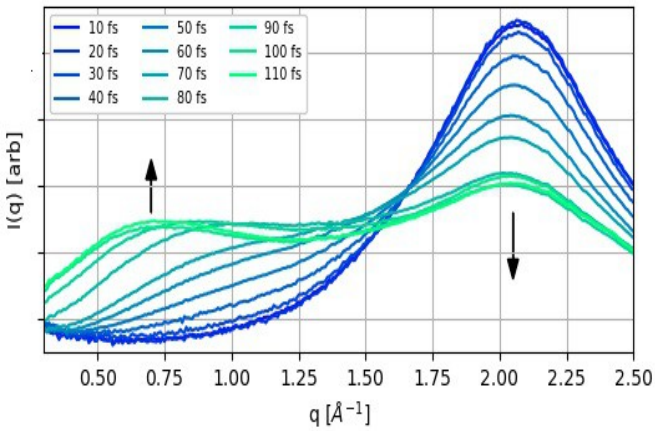

Figure 1. X-ray pump X-ray probe experiment reveals a new structural change in ionized water.

References

[1] M. Stransky, T. J. Lane, A. Gorel, S. Boutet, I. Schlichting, A. P. Mancuso, Z. Jurek, and B. Ziaja, Commun. Phys., accepted, (2024).

[2] I. Inoue et al., Phys. Rev. Lett. **131**, 163201 (2023).

* E-mail: ziaja@mail.desy.de

XFEL induced k-shell fluorescence in the solid to plasma regime

G .O. Williams[1]*, L. Ansia[1], M. Makita[2], P. Estrela[1], M. Hussain[1], T. Preston[2], J. Chalupsky[3], V. Hajkova[3] , T. Burian[3], M. Nakatsutsumi[2] J. Kaa[2], Z. Konopkova[2], J. C. P. Koliyadu[2], N. Kujala[2], K. Appel[2], V. Vozda[3], L. Juha[3], H.-K. Chung[4], P. Vagovic[5], H. Scott[6], P. Velarde[7], U. Zastrau[2], M. Fajardo[1].

[1] GoLP/Instituto de Plasmas e Fusão Nuclear, Instituto Superior Técnico, Universidade de Lisboa, 1049-001 Lisboa, Portugal
[2] European XFEL, Holzkoppel 4, 22869 Schenefeld, Germany
[3] Department of Radiation and Chemical Physics, Institute of Physics, Czech Academy of Sciences, Na Slovance 1999/2, 182 21 Prague, Czech Republic
[4] National Fusion Research Institute, Daejeon 34133, Republic of Korea
[5] Center for Free-Electron Laser Science CFEL, Deutsches ElektronenSynchrotron DESY, 22607 Hamburg, Germany
[6] Lawrence Livermore National Laboratory, Livermore, California 94550, USA
[7] Instituto de Fusión Nuclear, Universidad Politécnica de Madrid, José Gutiérrez Abascal 2, 28006 Madrid, Spain

High intensity XFELs have allowed uniform heating of solids on the micron scale and unique plasma diagnosis through x-ray spectroscopy and scattering. Here, we present results of XFEL heating and simultaneous fluorescence spectroscopy on mid-Z elements. The k-alpha and k-beta emission spectra are measured at several intensities and photon energies. The main features of the spectra are discussed and compared with models. We highlight the importance of features that persist from the solid-state to the plasma regime, that are important in the analysis of spectra in the warm dense regime, with temperatures near and below the Fermi temperature.

*E-mail: gareth.williams@tecnico.ulisboa.pt

Ultrahigh Resolution X-ray Thomson Scattering Measurements at the European XFEL

T. Gawne[1,2], Z. A. Moldabekov[1,2], O. S. Humphries[3], K. Appel[3], C. Baehtz[2], V. Bouffetier[3], E. Brambrink[3], A. Cangi[1,2], S. Göde[3], Z. Konôpková[3], M. Makita[3], M. Mishchenko[3], M. Nakatsutsumi[3], K. Ramakrishna[1,2], L. Randolph[3], S. Schwalbe[1,2], J. Vorberger[2], L. Wollenweber[3], U. Zastrau[3], T. Dornheim[1,2], T. R. Preston[3*]

[1]Center for Advanced Systems Understanding (CASUS), D-02826 Goerlitz, Germany
[2]Helmholtz-Zentrum Dresden-Rossendorf (HZDR), D-01328 Dresden, Germany
[3]European XFEL, D-22869 Schenefeld, Germany

Using an ultrahigh resolution ($\Delta E \sim 0.1$ eV) setup to measure electronic features in x-ray Thomson scattering (XRTS) experiments at the European XFEL in Germany, we have studied the collective plasmon excitation in aluminum at ambient conditions, which we can measure very accurately even at low momentum transfers. As a result, we can resolve previously reported discrepancies between *ab initio* time-dependent density functional theory simulations and experimental observations. The demonstrated capability for high-resolution XRTS measurements will be a game changer for the diagnosis of experiments with matter under extreme densities, temperatures, and pressures, and unlock the full potential of state-of-the-art x-ray free electron laser (XFEL) facilities to study planetary interior conditions, to understand inertial confinement fusion applications, and for material science and discovery.

References

T. Gawne et al., Phys. Rev. B, 109, L241112 (2024)
doi.org/10.1103/PhysRevB.109.L241112

*E-mail: thomas.preston@xfel.eu

PLASMA SPECTROSCOPY-II

High resolution, sub-picosecond x-ray spectroscopy of buried layers heated with high intensity, short pulse lasers[*+]

R. Shepherd[1], Hai Le[1], M. J. MacDonald[1], G. V. Brown[1], E. Magee[1], P. Beiersdorfer[1], H. Scott[1], L. Hobbs[2], C. R. D. Brown[2], M. Hill[2#], M. Martin[1], M. Foord[1], M. Patel[1], R. London[1], S. Pitt[2], D. Hoarty[2]

[1]Lawrence Livermore National Laboratory, Livermore, Ca., 94551, USA
[2]Atomic Weapons Establishment, Aldermaston, Reading, RG7 4PR,UK

Short pulse, laser (SPL) heated matter has opened an avenue to studying matter at conditions previously unobtainable. While SPLs can generate matter at extreme densities and temperatures, characterization of the heated matter can be extremely challenging. The conditions are extremely dynamic in nature, requirement a careful monitoring of the plasma evolution.

High temporal and spectral resolution spectroscopy can play an important role in understanding the heating dynamics of buried layers. At the onset of heating, the laser deposits energy into non-thermal electrons at the laser-target interaction plane. Some fraction of the non-thermals escapes the target, producing a charge imbalance and a return current. The spectral features during this heating phase result from thermal and non-thermal electron distributions. Temporally resolving the Li-like satellites along with the He_α complex provides an avenue for studying the plasma temperature as it transitions from a relatively low temperature to a high temperature. We look at the impact of the non-thermal electrons on the sulfur He_α and Li-like dielectronic complex using the LLNL sub-picosecond, high resolution-STreaked Orion High REsolution treX (STOHREX). The targets were 50 µm diameter "dots", made from 160nm of FeS and 60 nm KCl, tamped by 3 µm of parylene. The experiments were performed at the Orion laser facility using ~700 fs, 532 nm, 150 J focused to a 100 µm spot. The impact of non-thermal electrons on the inferred temperature rise is studied using recent adaptations to the Cretin code to account for non-Maxwellian electron distributions on spectral features. The preliminary results will be presented along with spectroscopic modeling.

[*]This work was performed under the auspices of the U.S. Department of Energy by Lawrence Livermore National Laboratory under Contract DE-AC52-07NA27344.
[#]Current address, Lawrence Livermore National Laboratory,
[+] Email: shepherd1@llnl.gov

Temperature determination of shock-compressed foams using x-ray fluorescence spectroscopy

M. J. MacDonald[1*], H. A. Scott[1], R. W. Falcone[2], K. B. Fournier[1], C. M. Huntington[1], S. R. Klein[3], C. C. Kuranz[3], K. H. Ma[3], E. V. Marley[1], A. M. Saunders[1], M. P. Springstead[3], P. A. Sterne[1], M. R. Trantham[3], B. G. Wilson[1], and T. Döppner[1]

[1] Lawrence Livermore National Laboratory, Livermore, California 94550, USA
[2] Department of Physics, University of California, Berkeley, California 94720, USA
[3] University of Michigan, Ann Arbor, Michigan 48109, USA

Temperature is a fundamental parameter in plasma physics and is a critical input to model and predict plasma properties. Despite its importance, experimental measurements of temperature in the high-energy-density regime are sparse due to the limited number of diagnostic techniques available for temperatures in the 10s of eV range. We present the use of x-ray fluorescence spectroscopy (XFS) to determine the temperature in shock-compressed foams at temperatures of 30–75 eV. XFS interrogates the plasma with an external energy source (typically x-rays or electrons) to fluoresce specific ions in a plasma to determine the ion distribution, and in turn the plasma temperature. Cobalt-doped foams were shock compressed using a planar drive at the OMEGA laser facility and probed with a Zn Heα x-ray source. Analysis of the resulting cobalt Kβ x-ray fluorescence spectra allow the temperature to be determined in the shocked foams. When properly calibrated, this method promises to provide a robust technique to infer temperatures in high-energy-density physics experiments in the 10s of eV temperature range of interest for hydrodynamics and equation of state experiments.

We present the analysis of XFS data using multiple codes, including rate matrix and Monte Carlo methods, and compare the results to hydrodynamic simulations. We find that hydrodynamic simulations predict a lower temperature in the shocked foams compared to analysis of the XFS data using collisional radiative codes. This disagreement can be explained by the radiation hydrodynamic codes underpredicting the plasma temperature or the collisional radiative codes underpredicting the cobalt ionization as a function of temperature, motivating future work to improve the models and cross-calibrate the temperature in the experiments to resolve this discrepancy.

This work performed under the auspices of U.S. Department of Energy by Lawrence Livermore National Laboratory under Contract DE-AC52-07NA27344 and supported by Laboratory Directed Research and Development (LDRD) Grant Nos. 18-ERD-033 and 22-ERD-005. RWF acknowledges support from DOE, National Nuclear Security Administration under Award Number(s) DE-NA0004147, and Office of Science, Office of Fusion Energy Sciences, under Federal Prime Agreement DE-AC02-05CH11231.

[*] E-mail: macdonald10@llnl.gov

Unveiling preplasma dynamics via collisional processes with nanosecond and sub-picosecond laser pulses

D. Khaghani[1 *], P. Neumayer[2], E. Galtier[1], H. J. Lee[1], G. Dyer[1] and O. Rosmej[2]

[1]SLAC National Accelerator Laboratory, Menlo Park, United States
[2]GSI Helmholtz Centre for Heavy Ion Research, Darmstadt, Germany

We present experimental results from the PHELIX laser facility in Darmstadt, Germany, utilizing both components of the PHELIX laser system: a nanosecond (ns) laser pulse and a 500 fs laser pulse [1]. Our study aimed to understand the interaction dynamics of Cu targets by inducing intentional preplasma formation with the ns laser and heating electrons to a suprathermal distribution with the sub-ps laser.

The experimental method involved recording time-integrated x-ray line emission spectra of highly ionized Cu atoms, focusing on the He-like Rydberg series and Lyman-alpha lines. We explored the impact of different energies in the ns pulse on preplasma formation, the effects of delays between the laser pulses on preplasma expansion dynamics, and the influence of short-pulse laser contrast by varying conditions of the ultrafast optical parametric amplifier (uOPA).

Our results show distinct changes in the x-ray line emission spectrum under different preplasma conditions. The suprathermal electron population generated by the short-pulse interaction serves as a pumping mechanism via collisional ionization in the nanosecond intentional preplasma, revealing the charge state distribution. We interpret these spectral signatures in terms of the plasma dynamics and its transient conditions.

This study enhances our understanding of laser-plasma interactions and provides insights into optimizing experimental conditions for future high-energy density physics research with both optical lasers and XFELs.

References

[1] Rosmej, O. N., et al. "Interaction of relativistically intense laser pulses with long-scale near critical plasmas for optimization of laser based sources of MeV electrons and gamma-rays." *New Journal of Physics* 21.4 (2019): 043044.

* E-mail: khaghani@slac.stanford.edu

OPACITY-IV

Production of an opacity table for air

Mark C. Zammit, James Colgan*, Isuru Ariyarathna, Christopher J. Fontes, Jeffery A. Leiding, Amanda J. Neukirch, Rodney W. Whitaker, and Eddy Timmermans

Los Alamos National Laboratory, Los Alamos, NM 87545, USA
*jcolgan@lanl.gov

Opacities are one of the most crucial ingredients in radiation-hydrodynamic simulations used to model a variety of astrophysical phenomena, laser-produced plasmas, and in shock-induced heating studies. For hot plasmas, it is usually only necessary to consider the opacities of atoms and their ions – a task that can still be very challenging for systems where a number of ion stages are populated and for complex ions where many atomic levels may retain population. For cooler plasmas (roughly temperatures in the range of 1 eV), it may be necessary to consider mixtures of atomic and molecular species. This can also be quite challenging, especially for scenarios where ionization and dissociation of molecules can lead to cases where contributions from atoms, molecules, and their ions are all important. Here we describe our recent work in calculating the opacity of air for a range of temperatures and densities. For room temperature cases, the opacity of air is dominated by the diatomic molecule contributions from N2 and O2. At temperatures of a few thousand Kelvin other molecular species, such as NO and NO2, make important contributions. At higher temperatures (approaching tens of thousands of Kelvin), molecular and atomic contributions are both significant. At even higher temperatures, atomic contributions finally start to dominate.

Our approach starts from the LANL Magpie code [1], which computes the equation-of-state of the air components for a given temperature and pressure in local thermodynamic equilibrium. The LANL MOLOP suite [2] is then used to compute the molecular absorption. We use a combination of detailed quantum chemistry (using the MOLPRO code [3]) and RKR methods to compute the potential energy curves and dipole matrix elements for the diatomic molecules of interest. NO2 contributions are provided from work done at Sandia National Laboratories [4]. The atomic contributions are computed using the LANL suite of atomic physics codes [5]. The LANL MOLOP code then assembles the monochromatic opacity of the air mixture and has recently been used to construct tables of air opacities. Examples of such opacities will be shown at the conference.
LANL is operated by Triad National Security, LLC, for the National Nuclear Security Administration of the U.S. Department of Energy under Contract No. 89233218NCA000001.

References

[1] C. Ticknor, S. A. Andrews, and J. A. Leiding, AIP Conf. Proc. 2272, 030033 (2020).

[2] M. C. Zammit, J. A. Leiding, J. Colgan, W. Even, C. J. Fontes, and E. Timmermans, J. Phys. B 55, 184002 (2022).

[3] H.-J. Werner, et al., J. Chem. Phys. 152, 144107 (2020).

[4] D. Osborn and D. Fisher, private communication (2024).

[5] C. J. Fontes, H. L. Zhang, J. A. Jr, R. E. H. Clark, D. P. Kilcrease, J. Colgan, R. T. Cunningham, P. Hakel, N. H. Magee, and M. E. Sherrill, Journal of Physics B: Atomic, Molecular and Optical Physics 48, 144014 (2015).

Implementation of a Super-Shell Refinement Algorithm for Plasma Opacities

Daniel Åberg*, **Paul E. Grabowski, Carlos A. Iglesias, and Brian G. Wilson**

Lawrence Livermore National Laboratory, P.O. Box 808, Livermore, California 94550, USA

The spectral fidelity of opacity spectra generated using Super-Transition Array (STA) formalism is strongly dependent by the choice of super-shell structure. We report on an algorithm where a parent super-configuration (SC) is iteratively refined into daughter SCs until the probabilities of the parent and daughter SCs are equal within a small tolerance. This naturally leads to an SC-dependent super-shell structure, avoiding redundant refinement of SCs that are already converged using a small number of super-shells. We further discuss some modifications of the scheme necessary to accelerate convergence of STA spectra when orbital relaxation, or finite-state effects, are considered. Benchmark calculations illustrating computational efficiency using LLNL's LTE opacity code OPUS will be showcased and discussed. Prepared by LLNL under Contract DE-AC52-07NA27344. LLNL-ABS-868727.

*E-mail: aberg2@llnl.gov

Full-potential treatment for multiple-scattering calculation of hot dense plasma opacity

H. B. Tran Tan[1]*, C. J. Fontes[1], and C. E. Starrett[1]

[1]Los Alamos National Laboratory, P.O. Box 1663, Los Alamos, New Mexico 87545, USA

The calculation of the optical properties of hot dense plasmas with a model that has self-consistent plasma physics is a grand challenge for high-energy density science. It is generally hoped that the development of such a model will reconcile discrepancies between theory and experiments such as the irons opacity problem [1, 2, 3]. Recently, an electronic structure model that uses multiple scattering to solve the Kohn-Sham density functional theory equations has been successfully applied to dense plasmas [4, 5]. A prominent advantage of this approach has over other state-of-the-art methods is that it does not use pseudopotentials; instead, the core electronic states are computed self-consistently. Results from this multiple scattering theory formalism are in good agreement with those obtained with other methods.

The existing implementation of the multiple scattering method is, however, not complete. For example, single-site scattering is treated by first averaging over the true three-dimensional potential then solving the scattering problem in this spherically symmetric average potential. It is expected that the asymmetry of the true potential, arising from the highly disordered nature of a plasma, will have appreciable effects on the plasma's properties such as its equation of state and opacity. Our work seeks to address this issue. We approach the full-potential scattering problem using the Siegert-states formalism [6, 7, 8], which accurately reproduces bound states, while yielding discrete complex-energy free states in contrast to the usual real-energy continuum. Siegert states are thus very convenient for the computation of physical quantities involving summations over complete sets of states. Indeed, the usefulness of Siegert states in the average-atom model has been recently demonstrated [9]. In this poster, we explain how Siegert states may be used for a full treatment of three-dimensional plasma potentials.

[1] J. Colgan *et al.*, Astrophys. J. **817**, 116 (2016)
[2] J. E. Bailey *et al.*, Nature **517**, 56–59 (2015).
[3] T. Nagayama *et al.*, Phys. Rev. Lett. **122**, 235001 (2019)
[4] C. E. Starrett and N. Shaffer, Phys. Rev. E **102**, 043211 (2020)
[5] N. Shaffer and C. E. Starrett, Phys. Rev. E **105**, 015203 (2022)
[6] O. I. Tolstikhin *et al.*, Phys. Rev. A **58**, 3 (1998)
[7] P. A. Batishchev and O. I. Tolstikhin, Phys. Rev. A **75**, 062704 (2007)
[8] L.O. Krainov *et al.* Phys. Rev. A **93**, 042706 (2016)
[9] C. E. Starrett and N. Shaffer, Phys. Rev. E **107**, 025204 (2023)

*E-mail: bao@lanl.gov

INERTIAL CONFINEMENT FUSION

Evaluation of Au L-shell spectroscopy as a T_e diagnostic for NIF hohlraum plasmas

N. Aybar[1 *], D. Liedahl[1], T. Woods[1], H. Chen[1], D. E. Hinkel[1], O. Landen[1], J. S. Ross[1], and M. B. Schneider[1]

[1]Lawrence Livermore National Laboratory, Livermore, USA

Obtaining accurate measurements of hohlraum plasma conditions is challenging, yet highly valuable in understanding hohlraum energy transport and achieving predictive modeling capabilities of indirect drive inertial confinement fusion. This is particularly true in the gold bubble region, a plasma plume generated where the outer beams strike the hohlraum, as subsequent laser energy propagates through and heats the gold bubble plasma. To attain such measurements, high quality spectral data were obtained from L-shell transitions of gold plasma self-emission which can serve as a powerful Te diagnostic, as the observed spectral features shift in energy depending on the charge state distribution. Experimental data collected from dedicated hohlraum science experiments include time resolved spectra of the Au L-shell. The measured spectra are compared against synthetic spectra produced by postprocessing radiation-hydrodynamics simulations performed in Lasnex [1] with atomic kinetics code SCRAM [2]. As a benchmark, these results are compared with dopant K-shell spectra from He-like and H-like charge states of Zn co-located in the gold. The differences obtained from both Te sensitive diagnostic approaches will be discussed and compared against simulation results.

This work was performed under the auspices of the U.S. Department of Energy by Lawrence Livermore National Laboratory under Contract No. DE-AC52-07NA27344.

LLNL-ABS-866222

References

[1] G. B. Zimmerman and W. L. Kruer, Plasma Phys. Controlled Fusion **2**, 51 (1975)

[2] S. Hansen, PhD dissertation, University of Nevada, Reno (2003)

* E-mail: aybar1@llnl.gov

Evidence of gold NLTE model in the deficiency of NIF ICF hohlraum x-ray drive prediction

Hui Chen, D. T. Woods, W. A. Farmer, N. A. Aybar, D. A. Liedahl, S. A. MacLaren, M. B. Schneider, H. A. Scott, D. E. Hinkel, O. L. Landen, J. D. Moody, M. D. Rosen, J. S. Ross, S. Rogers, N. Roskopf, G. Swadling and S. Vonhof

Lawrence Livermore National Laboratory, Livermore, California, USA

In the indirect-drive inertial confinement fusion (ICF) experiments on the National Ignition Facility (NIF) that have achieved ignition with energy gain of greater than one [1-3], advances in experimental design using hydrodynamic codes [3] have played critical role. To date, a less-than-unity artificial multiplier is often used in the design code, often referred as « drive-deficit », to match the implosion performance of deuterium-tritium fuel capsule [3]. We have performed a set of dedicated experiments using pairs of viewfactor targets [4] to understand the cause for such multiplier. The target and diagnostic setup is shown in Figure 1. The data revealed that the discrepancy between the simulation and data is larger when the measurement focus on the hotter (2-5 keV) region of non-Local thermal equilibrium (NLTE) plasma. Using an opacity multiplier on gold "M-band" emission in the code is shown to produce a much improved match to the measurements for both the radiation drive and the bubble temperature via K-shell dopant spectroscopy data. These experiments conclude that the inaccuracies in the atomic modeling of the NLTE gold plasma is likely responsible for the long standing "drive-deficient" hohlraum modeling [5].

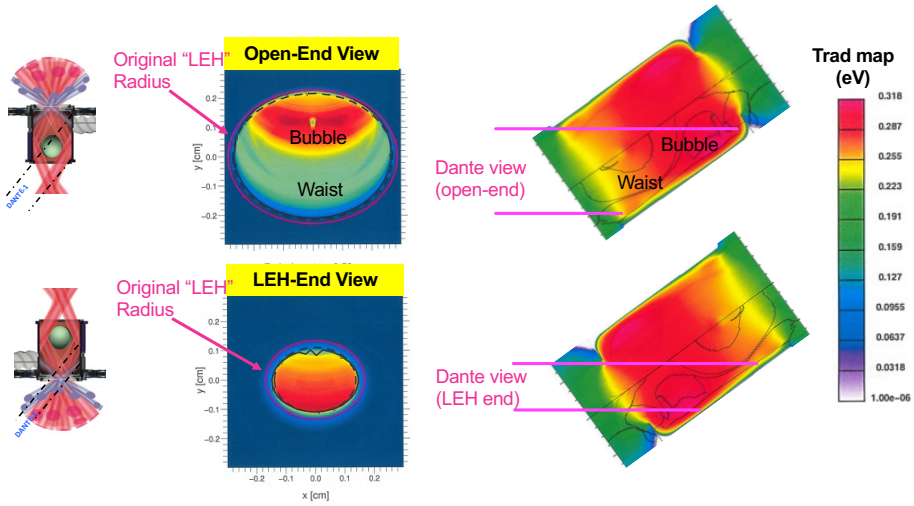

Figure 1. A pair of viewfactor targets provide different view of hohlraum internals and the target view of the Dante radiation flux diagnostic. The hohlraum plasma viewing through « LEH-end » is dominated by the NLTE Au bubble.

References

[1] H. Abu-Shawareb et al. (The Indirect Drive ICF Collaboration), Phys. Rev. Lett. **132**, 065102 (2024).
[2] O. A. Hurricane et al., Phys. Rev. Lett. **132**, 065103 (2024).
[3] A. L. Kritcher, et al., Phys. Rev. E **109**, 025204 (2024).
[4] S. A. MacLaren et al., Phys. Rev. Lett. **112**, 105003 (2014).
[5] M. B. Schneider et al, Phys. Plasmas **22**, 122705 (2015)
[5] H. Chen, et al., Phys. Rev. E **110**, L013201 (2024)

* E-mail: chen33@llnl.gov

Understanding the effects of preheat from the Au M-band and L-band hohlraum radiation on EOS experiments

Joseph Nilsen*, Rich London, Damian Swift, and Amy Lazicki

Lawrence Livermore National Laboratory, Livermore, CA 94551, USA

In this talk we look at the effect of the Au M-band and L-band hohlraum radiation on preheating the EOS sample in experiments done at the NIF laser facility. In particular we examine EOS experiments that were done using a Mach Stem shock wave created by putting a plastic CH cone inside the hohlraum with the EOS sample outside the hohlraum at the base of the cone, as shown in Fig. 1. The EOS sample consisted of Au and CH steps. The experiments measured the shock breakout times from the steps and used impedance matching of Au vs CH to determine a point on the Hugoniot for Au. The experiments were able to create planar shocks at pressures above 500 Mbar in the Au.

In this talk we show the importance of preheat effects from the Au M-band and L-band hohlraum radiation and how we were able to mitigate some of these effects by doping the plastic cone with Ge. The preheat causes the Au sample to heat and undergo hydrodynamic motion before the main Mach Stem shock arrives and it is important to minimize and understand the effect of the preheat on the interpretation of the experimental results. Unlike EOS experiments on lower-Z materials the effect of the L-band radiation is very important and more difficult to eliminate.

The preheat is a general issue for EOS experiments that needs to be understood and is not unique to the Mach Stem platform.

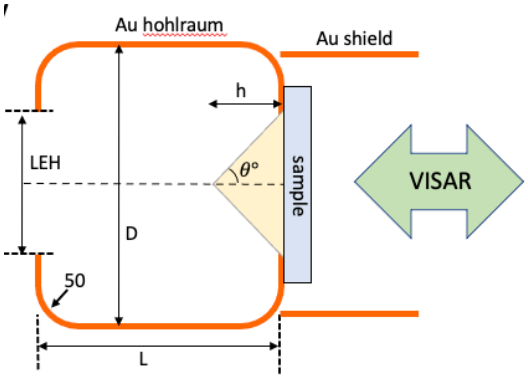

Figure 1. Mach Stem geometry for EOS experiments [1].

References

[1] Amy Lazicki (Jenei) et al., "Mach wave drive for ultra-high pressure plasma equation of state measurements," 63rd Annual Meeting of the APS Division of Plasma Physics, LLNL-PRES-829723.

This work was performed under the auspices of the U.S. Department of Energy by Lawrence Livermore National Laboratory under contract DE-AC52-07NA27344. Lawrence Livermore National Security, LLC.

* E-mail: nilsen1@llnl.gov

XFEL-II

Probing dense plasmas with high harmonics

P. Velarde[1]*, L. Ansia[1,2], A.G de la Varga[1], A. González[1], G. Williams[2], and M. Fajardo[2]

[1]Instituto de Fusión Nuclear, Universidad Politécnica de Madrid, José Gutiérrez Abascal 2, 28006 Madrid, Spain.

[2] GoLP/Instituto de Plasmas e Fusão Nuclear, Universidade de Lisboa, 1049-001 Lisboa, Portugal.

The advent of X-ray free electrons laser opened up new opportunities in the study of warm dense matter. With intensities previously achievable only by infrared and visible lasers, XFELs facilitate the creation of matter with precisely better defined properties, such as temperature and density. Recently, there has been a particular focus on the generation of dense plasmas from mid-Z materials, especially transition metals.

These experiments are typically complemented by collisional radiative models (CRMs), which have proven to be useful tools for understanding the temporal evolution of the sample. Recently, the non-thermal CRM BigBarT [1, 2, 3, 4] code has been extended to simulate arbitrary materials while maintaining a self-consistent approach for evolving non-thermal electron distributions and incorporating degeneracy effects. Additionally, time-dependent indexes of refraction have been derived using the Kronig-Kramers relations, allowing for the investigation of electromagnetic wave propagation in the plasmas.

The dielectric function is used to calculate the polarisation using the Havriliak–Negami method. This polarisation is used to calculate the propagation of a harmonic HHG beam in a target which has been isochorically heated by the XFEL. For this calculation, Maxwell's equations are solved numerically with a Godunov method with adaptive mesh, which allows to simulate the complete physical system during the whole HHG pulse. The phase differences of the outgoing HHG beam can be measured on a wavefront detector and the spatial variation of the sheet electron density can be derived. We present the results of simulations of this approach to measure density profiles in dense plasmas with HHG beams.

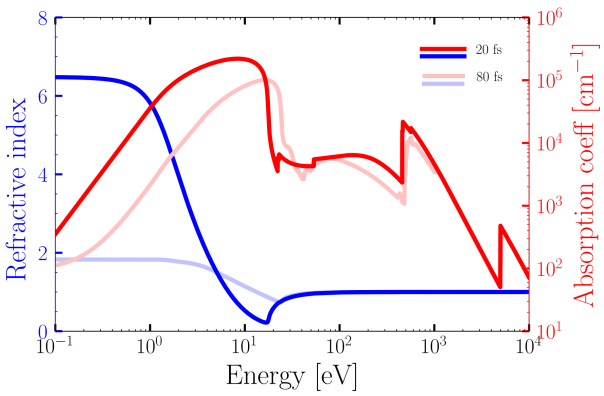

Refractive index and absorption coefficient for Ti illuminated by a XFEL pulse of I=10^{17} W/cm^2, FWHM=30 fs and hν=6 keV.

References

[1] A. G. de la Varga et al, HEDP **7**, 163-168 (2011).

[2] A. G. de la Varga et al, HEDP **9**, 542-547 (2013).

[3] Van Den Berg Q. Y. et al., Phys Rev Lett **120**, 055002 (2018).

[4] Ren S. et al., Comm Phys **6**, 99 (2023).

*E-mail: pedro.velarde@upm.es

Modelling non-thermal XFEL heating of Iron

L. Ansia[1,2]*, P. Velarde[2], M. Fajardo[1] and G. O. Williams[1]

[1] GoLP/Instituto de Plasmas e Fusão Nuclear, Universidade de Lisboa, 1049-001, Portugal.
[2]Instituto de Fusión Nuclear, Universidad Politécnica de Madrid, José Gutiérrez Abascal 2, 28006, Spain.

Over the past two decades, X-ray free-electron lasers (XFELs) have made significant progress, achieving peak brightness in the XUV and X-ray regions that were previously only attainable in the optical and infrared ranges. This advancement has opened up new possibilities in high-energy density science. It enables the creation of solid-density plasmas with larger volumes, greater uniformity, and well-defined properties, including temperature and density. XFEL heating proceeds through photoionisation and thermalisation, and as such initially creates a non-thermal electron distribution.

In the last years, several experiments have been focus in the creation of solid density plasmas of mid-Z materials, especially transition metals. Since collisional models have been proven to be a successful method to understand the time resolved atomic kinetics, we have adapted the non-thermal collisional radiative model BigBarT [1, 2, 3, 4] in order to simulate arbitrary elements.

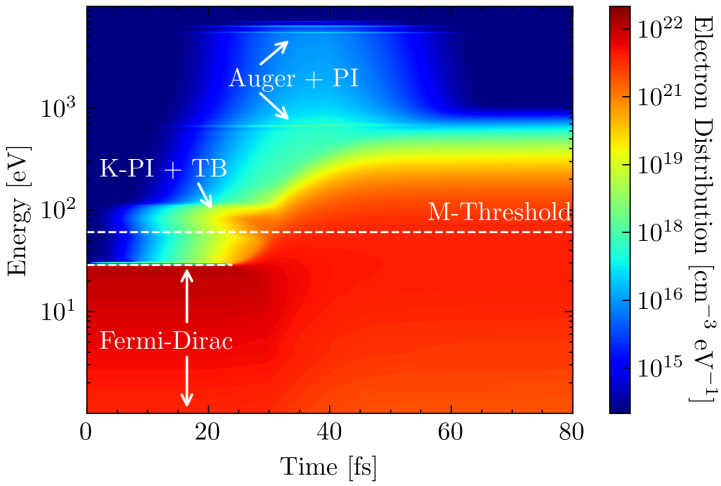

Figure 1. Electronic distribution temporal evolution of an Iron XFEL produced plasma, for a 15 fs FWHM pulse at 5×10^{17} W/cm^2

We investigate the effects of inelastic thermalization in iron under intense X-ray irradiation using the atomic model BigBarT , suited for the self-consistent evolution of the electron continuum, including degeneracy effects. A typical evolution of the distribution function is showed in Figure 1, for a 15 fs FWHM pulse at 5×10^{17} W/cm^2, and an incoming photon energy of 7200 eV. Our study focuses particularly on collisional M-shell ionization, which we identify as the most efficient relaxation process of non-thermal electrons. Comparison of calculated spectra with data could be used to refine collisional cross sections, that are otherwise difficult to compute due to their proximity to the continuum and the associated plasma screening effects.

References

[1] A. G. de la Varga, P. Velarde, High Energy Density Physics **7**, 163-168 (2011).

[2] A. G. de la Varga, P. Velarde, High Energy Density Physics **9**, 542-547 (2013).

[3] Van Den Berg Q. Y. et al., Phys Rev Lett **120**, 055002 (2018).

[4] Ren S. et al., Comm Phys **6**, 99 (2023).

*E-mail: lucas.ansia.fernandez@tecnico.ulisboa.pt

X-ray Imaging and Ionization dynamics in ultra-relativistic laser plasmas revelaled with an X-ray Free Electron Laser

Mikhail Mishchenko[1], Motoaki Nakatsutsumi[1], Erik Brambrink[1], Toma Toncian[2], Dominik Kraus[2], Irene Prencipe[2], Thomas Kluge[2], Thomas Cowan[2], Lingen Huang[2], Michal Smid[2], Alejandro Garcia[2], Hauke Höppner[2], Oliver Humphries[1,2], Eyal Kroupp[3], Evgeny Stambulchik[3], Ingo Uschmann[4], Robert Lötzsch[4], Paul B Neumayer[5], Byoung-ick Cho[6] and Ulf Zastrau[1] *

[1]European XFEL GmbH, Germany
[2] Helmholtz-Zentrum Dresden-Rossendorf (HZDR), Germany
[3] Weizmann Institute of Science, Israel
[4] Friedrich-Schiller-Universität Jena, Germany
[5] GSI Helmholtzzentrum für Schwerionenforschung, Germany
[6] Gwangju Institute of Science and Technology, South Korea

We present time-resolved resonant X-ray measurements of the micron-spatially resolved opacity, together with emission spectroscopy from laser-irradiated Cu foils. This study overcomes the limitations of earlier time-integrated observations of the characteristic K-lines and bremsstrahlung. The abundance of highly charged Cu ions is used as a marker for electron temperatures in the few 100 eV range during the first picoseconds after interaction.

We observe electron cooling inside the bulk within the first picosecond. The ionized region is limited spatially to a spot corresponding to the laser focal size and localized to the laser-irradiated side of the Cu foil. Despite the consistency of our experimental X-ray emission and opacity data in indicating a rapid plasma cooling and recombination, two-dimensional PIC simulations on the other hand predict a quasi-static temperature on this timescale. We find that the PIC simulations can only reproduce our experimental observations for a very narrow intensity and preplasma parameter space.

Moreover, the experimental data enables the assessment of enhancements to PIC codes with respect to the treatment of energy dissipation in three dimensions, atomic physics, and radiation transport.

References

[1] L. G. Huang, T Kluge, and T E Cowan, Phys. Plasmas 23, 063112 (2016)
[2] T. G. White et al., PRL 112, 145005 (2014)
[3] L. Gaus et al., Phys. Rev. Research, vol. 3, no. 4, 2021
[4] A. Laso Garcia et al., High Pow Laser Sci Eng, vol. 9, 2021
[5] U. Zastrau et al., JSR 28, 1393-1416 (2021)

* E-mail: ulf.zastrau@xfel.eu

Theoretical studies on M-shell localization of highly charged Mg produced by XFEL

Cheng Gao[1 *], Yongqiang Li[1] and Jianmin Yuan[2]

[1]College of Science, National University of Defense Technology, Changsha, Hunan 410073, P.R. China
[2]Institue of Atomic and Molecular Physics, Jilin University, Changchun Jilin 130012, P.R. China

The investigation of x-ray–matter interaction with x-ray free electron laser (XFEL) has attracted considerable attention in the past decade [1], which produces ultrafast ultra-intense x-ray pulses. Research on XFEL-matter interaction is significant for fundamental investigations and applications. In this work, we simulated the emission spectra of Mg in the interaction of XFEL with the photon energy of 1540 eV, duration of 100 fs and peak intensity of ~10^{17} W/cm^2[2]. A time-dependent rate equation is utilized to calculate the temporal evolution of the fine-structure level populations[3-4]. The emission spectra are compared with the experiment and reasonable good agreement is found. The relocalization of high orbtials of highly charged Mg ions in hot dense plasma environment are investigated using an a.b. init. method, in which the plasma screening effects on atomic wavefunctions are considered by introducing an effective screening potential into Hamiltonian.

References

[1] C. Bostedt et al., Rev. Mod. Phys. **88**, 015007 (2016).

[2] G. Pérez-Callejo, et al., Phys. Rev. E **109**, 045204 (2024)

[3] C. Gao et al., Phys. Rev. E 110, 015201 (2024)

* E-mail: gaocheng@nudt.edu.cn

X-RAY SOURCES

Recent advances on laser-plasma based soft x-ray lasers

Stephane Sebban[1], Adeline Kabacinski[1], Eduardo Oliva[2], Fabien Tissandier[1], Michaela Kozlova [3,4], Jean-Philippe Goddet[1], Igor Andriyash[1], Cédric Thaury[1], Philippe Zeitoun[1] and Julien Gautier[1]

[1]Laboratoire d'Optique Appliquée, ENSTA-Paris, CNRS, Ecole Polytechnique, Institut Polytechnique de Paris, Palaiseau, France

[2]Instituto de Fusion Nuclear "Guillermo Velarde" and Departamento de Ingenier´ıa Energética, E.T.S.I. Industriales, Universidad Politécnica de Madrid, Spain

[3]ELI Beamlines Project, Institute of Physics CAS, Praha 8, Czech Republic

[4]Institute of Plasma Physics CAS, Praha 8, Czech Republic

Intense and short soft X-ray light pulses offer unprecedented possibilities for studying ultrafast phenomena in matter at the nanometer scale. Plasma-based soft X-ray lasers (SXRLs) have the avantage of being compact sources. We report recent achievement aiming to demonstrate the control and reduction of duration of a seeded collisional soft X- ray laser induced by the anticipated interruption of the gain lifetime at high densities [1]. By controlling the peak intensity velocity of an ultrashort beam by spatio-temporal couplings we improve the performances of a SXRL, which intrinsically suffers from the group velocity (v_g) mismatch between the infrared pump beam used to generate the plasma amplifier and the XUV seed. The energy extraction was measured to raise from 19 to 59% when the pump v_g ranges from 0.55c to 1.05c. We also demonstrate that the SXRL pulse duration is governed by the pump beam velocity and can be maintained constant along its propagation, resulting in energetic pulses as short as 350 fs [2]. The measurements, in good agreement with simulations from a 3D Maxwell-Bloch code, have been performed thanks to an original method allowing to recover the temporal profile of any kind of soft X-ray laser pulse in single-shot operation.

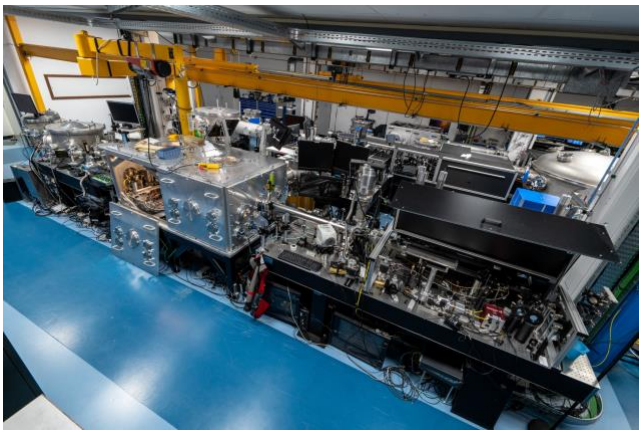

Figure 1. Soft X-ray laser beamline at LOA (Palaiseau, France)

References

[1] Adeline Kabacinski, Fabien Tissandier, Julien Gautier, Jean-Philippe Goddet, Igor Andriyash, Philippe Zeitoun, Stéphane Sebban, Eduardo Oliva, and Michaela Kozlová, Physical Review Research 4 (3), L03200

[2] Adeline Kabacinski, Eduardo Oliva, Fabien Tissandier, Julien Gautier, Michaela Kozlová, Jean-Philippe Goddet, Igor Andriyash, Cédric Thaury, Philippe Zeitoun, Stéphane Sebban, Nature Photonics, 202

* E-mail: stephane.sebban@ensta.fr

Laser-irradiated X-ray sources for X-ray diffraction of dynamically compressed matter on Sandia's Z-Machine

T. Ao*, M. Geissel, K. Fulford, P. Rambo and C. Yang

Sandia National Laboratories, Albuquerque, USA

Experiments on Sandia's Z-Machine have demonstrated the ability to produce dynamically compressed extreme-pressure states of matter with unique uniformity, duration, and size, which are ideal for investigations of fundamental material properties. X-ray diffraction (XRD) is a key material science measurement since it provides direct observation of the compression and strain of the crystal lattice, and is used to detect and identify phase transitions. To characterize phase transitions of dynamically compressed matter, XRD require both sufficient photon energy and fluence to produce data with high fidelity in a single shot. Recently, a novel XRD diagnostic has been implemented on the Z-Machine which enabled probing the phase changes of carbon samples that were dynamically compressed to pressures of 150–320 GPa [1].

Sandia's high-energy laser systems associated with the Z-Machine consist of the nanosecond Z-Beamlet (ZBL) laser and the sub-nanosecond Z-Petawatt (ZPW) laser. While the ZBL laser is currently being used to generate X-rays for the Z-XRD experiments, the ZPW laser is being developed as an X-ray source option for future campaigns. We present our latest data on absolute X-ray yields for mid-Z K-shell emission produced with ZBL and compare them to those produced with ZPW. We found that ZBL is a suitable X-ray driver up to 10 keV (Ge He_α), though the efficiency is very sensitive to pulse energy/intensity at this limit. However, for 15 keV (Zr K_α) X-rays and above, ZPW outperforms ZBL. We will compare the impact of target geometry, surface structure, and observation angle for X-ray generation with ZPW before and after recent improvements to focusability and pulse duration. These results will have important implications for future Z-XRD experiments, especially for high-Z materials.

References

[1] T. Ao, P. Kalita, C. Blada, N. P. Brown, K. Fulford, P. Gard, M. Geissel, H. Hanshaw, M. Montoya, S. Payne, E. Scoglietti, A. Smith, C. S. Speas, J. L. Porter, and C. T. Seagle, Minerals **13**, 1203 (2023).

* E-mail: tao@sandia.gov

Quantum coherence and inner-shell x-ray lasing in XFEL generated NLTE hot and dense plasmas

J. Yuan[1] *, J. Zeng[2] , Y. J. Li[3] , J. Liu[4] , C. Gao[4] , and Y. Q. Li[4]

[1]Institue of atomic and molecular physics, Jilin University, Changchun 130012, China
[2] College of Science, Zhejiang University of Technology, Hangzhou 310023, China
[3] Gradaute School of China Academy of Engineering Physics, Beijing 100193, China
[4] College of Science, National University of Defense Technology, Changsha 410073, China

High bright x-ray free electron laser (XFEL) with photon energy of hundreds to thousands eV can directly ionize the inner shell electrons of atoms, inducing sequential ionization processes such as Auger decay, electron impact excitation, ionization, and electron attachment. Dozens of electrons can be ionized from complex atoms within a few femtoseconds to tens of femtoseconds, resulting in a non-equilibrium plasma containing dozens of ionization stage of ions with exotic electronic configurations and hundreds of eV temperature free electrons [1]. Based on the classical rate equation and the quantum density matrix evolution equation, we have studied the ionization kinetics process and dynamics of gas/solid target [2] and possible atomic x-ray lasing [3,4] on the basis of detailed level accounting model. Based on finite difference and Monte Carlo numerical methods, the numerical calculation program can simulate the evolution process of rate equation containing tens of millions of atomic energy levels, as well as the time-dependent evolution process of density matrix containing thousands of quantum states. The results will demonstrate the precise atomic kinetics and the impact of quantum effects on ionic stage and energy level population evolutions.

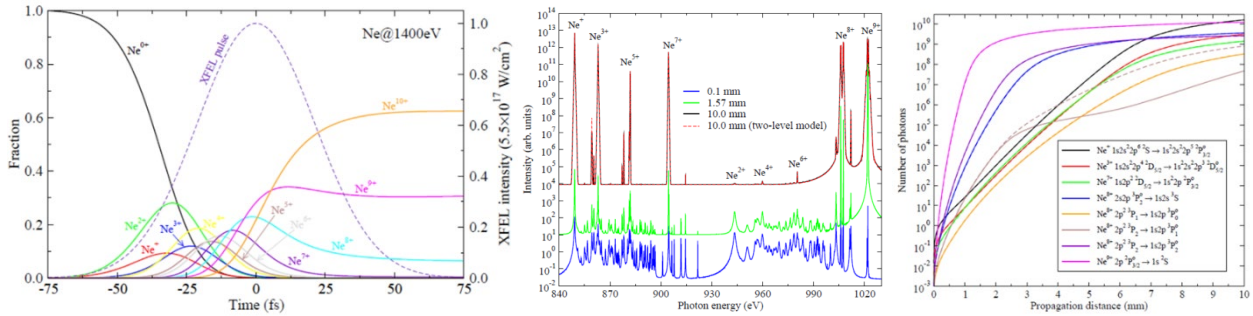

Figure 1. XFEL photoionization pumped Ne atom inner shell lasing amplification. (left) Evolution of different charged Ne ions populations with time, (middle) spectral distribution of emitted x-rays propagating at different distances in a medium, and (right) gain curves of some selected transitions.

References

[1]L. Young et al., Femtosecond electronic response of atoms to ultra-intense X-rays, Nature **466,** 56 (2010)

[2]Cheng Gao, Jiaolong Zeng, Yongqiang Li, Fengtao Jin, and Jianmin Yuan, Versatile code DLAYZ for investigating population kinetics and radiative properties of plasmas in non-local thermodynamic equilibrium, High Energy Density Physics **9,** 583(2013)

[3]Yongqiang Li, Cheng Gao, Wenpu Dong, Jiaolong Zeng, Zengxiu Zhao and Jianmin Yuan, Coherence and resonance effects in the ultra-intense laser-induced ultrafast response of complex atoms, Scientific Reports **6**, 18529(2016)

[4]Jianpeng Liu, Yongqiang Li, Li Wang, Jing Zhao, Jianmin Yuan, and Xiangjin Kong, Coherent control of atomic inner-shell x-ray lasing via perturbed valence-shell transitions, Physical Review A **104**, L031101 (2021)

* E-mail: yuanjianmin@jlu.edu.cn

Diagnosing surface heating in relativistic laser plasma interactions using GISAXS

S.V.Rahul[1], M. Banjafar[1], L. Randolph[2], T.Preston[1], M.Makita[1], J.P. Schwinkendorf[1], O.Oezturk[3], T.Yabuuchi[5], K. Miyanishi[5], M. Nishiuchi[6], M. Ota[7], L.Huang[4], T.Kluge[4], C.Gutt[3], M.Nakatsutsumi[1]

[1] European XFEL GmbH, Holzkoppel 4, 22869 Schenefeld, Germany
[2] Forschungszentrum Jülich GmbH, Wilhelm-Johnen-Straße, 52428 Jülich, Germany
[3] Universität Siegen D-57068 Siegen, Germany
[4] HZDR, Bautzner Landstraße 400, 01328 Dresden, Germany
[5] SACLA, 1-1-1 Kouto, Sayo-cho, Sayo-gun, Hyogo 679-5148, Japan
[6] National Institutes for Quantum and Radiological Science and Technology, 4-9-1 Anagawa, Inage-ku, Chiba-shi 263-8555, Japan
[7] National Institute of Fusion Science, 322-6 Oroshi, Toki, Gifu 509-5202, Japan

High field surface plasmons have recently attracted attention in producing the ultracompact sources electron accelerators and intense XUV sources via High order Harmonic Generation[1]. While these sources allow a diagnosis of the far field of the surface plasmons, an understanding of their transport and the consequent heating in the near field remains challenging. Propagating in a nm thin skin layer on the solid density plasma surface, these surface plasmons present the peculiar problem of requiring a probe with nm depth sensitivity in the solid density region - thus ruling out optical and proton imaging techniques.

Here, we present our results employing Hard X-ray Free Electron Lasers to probe sub-relativistic intensity laser driven solid density plasma surfaces. We irradiate Hard X-ray pulses at Grazing Incidence and monitor the Small Angle X-ray Scattering (GISAXS). This method, previously developed by us for laser ablation studies[2], allows us to obtain sensitivity to nm electron density fluctuations, with a picosecond resolution. We measure the dynamics of electron density correlations due to target neutralization inside a multilayered solid target, at several distances away from the laser irradiation spot. We infer the speed of the lateral heating front to be >0.77c. Finally, we present preliminary measurements of the surface heating due to resonantly generated surface plasmons.

`

References

[1] T. Ceccotti et al. Phys. Rev. Lett. 111, 185001 (2013) ; G. Cantono, Phys. Rev. Lett. 116, 015001(2016) ; A. Macchi, Phys. Plasmas 26, 042114 (2019)

[2] L. Randolph et.al. Phys. Rev. Research 4, 033038 (2022), M. Banjafar et..al., arXiv preprint arXiv:2404.15813 (2024)

* E-mail: sripati.rahul@xfel.eu

NLTE

NLTE-12, Benford's Law for Atomic Databases and All That

Yuri Ralchenko*

National Institute of Standards and Technology, Gaithersburg MD20899, USA

This talk will cover two topics. First, an overview of the 12th non-LTE Code Comparison Workshop that was held in Valladolid, Spain (Oct 2023) will be presented. This meeting was attended by more than 20 researchers who submitted case calculations with 14 different collisional-radiative (CR) codes. The proposed cases included (i) CR and photoionization kinetics and the L-shell emission of Fe for typical astrophysical conditions, (ii) CR kinetics and K-shell emission of Kr in dense plasmas of NIF imploded capsule experiments, and (iii) ionization balance and spectra of Au in hot laser-produced plasmas. We will present comparisons of the submitted data, main conclusions of the meeting, and future plans.

The second part of the talk (in collaboration with J.-C. Pain) will address applications of Benford's law to atomic spectra and opacity databases [1]. This intriguing, and yet not fully understood, law of anomalous numbers states that the significant digits of data follow a logarithmic distribution favoring the smallest values. We will discuss the compliance with this law of the atomic databases focusing on (i) line energies, oscillator strengths, and Einstein coefficients from the NIST Atomic Spectra Database [2] and (ii) radiative opacities from the NIST-LANL Lanthanide Actinide Opacity Database [3].

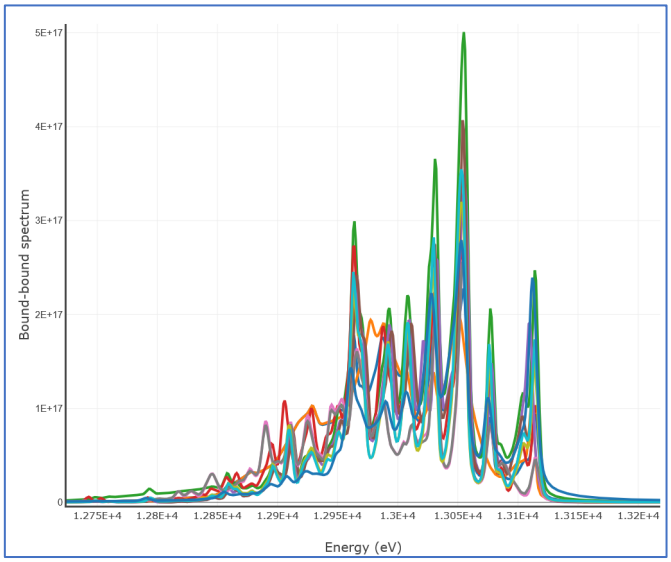

Figure 1. NLTE-12: Comparison of the bound-bound Kr spectra at 2000 eV and 3×10^{24} cm^{-3}.

References

[1] J.-C. Pain and Yu. Ralchenko, *J. Quant. Spectr. Rad. Transf.* **322**, 109010 (2024).

[2] URL https://www.nist.gov/pml/atomic-spectra-database.

[3] URL https://nlte.nist.gov/OPAC/.

* E-mail: yuri.ralchenko@nist.gov

Testing High Density XSTAR models with Fe Photoionized Plasma Experiments on Z

Patricia Cho[1*], Guillaume Loisel[2], Jim Bailey[2], Dan Mayes[1], Isaac Huegel[1], Taisuke Nagayama[2], Chris Fontes[4], Stephanie Hansen[2], Tim Kallman[3], Javier Garcia[5], Roberto Mancini[6]

[1]Lawrence Livermore National Laboratory, Livermore, CA, USA
[2]Sandia National Laboratories, Albuquerque, NM, USA
[3]NASA Goddard Space Flight Center, Greenbelt, MD, USA
[4]Los Alamos National Laboratories, Los Alamos, NM, USA
[6] University of Nevada Reno, Reno, NV, USA

The Z-machine at Sandia National Laboratories generates powerful X-ray radiation fluxes. This enables experiments to produce and study macroscopic quantities of matter at extreme conditions. Astronomers use spectra collected with satellite telescopes to construct models for the behavior of accretion powered plasmas around black holes in both active galactic nuclei and X-ray binaries. However, complex models for these radiation dominated non-Local-Thermodynamic-Equilibrium (NLTE) photoionized plasmas are mostly untested with laboratory data. A novel platform developed on the Z-machine for expanding-foil photoionized plasma experiments opens a new regime for benchmark measurements of NLTE photoionized plasmas. The data from these experiments reveal difficulties in modeling both emission intensities and the level of ionization in the plasma. Such data have been a laboratory astrophysics goal for two decades but are even more critical now because of the "Super-Solar" iron abundance problem. Iron abundances inferred from X-ray spectra emitted by photoionized plasma in many accretion disks around black holes appear to contain 5-20 times more iron than the Sun. This contradicts the widely held expectation that most objects in the universe have metallicities that are at most, only slightly larger than Solar. One prevailing theory is that effects of high electron density are not properly accounted for in the models. Reinterpreting astrophysical X-ray spectra with updated high density models resolved some of the discrepancy. However, much of the discrepancy remains along with a key question: do spectral models of photoionized plasmas accurately account for X-ray emission? I will describe my progress in using this dataset to inform the Super-Solar iron abundance problem and discuss the broader potential to evaluate model accuracy.

This work was performed under the U.S. Department of Energy LRGF Contract No. DE-NA0003960, WCAPP Contract Nos. DE-NA0003843 & DE-NA0004149, Sandia Contract No. DENA0003525, LANL contract 89233218CNA000001, and LLNL Contract No. DE-AC52-07NA27344.

References

[1] García et al., Mon. Not. R. Astron. Soc. **462**, 751 (2016).

[2] Heeter, et al., Review of Scientific Instruments **72**, 1224 (2001).

[3] Jiang et al Mon. Not. R. Astron. Soc. **484**, 1972 (2019).

[4] Loisel et al., Phys. Rev. Lett. **119**, 075001 (2017).

*E-mail: cho32@llnl.gov

ASTROPHYSICS

Structure of High Velocity Radiative Shocks from optically Thin to Thick

M. Koenig[1], D. Oportus[1], Y. Benkadoum[1], N. Ozaki[2,3], Y. Sakawa[3], K. Maeda[3], Y. Suzuki[3], M. Hanano[3], S. Orlando[4], A. Dearling[5], S. Yakura[6], R. Yamazaki[6], G. Rigon[7], C. Li[7], B. Albertazzi[1]

[1] LULI - CNRS, CEA, Sorbonne Universités, Ecole Polytechnique, Institut Polytechnique de Paris
[2] Graduate School of Engineering, Osaka University
[3] Institute of Laser Engineering, Osaka University
[4] INAF — Osservatorio Astronomico di Palermo
[5] York Plasma Institute, University of York
[6] Department of Physical Sciences, Aoyama Gakuin University
[7] Massachusetts Institute of Technology, Plasma Science and Fusion Center

In astrophysics, many phenomena involving strong radiative shocks (RS) disturb and inject energy into the interstellar medium, affecting the rate of star formation in galaxies. For instance, the compression and disturbance of the interstellar gas caused by shocks from supernova explosions can trigger the collapse of nearby molecular clouds, initiating the formation of new stars. Therefore, the interaction of strong radiative shock waves with other structures is a central problem in astrophysics. Moreover, magnetic fields play an important role additionally to radiation for example in protogalaxies giving rise to globular clusters. It also can stabilize thermal instability with a transverse magnetic field. Recent results of radiative shock (and their interaction with an obstacle) experiments on laser facilities are shown where we have measured many of the variables involved such as shock velocity, radiative precursor length and temperature, ablation of an obstacle by the radiation, shock generated in the obstacle after shock impact. We studied the transition between an optically thin medium (low xenon gas pressure) to optically thick (high xenon gas pressure) and observed a huge difference in the shock and radiative precursor length. In the meanwhile, we performed 2d numerical investigations using FLASH code when an external B field is present as it intervenes in the astropohysical situation. In the case of radiative magnetised shock, we do observe the generation of a magnetosonic wave ahead of the RS for a B field perpendicular to the shock propagation. Discussion on the impact in astrophysics will be presented.

* E-mail: michel.koenig@polytechnique.edu

Helioseismic inference of the solar radiative opacity

G. Buldgen[1 *], J. C. Pain[2,3], P. Cossé[2,3], A. Pradhan[4], C. Blancard[2,3], F.Gilleron[2,3], C.J. Fontes[5], J.Colgan[5], A. Noels[1]

[1]Star Institute, Université de Liège, Belgique
[2]CEA, DAM, DIF, F-91297 Arpajon, France
[3]Université Paris-Saclay, CEA, LMCE, F-91680 Bruyères le Châtel, France
[4]Dept. Astronomy,Ohio State University, Columbus, OH, 43210, USA
[5]Los Alamos National Laboratory, Los Alamos, NM, 87545, USA

The Sun is the most studied of all stars and constitutes a benchmark for stellar models. However, our vision of the Sun is still incomplete, as illustrated by the current debate on its chemical composition [1,2]. The problem reaches far beyond chemical abundances and is intimately linked to microscopic and macroscopic physical ingredients of solar models such as radiative opacity (see e.g. [3] for a review), for which experimental results have been recently measured that still await theoretical explanations. We present for the first time opacity profiles derived from helioseismic inferences and compare them with detailed computations of individual element contributions using four different opacity codes (OPAS, OP, SCO-RCG and OPLIB) in a complementary way to experimental results. We find that our seismic opacity is ~10% higher than theoretical values used in current solar models around 2 million degrees, but lower by 35% than some available theoretical values (See Figure 1 below). Using the Sun as a laboratory of fundamental physics [4], we show that quantitative comparisons between various opacity tables are required to understand the origin of the discrepancies between reported helioseismic, theoretical and experimental opacity values.

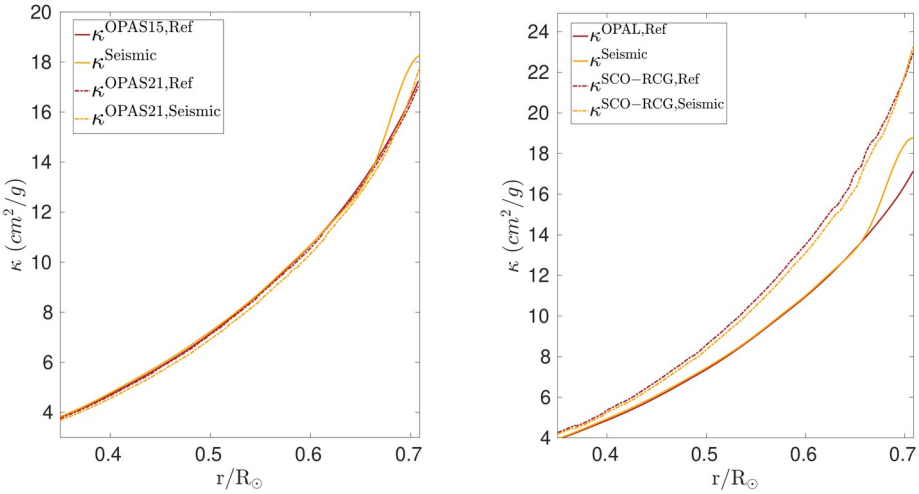

Figure 1. Comparison of the mean Rosseland opacity profiles of solar models, seismic reconstruction and theoretical computations for the thermodynamical. *Left panel:* Opacity profiles from evolutionary computations with 2015 OPAS tables (brown-plain line), from seismic reconstruction (orange-plain line), and from detailed computations with the OPAS code for both model and seismic thermodynamical paths (brown and orange dashed lines, respectively). *Right panel:* Opacity profiles for evolutionary computations using OPAL tables (brown-plain line), from seismic reconstruction (orange-plain line) and from detailed SCO-RCG computations for both model and seismic thermodynamical paths (brown and orange dashed lines, respectively).

References

[1] Asplund, M., Amarsi, A.M. Grevesse, N., A&A. **653**, id.A141 (2021).
[2] Magg. E., et al. A&A. **661**, id.A140 (2022).
[3] Christensen-Dalsgaard, J. Living Reviews in Solar Physics, **18**, Issue 1, article id.2 (2021)
[4] Buldgen, G. et al., accepted for publication in Nature Communications (2024)

* E-mail: gbuldgen@uliege.be

DENSE PLASMAS-I

Interogating the population kinetics in dense plasmas using X-ray Free Electron Laser resonant photopumping

E. Galtier[1]*, F. Condamine[2], E. Cunningham[1], G. Dyer[1], L. Gournay[3], M. Greenberg[1], P. Heimann[1], D. Khaghani[1], H. J. Lee[1], A. McKelvey[6], B. Nagler[1], Y. Ralchenko[7], O. Renner[2,8], F. B. Rosmej[3,4], J. Seely[9], R. Shepherd[6]

[1]SLAC National Accelerator Laboratory, Menlo Park, USA [2]The Extreme Light Infrastructure ERIC, ELI Beamlines Facility, Dolní Břežany, Czech Republic [3]Sorbonne University, Faculty of Science and Engineering, Paris, France [4]LULI, Ecole Polytechnique, CEA-CNRS-SU, Palaiseau, France [6]Lawrence Livermore National Laboratory, USA [7]National Institute of Standards and Technology, USA [8]Institute of Plasma Physics, Czech Academy of Sciences, Prague, Czech Republic [9]Artep Inc., Maryland, USA

Atomic physics can provide unique information on the detailed processes at play during the evolution of a plasma [1]. However, it suffers critical issues when invetigated in dense plasma conditions, where reabsorption, opacities and/or broadening mechanisms prevent its precise investigation (e.g. [2]). Fifteen years ago, when X-ray Free Electrons Lasers (X-ray FELs) first emerged as user facilities, they allowed breakthrough studies of some key elements of dense plasmas (e.g. opacity [3, 4], continuum lowering [5], population kinetics [6]). Still, because the X-ray pump and the X-ray probe are coupled, the available plasma conditions to be reached are limited in temperature and density space (due to the limited peak intensity an X-ray FEL can reach) as well as time scales (due to the X-ray pulse duration). In this work, we have investigated the population kinetics of a laser-driven modestly-dense copper plasma via X-ray FEL resonant photo-pumping. While we start by presenting on known state-of-the-art full scale analysis of its kinetics, with 3D hydrodynamic simulations coupled to detailed collisional radiative modeling, the emission spectra obtained during this experiment are found to be remarquably similar to fundamental atomic physics spectra obtained from relatively simple atomic physics code only. This work sheds light on the ability to use X-ray FELs to interogate the detailed atomic physics even in the hot and dense plasmas found in fundamental laser/matter interaction or in plasmas relevant to inertial confinement fusion experiments.

References

[1] D. Mihalas *et al.*, Foundations of radiation hydrodynamics, New York, Oxford University Press, 731 p., (1984)

[2] J. E. Bailey *et al.*, Nature, 7532, 56–59, **517**, (2015)

[3] O. Ciricosta *et al.*, Phys. Rev. Lett., **109**, 6, 065002, 4 (2012)

[4] T. R. Preston *et al.*, Phys. Rev. Lett., **119**, 8, 085001, 5 (2017)

[5] S. Vinko *et al.*, Nature, **482**, 59 EP (2012)

[6] E. Galtier *et al.*, Phys. Rev. Lett., **106**, 16, 164801, 4, (2011)

*E-mail: egaltier@slac.stanford.edu

Population Kinetics for Laser Plasma Interactions

B.E. Marré [1]*, A. Huebl [2], M. Bussman [1,3], U. Schramm [1], R. Widera [1], T. Cowan [1], T. Kluge [1]

[1]HZDR, Dresden, Germany [2]Berkley National Lab, Berkley, USA [3]CASUS, Görlitz, Germany

Standard atomic physics models in Particle-In-Cell(PIC) simulations either neglect excited states, predict atomic state populations in post processing only, or assume quasi-thermal plasma conditions.

This is no longer sufficient for high-intensity laser plasma interactions such as direct-drive ICF and laser plasma accelerators, due to their non-equilibrium, transient and non-thermal plasma conditions, which are now accessible in XFEL experiments at HIBEF (EuropeanXFEL), SACLA (Japan) or at MEC (LCLS/SLAC).

To remedy this, we have developed FLYonPIC, a extension of the PIC code PIConGPU, to self-consistently and time-dependent model atomic population kinetics inline in PIC-Simulations, in transient plasmas and without assuming equilibrium or steady state temperatures.

This new approach to atomic physics modeling will be useful in predicting plasma emission prediction, plasma condition probing with XFELs and better understanding of isochoric heating processes, all relying on an accurate prediction of atomic state populations inside transient plasmas.

I will show comparisons of FLYonPIC-PIConGPU, SCFLY, and ground state only PIC simulations for different plasma conditions relevant to ICF and laser plasma accelerators.

*E-mail: b.marre@hzdr.de

Ionization and temperature measurements in warm dense copper using x-ray absorption spectroscopy

T. Cordova[1,2†], E. V. Marley[2], D. Chin[3], T. Döppner[2], R. A. London[2], M. K. G. Kruse[2], H. A. Scott[2], F. N. Beg[1], F. Coppari[2], J. Emig[2], S. B. Hansen[4], C. C. Kuranz[5], M. Millot[2], P. Nilson[3], M. P. Springstead[5], P. Sterne[2], and M. J. MacDonald[2]

[1]*University of California San Diego, San Diego, CA, USA*
[2]*Lawrence Livermore National Laboratory, Livermore, CA, USA*
[3]*Laboratory for Laser Energetics, University of Rochester, Rochester, NY, USA*
[4]*Sandia National Laboratories, Albuquerque, NM, USA*
[5]*University of Michigan, Ann Arbor, MI, USA*

Warm dense matter exists at temperatures of order 10 eV and a few times solid density, where the complex balance of collective and quantum effects precludes standard approximations used in plasma physics or condensed matter physics. Understanding ionization in the warm dense matter regime, in particular, is an active area of research requiring additional experimental data to benchmark and improve current predictive capabilities. In this study, we present the experimental results and analysis of K-shell x-ray absorption spectra to infer temperature and ionization state distribution of copper uniformly heated to temperatures 10–30 eV and compressed to densities of 9–30 g/cm^3. The experiments were conducted at the OMEGA laser facility using a buried layer of copper tamped by plastic on both sides. The two sides were then irradiated by a symmetric laser pulses and probed by a laser-generated x-ray source. Experimental results are compared to collisional-radiative models where we find large discrepancies in the predicted x-ray absorption spectra at these conditions. We also explore the role of including density effects in the underlying atomic data used in the collisional-radiative models and compare the results to our experimental data.

This work was performed under the auspices of the U.S. Department of Energy by Lawrence Livermore National Laboratory under Contract DE-AC52-07NA27344 and was supported by the LLNL-LDRD Program under Project No. 22-ERD-005. SNL is managed and operated by NTESS under DOE NNSA contract DE-NA0003525.

†Corresponding Author Email: tcordova@ucsd.edu

Influence of two-temperature effect on the ionization potential depression in hot dense plasma

Qingbo Luo[1], **Yong hou**[1 *], **Cheng Gao**[1], **and Jianmin Yuan**[1,2]

[1]College of Science, National University of Defense Technology, Changsha Hunan 410073, People's Republic of China;
[2]Institute of Atomic and Molecular Physics, Jilin University, Changchun Jilin 130012, People's Republic of China

The interaction between charged particles in hot dense plasma will cause ionic energy level shift and broadening, resulting in reduction of ionization potential, which alter the electronic structures and physical properties of hot dense plasma, such as opacity and equation of state. The experiment~(O. Ciricosta, et al. Nat. Commun. 7:11713)~on ionization potential depression (IPD) of solid-density Al plasma have indicated that present theoretical models cannot give reasonable desciption of the IPD in hot dense plasma, especially for highly charged ions where the discrepancy between experiment and theory is even greater. The reasonable theoretical methods are needed to describe the effects of dense environments on IPD, and the process of generating hot dense plasmas through the interaction between ultrashort laser pulse and solid-density matter also needs to be carefully considered. Here, the electronic structure is computed by the modified flexible atomic code~(FAC), which has included the correlations of free electrons and other ions by correlaiton functions from the hypernetted chain (HNC) approximation. A self-consistent-field method is used to calculate the electronic structures, and the temperatures for electron and ion in hot dense plasma are considered, seperately. Based on the calculations, the IPD is obtained through two-step model. Considering the interaction of the femeto-second laser on the solid-density Al plasma of Circosta's experiment, we use the two-temperature model to calculate the IPD with increasing the ionic temperature. The theoretical results are good agreement with the experimental results.

References

[1] O. Ciricosta, S.M. Vinko, B. Barbrel, et al., Measurements of continuum lower ing in solid-density plasmas created from elements and compounds, Nature communications 7, 11713 (2016)

[2] P. Zhang, Y. Jin, X. Zan, P. Liu, Y. Li, C. Gao, Y. Hou, J. Zeng, and J. Yuan, Enhancement of electron-impact ionization induced by warm dense environments, Physical Review E 104, 035204 (2021).

* E-mail: yonghou@nudt.edu.cn

MAGNETIZED PLASMAS

Tungsten VUV spectroscopy in WEST tokamak 1-4 keV plasmas

R. Guirlet[1*], C. Desgranges[1], O. Peyrusse[2], N. Saura[3], J. L Schwob[4], P. Mandelbaum[4,5]

[1]CEA, IRFM, F-13108 Saint-Paul-lez-Durance, France
[2]Aix-Marseille Université, CNRS, Laboratoire LP3, UMR7341, 13288 Marseille, France
[3]Aix-Marseille Université, CNRS, Laboratoire PIIM, UMR7345, 13288 Marseille, France
[4]Racah Institute of Physics, Hebrew University of Jerusalem, Jerusalem, Israel
[5]Jerusalem College of Engineering, Ramat Beth Hakerem, 91035 Jerusalem, Israel

Since Tungsten (W) was chosen as the plasma-facing material in the future tokamak ITER, several magnetic fusion devices have been equipped partly (JET) or entirely (ASDEX-Upgrade) with W components. Among them, the WEST tokamak has a prominent place because of its capability to sustain 2-5 keV plasma discharges for minutes in a complete W environment.

WEST is equipped with two extreme UV spectrometers, one of which provides a wide variety of measurements thanks to its versatility. It covers the range 5-340 Å with two mobile detectors, each viewing a narrow interval (~20 Å at 15 Å, 60 Å at 310 Å) and a spectral resolution of ~0.2 Å. Its single line of sight can scan the lower half of the plasma with a minimum period of 4 s.

Spectra measured with this spectrometer are very complex due to the large number of spectral structures emitted by W. We have undertaken an extensive work of spectral line assignment using the HULLAC code and the NIST atomic database [1]. W^{25+} to W^{45+} ionisation stages have been identified. From four spectral lines from the higher stages we estimate the W density profile in the core plasma provided the electron temperature is high enough [2].

The strong and broad quasicontinuum (QC) at 45-65 Å has been extensively observed in magnetic fusion devices [3]. It has been attributed to W^{28+}-W^{45+} with additional lines from various ionisation stages. Up to now collisional-radiative modelling has not allowed to reproduce it in a satisfactory way, which suggests that the atomic structure of W or the radiative transitions and their probabilities are not well understood. A semi-statistical approach used in dense plasmas [4] has been applied with encouraging results, concerning both the ionisation degree of W and the quasicontinuum itself.

Given the complexity of this spectral feature, in parallel we have recently started to use artificial intelligence (AI) tools to investigate the relation between the spectral shape of the QC and the thermodynamic profiles of the plasma, in particular the electron temperature. The first step is to establish a relation between the spectrum and the maximum temperature along the line of sight. We have found that the temperature can be predicted with a very satisfactory accuracy (± 50 eV) in a boad range (300-3500 eV) if the AI algorithm is trained with plasma discharges performed on the same day. Plasma discharges performed several days from each other do not provide good results, possibly due to the changing vessel status. The next step is to investigate the possibility of extracting the whole temperature distribution from the QC analysis.

References

[1] Kramida, A. et al., NIST Atomic Spectra Database, online https://physics.nist.gov/asd , National Institute of Standards and Technology, Gaithersburg, MD. DOI: https://doi.org/10.18434/T4W30F
[2] Guirlet R. et al., Plasma Phys. Control. Fusion 64 (2022) 105024, DOI: https://doi.org/10.1088/1361-6587/ac8d2c
[3] Harte C. S. et al., J. Phys. B 43 (2010) 205004, DOI: 10.1088/0953-4075/43/20/205004
[4] Bauche J. et al., Atomic Properties in Hot Plasmas, Springer, 2015

*Email: remy.guirlet@cea.fr

Spectroscopic characterization of compressed core conditions in directly-driven magnetized cylindrical implosions

R. Florido[1 *], A. Bordón[1], M. A. Gigosos[2], G. Pérez-Callejo[2], M. Bailly-Grandvaux[3], C. A. Walsh[4], F. Beg[3], R. C. Mancini[5], C. McGuffey[6], J. Saret[3], F. Suzuki-Vidal[7], C. Vlachos[8], J. J. Santos[8]

[1]Departamento de Física, Universidad de Las Palmas de Gran Canaria, Las Palmas de Gran Canaria, Spain
[2]Departamento de Física Teórica, Atómica y Óptica, Universidad de Valladolid, Valladolid, Spain
[3]Center for Energy Research, University of California San Diego, California, USA
[4]Lawrence Livermore National Laboratory, California, USA
[5]Department of Physics, University of Nevada, Reno, USA
[6]General Atomics, California, USA
[7]First Light Fusion, Oxfordshire, United Kingdom
[8]Centre Lasers Intense et Applications, Universitè de Bordeaux, CNRS, CEA, Bordeaux, France

The application of external magnetic fields in inertial confinement fusion (ICF) implosions has been identified as a method to enhance hot-spot performance, reducing thermal losses and enabling higher fusion yields. To facilitate the investigation of the magnetic-field compression mechanism, a cylindrical geometry is particularly appropriate. This works discusses the use of Ar K-shell spectroscopy to characterize the core conditions in magnetized cylindrical implosion experiments conducted at the OMEGA laser facility. The targets, filled with Ar-doped deuterium, were symmetrically imploded using a 40-beam, 14.5 kJ, 1.5 ns laser drive. Recorded space- and time-integrated Ar K-shell spectra exhibit highly reproducible, distinctive features both with and without an imposed magnetic field. A uniform spectroscopic model was insufficient to replicate the observations; however, a multizone spectroscopic model, combined with a random-search χ^2 minimization procedure, successfully fitted the experimental spectra. The analysis allows to extract intensity-weighted average conditions of the cylindrical imploded core, namely revealing a 50% core temperature rise at half mass density when a 30 T seed B-field was applied. Additionally, the methodology shows potential for deriving a coarse-grained radial profile of core conditions at stagnation, supporting the formation of a hotter central spot in the magnetized scenario. Concurrently, the experimental spectra align well with synthetic spectra obtained by post-processing extended-magnetohydrodynamics simulations, incorporating detailed atomic-kinetics and Stark-broadened line shapes. This provides strong evidence that the attained core conditions at peak compression are consistent with the impact of a 10-kT compressed field.

References

[1] M. Bailly-Grandvaux *et al.*, Phys. Rev. Research **6**, L012018 (2024).

* E-mail: ricardo.florido@ulpgc.es

DENSE PLASMAS-II

Scattering of ultrashort X-ray pulses in optically dense plasma: account for pulse duration and propagation effects

F.B. Rosmej[1,2*], V.A. Astapenko[3] and V.S. Lisitsa[3,4]

[1] Sorbonne University SU, Faculty of Science and Engineering, Paris, France
[2] Ecole Polytechnique, LULI, Palaiseau, France
[3]Moscow Institute of Physics and Technology MIPT, Dolgoprudnyi, Russia
[4]National Research Center "Kurchatov Institute", Moscow, Russia

Scattering of electromagnetic radiation in media is an important experimental tool to obtain information about the properties and state of matter. Recent advances in generating ultrashort laser pulses (USP) open perspectives of sub-femtosecond scattering processes. For ultra-short electromagnetic fields the scattering differs considerably from the standard long-pulse theory. One of the interesting properties is associated with the interaction of ultrashort pulses with dense matter: here, the short pulse propagation is characterized by possible resonance processes in the optically dense medium due to the large width of the frequency spectrum.

We consider a semi-analytical approach [1] that overcomes the failure of Fermi's Golden Rule in the description of the ultra-short photoprocess but maintains the possibility to employ cross sections (note, that the complex numerical solution of the time-dependent Schrodinger equation makes it difficult to employ measured cross sections). A central element of this approach is the probability induced by USP during all time of pulse action:

$$W(\tau)=\frac{c}{(2\pi)^2}\int_0^\infty \frac{\sigma(\omega)}{\hbar\omega}\left|E(\omega,\tau)\right|^2 d\omega. \tag{1}$$

$\sigma(\omega)$ is the cross section of the photoprocess and $E(\omega,\tau)$ is the Fourier transform of electric field strength in the pulse, τ is the pulse duration. This approach has been used [2] for the study of femtosecond X-ray pulse driven resonance scattering on ions in plasmas. It was shown particularly that the dependence of the scattering probability on the pulse duration can be nonlinear for certain values of pulse parameters even if the radiation intensity is small (1st order perturbation theory). The approach was generalized to account for the dependence on the pulse propagation length in optically dense hydrogen plasmas [3].

In the present work we account for the absorption of USP in optically dense hot plasmas employing the integral expression for the scattering probability:

$$W_{scat}(\tau,z)=\frac{c}{(2\pi)^2}\int_0^\infty \frac{\sigma_{scat}(\omega)}{\hbar\omega}\left|E(\omega,\tau)\right|^2 \exp\left[-N\sigma_{abs}(\omega)z\right]d\omega. \tag{2}$$

$\sigma_{scat}(\omega)$ and $\sigma_{abs}(\omega)$ are the scattering and absorption cross sections, respectively, N is the density of the scattering ions, z is the propagation length of the USP in the plasma. This expression allows to consider two new fundamental parameters in dense plasmas: (i) the ratio of the spectral resonance line width and the width corresponding to the pulse duration, (ii) the optical thickness of the medium.

Numerical calculations of the scattering probability (2) have been carried out for femtosecond USP resonance scattering on highly charged ions in hot dense plasmas with account for the fine structure splitting of the ionic energy levels and the Doppler effect. The dependencies of the scattering probability on pulse duration and propagation length were analyzed for different ionic charges at temperatures of about 100 eV and densities 10^{21}-10^{23} cm^{-3}. We also examine the influence of the pulse duration τ and plasma length z on the spectrum of the USP scattering probability for various ions. The analysis allows to explore the main features of USP scattering in dense hot plasmas.

* E-mail corresponding author: frank.rosmej@sorbonne-universite.fr

References

[1] V.A. Astapenko, Phys. Lett. A **374**, 1585-1590 (2010).

[2] F.B. Rosmej, V.A. Astapenko, V.S. Lisitsa, N.N. Moroz, Phys. Lett. A **381**, 3576-3579 (2017).

[3] A. Calisti, V.A. Astapenko, V.S. Lisitsa, Contr. Plasma Phys. **57**, 414-420 (2017).

Toward electron temperature profiles in hot-dense plasmas from x-ray spectral ensembles

B. F. Kraus[1 *], S. P. McPoyle[1], K. Atay[1], E. Kriz[2], R. C. Hollinger[3], S. N. Benjamin[4], S. Malko[1], Lan Gao[1], P. C. Efthimion[1], Shoujun Wang[3], J. King[3], S. Zahedpour Anaraki[3], V. N. Shlyaptsev[3], and J. J. Rocca[3]

[1]Princeton Plasma Physics Laboratory, Princeton University, Princeton, New Jersey, USA
[2]McGill University, Montreal, Quebec, Canada
[3]Colorado State University, Fort Collins, Colorado, USA
[4]Mercer County Community College, West Windsor, New Jersey, USA

High repetition rate laser systems enable new strategies for diagnosing plasma behavior with large datasets. We define an ensemble technique that relies on randomized targeting of x-ray tracer micro-stripes. On each shot, a high-intensity laser pulse is focused on a solid target with Ti tracer stripes embedded in an Al foil, randomly targeting a micro-stripe, a portion of a stripe, or a gap between stripes. High-resolution, time-integrated x-ray spectrometers capture line emission from the portion of the micro-stripe that is heated to sufficiently high electron temperatures. Accumulation of many such cases is used to construct ensemble distributions of x-ray line intensities that encompass all relative offsets of the laser focus to the micro-stripe centers. Synthetic intensity distributions are likewise generated using collisional-radiative modeling. Bayesian fitting of modeled to measured intensity distributions establishes the most likely radial temperature profiles, enabling comparison to hydrodynamic models and calling into question the cylindrical symmetry of these micro-stripe-embedded systems [1]. Ensemble techniques have significant potential for high-energy-density plasma diagnostics, especially with the advent of high repetition rate experiments.

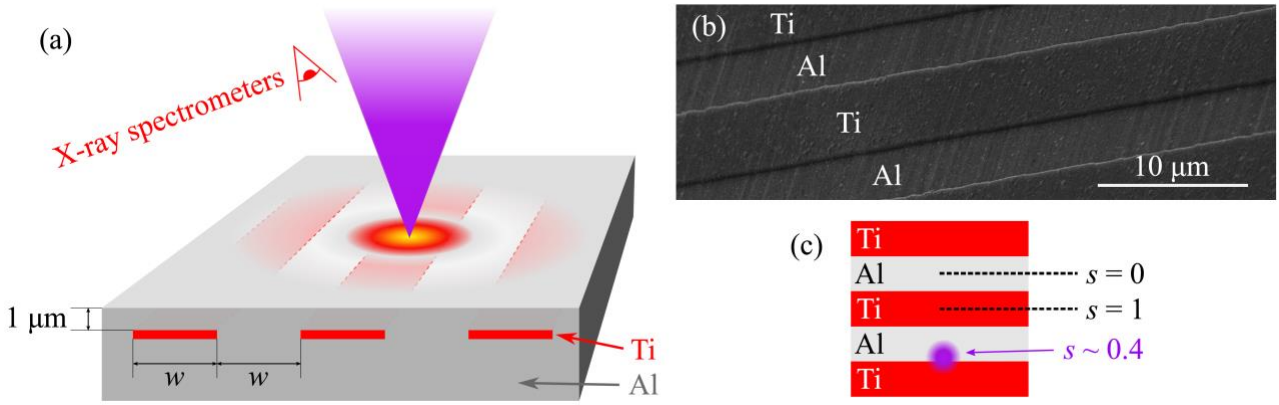

Figure 1. Schematic of micro-stripe layout. (a) A cartoon showing the laser focusing above embedded micro-stripes. (b) An electron microscope image of untamped Ti stripes deposited on Al. (c) An indication of *s*, the relative alignment of the laser focus with a stripe center, which randomly varies between 0 and 1.

References

[1] B. F. Kraus et al., submitted to Phys. Plasmas (2024).

* E-mail: fkraus@pppl.gov

Line shifts induced by plasma screening in x-ray heated matter

M. Šmíd

[1] Helmholtz Zentrum Dresden Rossendorf, HZDR, Dresden, Germany

The electronic structure of ions in dense plasma is influenced by changes in the microscopic electric fields, a phenomenon referred to as plasma screening. In our study, we have experimentally measured plasma screening by observing energy shifts in bound-bound transitions induced by an x-ray free electron laser (XFEL). This was achieved by identifying the specific electronic configurations corresponding to the Kα, Kβ, and Kγ lines of copper heated to roughly 100 ev. Our findings provide a foundation for refining plasma screening models, incorporating related effects such as ionization potential depression and continuum lowering, thereby enhancing our understanding of atomic physics within the Warm Dense Matter regime.

[*] E-mail: m.smid@hzdr.de

Ionisation equilibrium in dense carbon and beryllium plasmas

Dirk O. Gericke*

Centre for Fusion, Space and Astrophysics, Department of Physics, University of Warwick,
Coventry CV4 7AL, United Kingdom

Ionisation is central in defining many radiative and transport quantities in dense plasmas. For plasmas with pressures in the Mega- and Gigabar range, models tend to deviate significantly even for light elements which puts large uncertainties on any calculation relying on inputs for the ion charge state. Moreover, the few experimental results available deviate also significantly from often-used models for the ionisation degree. This situation gets even more complicated as the charge state is not well a defined quantity in dense media and one has to be careful when comparing models and experimental results.

This contribution will review the recent experimental results and compare them with predictions from a variety of theoretical approaches. The focus will be on light elements, that is carbon and beryllium, where the degree of K-shell ionisation is the most relevant question. These elements have been probed at the extreme pressures using the National Ignition Facility [1, 2] and large deviations from standard descriptions [3] have been found while the data agree with results from DFT-MD simulations [4]. Both experiments and *ab initio* simulations show also a different trend with increasing density and pressure than the standard models. This deviation can't be explained by a different model for the ionisation potential depression. Details of this comparison as well as details of the extraction of the mean ion charge states from the X-ray scattering data and possible sources of uncertainties will be discussed. One possible source for the different trends in charge state distributions at high pressures can be the distribution of local environments for the ions with allows for an additional spread of the charge states of ions. The significance of these results for astrophysics and inertial confinement fusion will be briefly highlighted at the end.

References

[1] D. Kraus et al., Phys. Rev. E **94**, 011202(R) (2016).

[2] T. Döppner et al., Nature **618**, 270 (2023).

[3] J.C. Stewart & K.D. Pyatt, Astrophys. Journal **144**, 1203 (1966).

[4] M. Bethkenhagen et al., Phys. Rev. Res. **2**, 023260 (2020).

*D.Gericke@warwick.ac.uk

POSTERS/ASTRO

Photoionized plasma experiments at NIF driven by a long-duration x-ray drive

R. C. Mancini[1], J. J. Rowland[1], A. Peterson[1], R. Heeter[2], R. London[2], P. Cho[2], Y. P. Opachich[2], T. Perry[2], M. Hohenberger[2], H.M. Johns[3]

[1] Physics Department, University of Nevada, Reno, Nevada, US
[2]Lawrence Livermore National Laboratory, Livermore, California, US
[3]Los Alamos National Laboratory, Los Alamos. New Mexico, US

A new experimental platform has been established at the NIF laser facility in which a plastic-tamped iron-magnesium sample is driven by two gold-halfraum x-ray sources characterized by a bright and broadband x-ray flux with a sustained radiation temperature of 180eV for 12ns. The x-ray flux produces and sustains a photoionized plasma populated with magnesium K-shell and iron L-shell ions. The suite of diagnostics includes DANTE to monitor the performance of the radiation source, gated x-ray imaging to observe the expansion of the photoionized iron-magnesium plasma and thus extract the density, and two OPSPEC x-ray spectrometers equipped with elliptically bent KAP crystals to record self-emission and transmission spectra from iron and magnesium ions to characterize charge state distribution, temperature, and plasma emissivity and opacity. We discuss the measurements obtained in two experimental campaigns performed at the NIF, data interpretation and analysis, and the application of the data to benchmark astrophysical models and codes employed in the analysis of x-ray astronomy observations.

This work is supported by DOE NNSA grant DE-NA0004038, and the NIF Discovery Science Program of LLNL.

* E-mail: rcman@unr.edu

Magnetized radiative Shocks: their role in global evolution of the interstellar medium

D. Oportus[1 *], A. Triantafyllidis[1], J-R Màrques[1], F. Lefevre[1], C. K. Li[2], T. Michel[1], S. Orlando[3], C. A. J. Palmer[4], G. Rigon[2], N. Vanderloo[2], M. Koenig[1], B. Albertazzi[1]

[1] LULI, Sorbonne Université, CNRS, CEA, École Polytechnique, Institut Polytechnique de Paris, Paris, France
[2] Plasma Science and Fusion Center, Massachusetts Institute of Technology, Cambridge, Massachusetts 02139, USA
[3] INAF - Osservatorio Astronomico di Palermo, Piazza del Parlamento 1, Palermo 90134, Italy
[4] School of Maths and Physics, Queen's University Belfast, Belfast, UK

Radiative Shocks (RS) can be found in many astrophysical scenarios [1,2], injecting energy into the interstellar medium (ISM) and having an important impact on a multitude of phenomena. Furthermore, recent astronomical observations highlight the role of magnetic fields shaping these interactions [3], making them an essential part of understanding the many related processes. However, as the shocked structure becomes optically thick, giving its own radiation [4], quantitative data is hard to obtain. Thus, it becomes essential to study RS in laboratory. Under this context, experiments at high-power laser facilities confirms the impact of radiation effects [5] over the structure, dynamics and properties of the system [6], but until now the influence of magnetic fields in RS has not been study experimentally in detail. Hence, including those effects in this framework is essential.

In our work, carry out in LULI2000 facility, we generated a strong shock into a solid multi-layer target drive by two lasers beams (2ω, 400-600J, 1.5ns FWHM each one) that produced a high RS in a gas cell filled with xenon at different initial pressures. An external pulsed B-field up to 21T is added. The main diagnostics were a combination of visible interferometry, spectroscopy and optical emission, which allowed us to estimate crucial parameters as electron density, radiative precursor length and shock velocity. In this poster we will present preliminary experimental analysis aims to show how depending of the orientation and amplitude of the B-field the RS structure was modified, having an impact on its dynamics and comparing these results with analytical models [7,8].

This new platform paves the path for future developments to complement these results to theoretical models and hydrodynamics/radiative simulations. It is also expected to carry future experimental campaigns on large facilities such as NIF or LMJ.

References

[1] K. Schawinski, et al., Science **321**, 223 (2008).

[2] S. Orlando, et al., Astronomy & Astrophysics **559** (2013), A127.

[3] A. Gusdorf, et al., Astronomy & Astrophysics **542**, L19 (2012).

[4] R. P. Drake, Physics of Plasmas **14**, 043301 (2007).

[5] T. Vinci, et al., Physics of Plasmas **13**, 010702 (2006).

[6] J. Hansen, et al., Physics of plasmas **13**, 112101 (2006).

[7] T. Michel, et al., The Astrophysical Journal **888**, 25 (2019).

[8] P. Mabey, et al., Physics of Plasmas **27**, 083302 (2020).

[*] E-mail: diego.oportus@polytechnique.edu

Radiative decay parameters for spectral lines in lanthanide ions of interest for the study of kilonovae in their nebular phase

L. Maison[1], P. Palmeri[1] and P. Quinet[1,2*]

[1]Atomic Physics and Astrophysics, University of Mons, Mons, Belgium
[2]IPNAS, University of Liège, Liège, Belgium

Most heavy elements have a fairly complex atomic structure, in particular the lanthanides (Z = 57 – 71) and the actinides (Z = 89 – 103) which present electronic configurations in which the 4f or 5f subshell is partially filled, giving rise to numerous energy levels and therefore many possible radiative transitions between these energy levels. Consequently, in the kilonova phostospheric phase, i.e. in the first few days after a neutron star merger (NSM), the spectrum is greatly affected by a significant opacity due to the absorption of light by millions of allowed electric dipole transitions (E1) belonging to the different heavy ions present in the ejecta [1].

At later times, as the NSM ejecta continues to expand, temperatures and densities decrease rapidly, leading to non-local thermodynamic equilibrium (NLTE) conditions in which the kilonova is considered to be in the nebular phase. This has the consequence that the spectrum is then emission line dominated, unlike the quasi-blackbody continuum spectrum observed in the phostospheric phase. Moreover, the infrared nebular phase kilonova spectrum detected by the *Spitzer Space Telescope* was assumed to contain forbidden lines of magnetic dipole (M1) and electric quadrupole (E2) types [2] The key role of such forbidden transitions in kilonova modeling was also underlined by Gillanders *et al*. [3] who showed how the inclusion of M1 and E2 lines of heavy elements could lead to the identification of elemental signatures through radiative transfer calculations, while emphasizing the lack of accurate atomic data available for these lines in order to perform reliable kilonova spectral analyses.

The main goal of the present work is to provide new radiative decay rates corresponding to forbidden lines in lanthanide ions. To do so, two computational approaches are used, namely the pseudo-relativistic Hartree-Fock (HFR) method [4] and the fully relativistic Multiconfiguration Dirac-Hartree-Fock (MCDHF) method [5]. New transition probabilities for M1 and E2 lines within the ground configurations of Pr III, Nd III and Er III will be reported at the conference. Astrophysical implications will also be discussed in the context of spectral investigations of kilonovae in their nebular phase.

References

[1] D. Kasen *et al*., Nature 551, 80 (2017).
[2] M.M. Kasliwal *et al*., MNRAS 510, L7 (2022).
[3] J.H. Gillanders *et al*., MNRAS 506, 3560 (2021).
[4] R.D Cowan, *The Theory of Atomic Structure and Spectra*, University of California Press, Berkeley (1981).
[5] I.P. Grant, *Relativistic Quantum Theory of Atoms and Molecules*, Springer, Berlin (2007).

* E-mail: pascal.quinet@umons.ac.be

POSTERS/DENSE PLASMAS

Thomas-Fermi version of the VAMPIRES model

T. Blenski[1] **and R. Piron**[2,3]

[1] Laboratoire "Interactions, Dynamiques et Lasers", UMR 9222, CEA-CNRS-Université Paris-Saclay, Centre d'Études de Saclay, F-91191 Gif-sur-Yvette Cedex, France.
[2] CEA, DAM, DIF, F-91297 Arpajon, France.
[3] Université Paris-Saclay, CEA, Laboratoire Matière en Conditions Extrêmes, F-91680 Bruyères-le-Châtel, France.

We proposed recently a model of ion-electron plasma (or nucleus-electron plasma) that accounts for the electronic structure around nuclei (i.e. ion structure) as well as for ion-ion correlations, the VAMPIRES model [1]. In this poster we discuss with more detail the Thomas-Fermi version of the model.

References

[1] Blenski, Piron, Phys Rev E **107**, 035209 (2023).

Consistent Treatment of Dense Plasma Effects on Atomic Structures, Collisions, and Spectral Signatures

I. E. Golovkin[1] *, M. F. Gu[1] and J. J. MacFarlane[1]

[1]Prism Computational Sciences, Inc., Madison, WI, USA

Many existing models for dense plasma effects on the atomic structure often rely on ad-hoc ionization potential depression formulas. However, these models do not capture the entire influence of the plasma screening effects at high densities [1-3]. We report on development of a complete and consistent atomic database, with all atomic parameters required for collisional radiative modeling computed from appropriate plasma screening potentials. A grid of models depending on plasma temperature and density will be calculated with the Flexible Atomic Code (FAC) [4], and new capability in the suite of Prism modeling codes [5] will be developed to utilize such a database. We will explore several different forms of plasma screening potentials, such as ion-sphere, Stewart-Pyatt, and those based on the average atom models. The resulting spectral models will not only address the modification of ionization balance due to the continuum lowering, but also shifts of spectral lines from the altered energy level structures, as well as the effects of screening potentials on other collisional and radiative process, such as radiative transition, electron impact excitation, photo-ionization, autoionization, and collision ionization. The new development required in FAC, and the resulting atomic data from this project will be made publicly available and hosted in the GitHub repository for FAC.

Some presented material is based upon work supported by the U.S. Department of Energy, Office of Science, Fusion Energy Sciences (FES) under Award Numbers DE- SC0024331

References

[1] A. Saemann, et al. "Isochoric Heating of Solid Aluminum by Ultrashort Laser Pulses Focused on a Tamped Target." Phys. Rev. Lett., **82**(24):4843–4846, Jun 1999.

[2] O. Ciricosta, et al. "Direct Measurements of the Ionization Potential Depression in a Dense Plasma." Phys. Rev. Lett., **109**(6):065002, Aug 2012.

[3] S. B. Hansen, et al. "Changes in the electronic structure of highly compressed iron revealed by X-ray fluorescence lines and absorption edges." High Energy Density Physics, **24**:39–43, Sep 2017

[4] M. F. Gu. The flexible atomic code. Canadian Journal of Physics, **86**(5):675–689, January 2008.

[5] J. J. MacFarlane, et al. "SPECT3D - A multi-dimensional collisional-radiative code for generating diagnostic signatures based on hydrodynamics and PIC simulation output." High Energy Density Physics, **3**(1-2):181–190, May 2007.

* E-mail: golovkin@prism-cs.com

Radiation-Hydrodynamics code HELIOS-CR: improved models for dense plasma effects and IFE simulations

V. N. Golovkina[1] [*], I. E. Golovkin[1], M. F. Gu[1] and J. J. MacFarlane[1]

[1]Prism Computational Sciences, Inc., Madison, WI, USA

HELIOS-CR is a 1-D radiation-magnetohydrodynamics code that is used to simulate the dynamic evolution of plasmas created in high energy density physics (HEDP) experiments [1]. The energy sources include lasers, radiation sources, electric currents (in cylindrical geometry), and particle beams. It has been extensively used for modelling low-yield ICF experiments. We will discuss several model improvements that makes HELIOS more suitable for IFE simulations including accounting for burned fuel, improved fusion cross-sections, more accurate and efficient charged particle transport algorithms, and support for non-monoenergetic particle beam specifications. We will also discuss new models that account for dense plasma effects on atomic structures and their effect on the results of hydrodynamics simulations with inline collisional-radiative atomic kinetics.

References

[1] J.J. MacFarlane, I.E. Golovkin, P.R. Woodruff, HELIOS-CR - a 1-D radiation-magnetohydrodynamics code with inline atomic kinetics modeling, JQSRT, Vol. **99**, Issues 1-3, pp. 381-397 (2006).

[*] E-mail: vgolovkina@prism-cs.com

An explicit numerical scheme for Milne's phase-amplitude equations

Robin PIRON[1,2] * **and Mikael TACU**[1,2]

[1] CEA, DAM, DIF, F-91297 Arpajon, France.
[2] Université Paris-Saclay, CEA, Laboratoire Matière en Conditions Extrêmes, F-91680 Bruyères-le-Châtel, France.

Models used in atomic physics of plasma should in principle account for continuum electrons in the atomic structure. This can lead to rather intensive computation and memory storage, because accounting for the continuum requires sampling of the radial wavefunctions in both the radius and momentum spaces (see, for instance, [1, 2, 3]).

Alternative formalisms for the one-electron basis may bring a more efficient numerical representation of the continuum. For instance, an average-atom numerical algorithm resorting to the basis of Siegert states was recently proposed and studied [4], using the method of solution of [5].

Milne's phase-amplitude (MPA) representation [6] is based on a slowly varying amplitude function. It has a direct link with the Wentzel-Kramers-Brillouin approximation. It also has a strong numerical interest, for it resorts to slowly varying, nonperiodic functions, and thus allows one to circumvent the Shannon sampling limit. This interest has long been recognized in the literature, and MPA representation was used for Bessel functions calculations [7] and atomic-physics computations [8, 9].

In this poster, we first discuss the limitations of some known methods for solving the MPA equations [8, 9]. We then propose a new explicit method of solution, which addresses these limitations. Such a method may prove itself useful in dense-plasma modeling and in the calculation of atomic-processes cross-sections. Examples of such applications are given.

References

[1] Liberman, Phys Rev B **20**, 4981 (1979).

[2] Wilson, Sonnad, Sterne, Isaacs, JQSRT **99**, 658 (2006).

[3] Piron, Blenski, Phys Rev E **83**, 026403 (2011).

[4] Starrett, Shaffer, Phys Rev E **107**, 025204 (2023).

[5] Batishchev, Tolstikhin, Phys Rev A **75**, 062704 (2007).

[6] Milne, Phys Rev, **35**, 863 (1930).

[7] Goldstein, Thaler, Math. Tables and Other Aids to Comput. **12**,18 (1957).

[8] Bar-Shalom, Klapisch, Oreg, Comput. Phys Commun. **93**, 21 (1996).

[9] Wilson, Iglesias, Chen, JQSRT **81**,499 (2003).

*E-mail: robin.piron@cea.fr

POSTERS/ICF

NIF x-ray crystal calibration via mulptiple throughput measurement techniques

M. Dozieres-Aybar[1], M. Wu[2], P. Lake[2], A. Lejars[3], C. Reverdin[3], B. Vauzour[3], S. Darbon[3], L. Webster[4], S. Stoupin[5], N. B. Thompson[5], J. Buscho[5], P. Parker[1], M. B. Schneider[5], C. M. Krauland[1]

[1]General Atomics, San Diego, CA 92121, USA
[2]Sandia National Laboratory, Albuquerque, NM 87123, USA
[3]Commissariat à l'énergie atomique et aux énergies alternatives (CEA), Paris, France
[4]University of New Mexico, Albuquerque, NM 87131, USA
[5]Lawrence Livermore National Laboratory, Livermore, CA 94550, USA

Over the past three years, the National Ignition Facility (NIF) Spectrometer Calibration Station (SCS) has developed a methodology to calibrate x-ray crystals by measuring their absolute throughput. From this full instrument response measurement, we can infer the integrated reflectivity as a function of energy for the individual bent crystals used in such diagnostics.
In considering multiple crystals and/or crystal geometries, this work has revealed the importance of experimentally calibrating crystals as we show that theoretical calculations are not always a good estimate and that even crystals with identical fabrication specification can display different behavior. Multiple comparisons with theoretical calculations will be presented as well as a modeling study of the effect of in-plane crystal orientation on reflectivity. Additionally, our findings initiated a cross calibration effort through collaborative engagements, in order to ensure the quality of the experimental data. We will show and discuss the different calibration techniques used by the x-ray spectroscopy community, from both in-house NIF SCS work and external facilities. We will show results of cross calibration for different NIF spectrometers and present comparison with direct rocking curve measurement.

This work was performed under the auspices of the U.S. Department of Energy by General Atomics under Contract 89233119CNA000063 and by Lawrence Livermore National Laboratory under Contract DE-AC52-07NA27344.

* E-mail: dozieresayba1@llnl.gov

Electron heat transport in plasmas through Molecular Dynamics and Particle-In-Cell simulations

D. Guerroudj[1] *, A. Calisti[1], A. Debayle[2,3], J. Rosato[1], and S. Ferri[1]

[1]Aix-Marseille Université, CNRS, PIIM, UMR7345, Marseille, France
[2]CEA, DAM, DIF, F-91297 Arpajon, France
[3]Université Paris-Saclay, CEA, LMCE, 91680 Bruyères-le-Châtel, France

Understanding electron heat transport in Inertial Confinement Fusion (ICF) plasmas is both a challenging and essential task, as it plays a crucial role in transferring laser energy to the fusion capsule. In this study, we investigate electron heat transport properties using two simulation approaches: Particle-In-Cell (PIC) simulations with the SMILEI code [1], which are based on a kinetic closure using the Vlasov-Landau equation to model plasma behavior, and classical Molecular Dynamics (MD) simulations using the Bingo-TCP code [2], which solve the full N-body problem. This preliminary work focuses on heat transport in the Spitzer-Härm regime [3], where the thermal transport coefficient κ is determined through spectral analysis of the temperature profile evolution in both PIC and MD simulations. This study serves as an initial step toward other tasks, such as the reconstruction of the complete generalized Ohm's law, and should be extended to the non-local regime, where additional effects can limit heat transport efficiency. Furthermore, we will account for the effects of an external magnetic field in the MD simulations [4] to guide our research toward Magneto-Inertial Fusion (MIF) experiments.

References

[1] J. Derouillat, et al., Comput. Phys. Commun. **222**, 351-373 (2018).

[2] A. Calisti, et al., High Energy Density Physics **50**, 101084 (2024).

[3] L. Spitzer, and R. Härm, Phys. Rev. **89**, 977 (1953).

[4] Q. Spreiter, and M. Walter, Journal of Computational Physics **152**, 102-199 (1999).

*E-mail: daniel.guerroudj@univ-amu.fr

POSTERS/MAG

Transition energy measurements of highly-charged Xe and W in support of ITER's XRCS and SPARC's XRS

A. J. Fairchild[1] *, N. Hell[1], G. V. Brown[1], M. E. Eckart[1], M. Bitter[2], L. Gao[2], S. B. Hansen[3], K. W. Hill[2], R. L. Kelley[4], C. A. Kilbourne[4], N. A. Pablant[2], C. Perks[5], F. S. Porter[4], J. Rice[5], R. Tieulent[6], D. Vezinet[7], and Z. Cheng[6]

[1]Lawrence Livermore National Laboratory, Livermore, CA, USA
[2]Princeton Plasma Physics Laboratory, Princeton, NJ, USA
[3]Sandia National Laboratories, Albuquerque, NM, USA
[4]NASA Goddard Space Flight Center, Greenbelt, MD, USA
[5]MIT Plasma Science and Fusion Center, Cambridge, MA, USA
[6]ITER Organization, St. Paul-lez-Durance, France
[7]Commonwealth Fusion Systems, Devens, MA, USA

High-resolution x-ray crystal spectroscopy diagnostics continue to be an indispensable tool for determining important plasma parameters such as ion temperature, plasma flow, and impurity abundances in tokamak devices. However, both the design and successful operation of these diagnostics require accurate transition energies for the diagnostic lines themselves, for line emission from nearby charge states of the same Z, and for line emission from other relevant impurity ions present in the device. ITER's X-Ray Crystal Spectrometer, Core Viewing (XRCS-Core) is a key diagnostic that will utilize high-resolution spectroscopy to measure time-resolved profiles of plasma parameters such as ion and electron temperature for the ITER tokamak. Line surveys and accurate reference energies are the first critical step to identify suitable lines for these diagnostics. XRCS-Core is designed to observe the Ne-like Xe^{44+} $2p^5_{1/2}3d_{3/2}(J = 1) \rightarrow 2p^6$ emission line known as 3C and a nearby N-like Xe^{47+} emission line. SPARC is a planned commercial D-T tokamak fusion device. SPARC's XRS-HR-Xe high-resolution x-ray crystal spectrometer is designed to observe the Ne-like Xe^{44+} $2p^5_{3/2}3d_{5/2}(J = 1) \rightarrow 2p^6$ line known as 3D. For both the XRCS-Core and XRS-HR-Xe diagnostics, a complete set of measured transition energies from highly-charged xenon and from highly-charged impurity ions, such as tungsten, which may limit the Xe diagnostics, is needed. In order to address these atomic data needs, we have used the LLNL EBIT-I electron beam ion trap and EBIT calorimeter spectrometer (ECS) to measure the transition energies of x-ray line emission from highly charged Xe and W ions.

This work was performed under the auspices of the U.S. Department of Energy by Lawrence Livermore National Laboratory under Contract DE-AC52-07NA27344 and is also supported by funding from US-ITER and the DOE Fusion Energy Science Program. SNL is managed and operated by NTESS under DOE NNSA contract DE-NA0003525. The views and opinions expressed herein do not necessarily reflect those of the ITER Organization.

*E-mail: fairchild8@llnl.gov

POSTERS/NLTE

Effects of super-Gaussian electron velocity distribution functions on atomic kinetics and radiative emission of hot under-dense Gold plasmas

C. Blancard[1,2], Ph. Cossé[1,2] and G. Faussurier[1,2]

[1]CEA, DAM, DIF, F-91297 Arpajon, France
[2]Université Paris-Saclay, CEA, LMCE, 91680 Bruyères le Châtel, France

Numerous studies in plasma physics are performed assuming that the electron distribution functions (EDFs) are Maxwell-Boltzmann or Fermi-Dirac distributions. However, these widely used assumptions appear to be invalid in various situations.

A source of non-Maxwellian EDF in a laser-produced plasma occurs when the inverse Bremsstrahlung process is the dominant heating mechanism. In the plasma zone where the laser energy is efficiently deposited, media are characterized by high temperatures, large density gradients, and EDFs depleted, both in their low- and the high-energy regions, compared to a Maxwellian distribution. It has been predicted [1] that such EDFs can be described as super-Gaussian (SG) distribution functions where the SG exponent (m) is greater than 2. Recently, the effects of such flat-top electron distributions on the crossed beam energy transfer and on the laser heating have been experimentally demonstrated in low-Z and mid-Z plasmas [2, 3].

Mega-Joule class laser-produced plasmas should enhance the presence of SG-like distributions during the laser heating of high-Z materials, since higher will be the values of the laser intensity and the average ionization, higher could be the deviation between the SG-like and the Maxwellian-Boltzmann distributions. This assumption has motivated the present study, where the effects of non-Maxwellian EDFs on properties of hot under-dense gold plasmas are numerically investigated for conditions existing in laser-heated hohlraums downstream the critical density. A non-thermal collisional-radiative model is used to perform the atomic kinetics and spectral emissivity calculations. Deviations from the case of the Maxwellian distribution, are examined as illustrated in Fig 1.

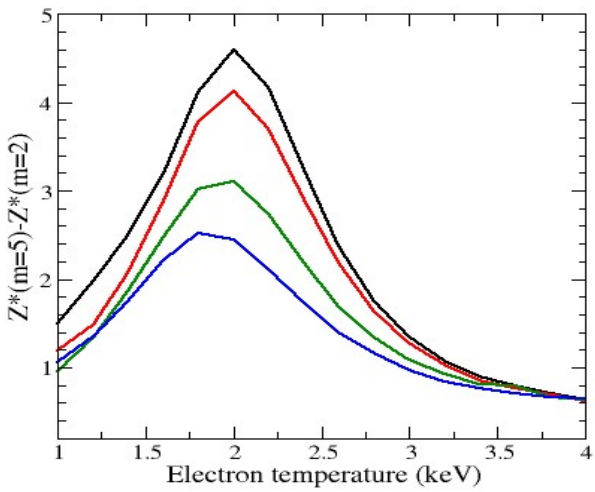

Figure 1. Deviation of Gold average ionizations calculated for two super-Gaussian exponent values (m = 2 and m = 5) as function of the electron temperature and for various electron densities: 10^{19} cm^{-3} (black line), 10^{20} cm^{-3} (red line), 5×10^{20} cm^{-3} (green line), and 10^{21} cm^{-3} (blue line).

References

[1] A.B. Langdon, Phys. Rev. Lett. **44**, 575 (1980).

[2] D.P. Turnbull, A. Colaitis, A.M. Hansen, A.L. Milder, J.P. Palastro, J. Katz, C. Dorrer, B.E. Kruschwitz, D.J. Strozzi, and D.H. Froula, Nature Physics **16**, 181 (2020).

[3] A.L. Milder, J. Katz, R. Boni, J.P. Palastro, M. Sherlock, W. Rozmus, and D.H. Froula, Phys. Rev. Lett. **127**, 015001 (2021).

The role of collisions and radiation transport on the emision signature from x-ray driven plasma

Sebastian Cardoch[1] *, Thomas M. Baumann[2], Sang-Kil Son[3], Jan-Erik Rubensson[1], Nicuşor Tîmneanu[1]

[1]Department of Physics and Astronomy, Uppsala University, Uppsala, Sweden [2]European XFEL, Holzkoppel 4, 22869 Schenefeld, Germany [3]Center for Free-Electron Laser Science CFEL, Deutsches Elektronen-Synchrotron DESY, Notkestr. 85, 22607 Hamburg, Germany

High-intensity and femtosecond duration x-rays from Free Electron Lasers, enable the study of out-of-equilibrium states. As a pump, x-rays induce electronic changes that may lead to ionization and rapid isochoric heating, reaching extreme conditions such as warm and hot dense matter. Emission spectroscopy has been an important tool to diagnose these transient states [1]. We employed a rate equation model [2] and level-resolved atomic data that includes radiative and collisional processes [3] to simulate time-resolved spectra from neon gas driven into plasma by x-rays. We explored gas densities that extend beyond an isolated atom environment. Using experimentally relevant pulse duration and intensity values, simulations show that post-pulse electron impact drives the photo-ionized gas to further ionization. For excitation energy above neon's 1s ionization threshold, collisions culminate with an abundance of ground-state Ne 8+ ions in sub-nanoseconds. To assess the effects of collisions, we focused on the emission from He-like neon 1s2p $^1P_1$ singlet and 1s2p $^3P_1$ triplet. In the isolated atom limit, these states have distinct fluorescence lifetimes of ∼100 fs and ∼400 ps, respectively. In sub-nanosecond timescales and for the pressures explored, we find the gas maintains a high energy density state with electron temperatures ∼200–300 eV. These hot electrons, capable of core-level collision excitation from Ne 8+ $1s^2\,{}^1S_0$, populate the singlet in picosecond timescales and extend its effective lifetime. Selection rules hinder the same channel from feeding the triplet, and electron de-excitation suppresses the triplet's lifetime. We compared time-dependent and time-integrated calculations with preliminary experimental spectra obtained with a high-resolution spectrometer [4] at the European X-ray Free Electron Laser. The process revealed the importance of radiation propagation, electron collisions and electron-ion temperature relaxation that extend beyond the isolated atom approximation.

References

[1] Ziaja, B. et al. Philosophical Transactions 381, 20220216 (2023).

[2] Scott, H. A. & Mayle, R. W. Applied Physics B 58, 35-43 (1994).

[3] Gu, M. F. Canadian Journal of Physics 86, 675-689 (2008).

[4] Agåker, M. et al. Journal of Synchrotron Radiation 31, 1264-1275 (2024).

*E-mail: sebastian.cardoch@physics.uu.se

Alignment-transfer rate coefficients for collisional excitation of O V ion in an anisotropic two-temperature plasma

A. F. Sekkal-Haddouche, M. K. Inal* and M. Benmouna**

Faculty of Sciences, Abou-Bekr Belkaid University, 13000 Tlemcen, Algeria

Rate coefficients for the transfer of alignment in the electron-impact excitation of ions are required for collisional-radiative modeling of polarized line emissions from non-thermal plasmas with cylindrically symmetric electron velocity distributions [1]. These coefficients, denoted $C_0^{KK'}$ with K, K'=2,4,…, are obtained from the multipole cross sections $\sigma_Q^{KK'}$ with $|Q| = 0,1,2,\ldots,\min(K,K')$ [2]. Unlike $\sigma_{Q=0}^{KK'}$, the $\sigma_{Q\neq 0}^{KK'}$ cannot be deduced from the usual cross sections for transitions between magnetic sublevels. Their calculations are much more difficult since they must include coherences between different magnetic sublevels within the initial and final ion levels. Until now, there have been no published calculations of $C_0^{KK'}$ taking into account $\sigma_{Q\neq 0}^{KK'}$.

In an attempt to fill this gap, we report here calculations of the alignment-transfer rate coefficients C_0^{22} and C_0^{44} for excitations of the Be-like ion O V from its metastable levels 2s2p $^3P_1$ and $^3P_2$, using an anisotropic Maxwellian electron distribution. The calculations are made in terms of the ratio $T_\perp/T_{//}$ characterizing the anisotropy degree of the electron distribution, for different values of the mean electron energy $\langle\varepsilon\rangle = k(T_\perp + T_{//}/2)$ in the range 30−450 eV, $T_{//}$ and $T_\perp$ being respectively the longitudinal and transverse temperatures with respect to the quantization axis z. The multipole cross sections $\sigma_{Q=0-2}^{22}$ and $\sigma_{Q=0-4}^{44}$ are computed in the factorized method of the relativistic distorted-wave approximation from an extended version of the Flexible Atomic Code [3].

In order to illustrate the effects of coherences, we give in figure 1 typical results of C_0^{22} versus $T_\perp/T_{//}$ for two selected excitations. Clearly, as the electron distribution deviates from the perfect beam along the z axis ($T_\perp/T_{//} \to 0$), the coherences lead to an important increase of C_0^{22} besides a reversal trend of the curves.

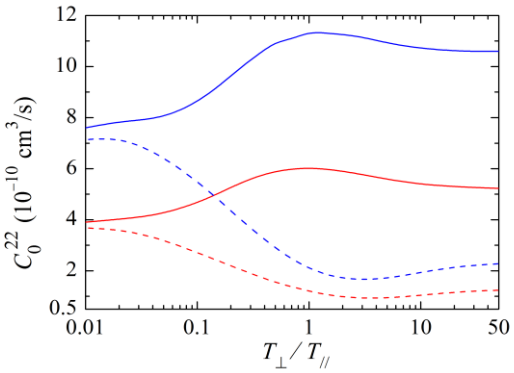

Figure 1. C_0^{22} versus $T_\perp/T_{//}$ with $\langle\varepsilon\rangle = 120$ eV for 2s2p $^3P_2$ →2s3p $^3P_2$ (lower curves in red) and 2s2p $^3P_2$→2s3d $^3D_3$ (upper curves in blue). Solid curves include coherences via $\sigma_{1,2}^{22}$, dashed curves do not.

References

[1] T. Fujimoto, *Plasma Polarization Spectroscopy* (Spinger, Berlin, 2008), chapter 4.

[2] G. Csanak, C. J. Fontes, P. Hakel and D. P. Kilcrease, J. Phys. B **44**, 215701 (2011).

[3] M. Belabbas, M. K. Inal and M. Benmouna, Phys. Rev. A **104**, 042818 (2021).

*E-mail: mokhtar.inal@univ-tlemcen.dz **Retired

Electron-impact ionization cross sections and rates for Si IV-VIII

J.-C. Pain[1,2]* and D. Benredjem[3]

[1]CEA, DAM, DIF, F-91297 Arpajon, France
[2]Université Paris-Saclay, CEA, Laboratoire Matière en Conditions Extrêmes, F-91680 Bruyères-le-Châtel, France
[3]Université Paris-Saclay, CNRS, Laboratoire Aimé Cotton, F-91405 Orsay, France

We investigate the ionization of silicon ions Si IV-Si VIII by electron impacts in hot plasmas. Our calculations of the cross sections and rates rely on the Coulomb-Born-Exchange, Binary-Encounter-Dipole and Distorted-Wave methods implemented in the Flexible Atomic Code (FAC) [1]. Our results are compared with measurements [2, 3] and other calculations [4]. We use a semi-empirical formula for the cross section, which involves a small set of adjustable parameters [5]. The rate coefficient is then expressed in terms of these parameters and is represented in a large temperature interval, up to 10^8 K. As expected, the agreement with measurements improves for increasing ion charges, confirming the applicability of our approach to hot plasma studies involved in inertial confinement fusion, and its reliability. The configuration interaction is taken into account and is shown to affect the cross section at low energy, in particular for Si^{3+}.

References

[1] M. F. Gu, Can. J. Phys. **86** 675-689 (2008).

[2] D. H. Crandall, R. A. Phaneuf, R. A. Falk, D. S. Belić and G. H. Dunn, Phys. Rev. A **25**, 143-153 (1982).

[3] P. A., Zeijlmans van Emmichoven, M. E. Bannister, D. C. Gregory, C. C. Havener, R. A. Phaneuf, E. W. Bell, X. Q. Guo and J. S. Thompson, Phys. Rev. A **47**, 2888-2892 (1993).

[4] N. R. Badnell, M. S. Pindzola, I. Bray and D. C. Griffin, J. Phys. B: At. Mol. Opt. Phys. **31**, 911-924 (1998).

[5] D. Benredjem and J.-C. Pain, J. Phys. B: At. Mol. Opt. Phys. **57**, 115001 (2024).

*E-mail: jean-christophe.pain@cea.fr

POSTERS/OPACITY

Two decades of stellar interior opacity research at Z.

J.E. Bailey[1,*], G.P. Loisel[1], T. Nagayama[1], G.A. Rochau[1], P.W. Lake[1], G.S. Dunham[1], S.B. Hansen[1], D.C. Mayes[2], C. Blancard[3], Ph. Cosse[3], G. Faussurier[3], F. Gilleron[3], J.-C. Pain[3], J. Colgan[4], C.J. Fontes[4], D.P. Kilcrease[4], M. Sherrill[4], and J. Abdallah Jr. [4], C.A. Iglesias[5], B.G. Wilson[5], R.C. Mancini[6], R. More[7], C. Orban[8], A.K. Pradhan[8], S.N. Nahar[8], I. Golovkin[9], M.F. Gu[9], W. Ping[9], J.J. MacFarlane[9], and T.A. Gomez[10]

[1]Sandia National Laboratories, Albuquerque, New Mexico, USA
[2]University of Texas, Austin, Texas, USA
[3]CEA, DAM, DIF, F-91297 Arpajon, France
[4]Los Alamos National Laboratory, Los Alamos, New Mexico, USA
[5]Lawrence Livermore National Laboratory, Livermore, California, USA
[6]University of Nevada, Reno, Nevada, USA
[7]Retired from the National Institute for Fusion Science, Toki, Gifu, Japan
[8]Ohio State University, Columbus, Ohio, USA
[9]Prism Computational Sciences, Madison, Wisconsin, USA
[10]University of Colorado, Boulder, Colorado, USA

Nearly a century ago, Eddington [1] recognized that the attenuation of radiation by stellar matter controls the internal temperature and density profiles within stars like the Sun. Opacity calculations for high energy density (HED) matter are challenging because accurate and complete descriptions of the energy level structure, equation of state, and plasma effects such as continuum lowering and spectral line broadening are needed for partially ionized atoms. This requires approximations. Opacity calculations, however, have never been benchmarked against laboratory measurements at stellar interior conditions until now. The measurements are challenged by creating and diagnosing sufficiently large and uniform samples at stellar interior conditions. Over the last two decades, we developed an experimental platform on the Z facility and measured [2] spectrally-resolved opacity at electron temperatures T_e = 150-200 eV and densities $n_e = 0.6 – 5.0 \times 10^{22}$ cm^{-3} - conditions very similar to the solar radiation/convection boundary zone. Models agree with iron data at the lower temperature and densities, but notable model-data discrepancies arise at higher temperatures and densities. The comparisons raise questions about how well we understand atoms embedded in high energy density plasma. These measurements may also help resolve two-decade-old discrepancies between solar model predictions and helioseismic observations. So far, however, there is no reconciliation of the model-data discrepancy and both theory and experiment scrutiny must continue. The experiments have now been expanded to include opacity data for chromium, nickel [3], and oxygen. The wavelength range has also been expanded to cover 5-20 Angstroms, a span that is unprecedented in opacity research. This presentation will describe experiment design considerations for benchmark quality results. It will provide an overview of the results, investigations of possible errors, and ongoing experiments.

Sandia National Laboratories is a multimission laboratory managed and operated by NTESS LLC, a wholly owned subsidiary of Honeywell International Inc. for the U.S. DOE's NNSA under contract DE-NA0003525. Experimental time on the Z facility was provided in part through the Z Fundamental Science Program. DAM and TAG acknowledge support from the Wootton Center for Astrophysical Plasma Properties.

[1] A.S. Eddington, The Internal Constitution of the Stars (Cambridge Univ. Press, Cambridge, 1926).
[2] J.E. Bailey *et al*., *Nature* **517**, 56 (2015).
[3] T. Nagayama *et al*., *Physical Review Letters* **122**, 235001 (2019).
[*] E-mail: jebaile@sandia.gov

Opacity determination of photospheric-phase kilonova ejecta based on detailed atomic data calculations

J. Deprince[1,2] *, S. Ben Nasr[1], H. Carvajal Gallego[1], G. Wagle[2] , M. Godefroid[3], S. Goriely[2], O. Just[4], P. Palmeri[1] and P. Quinet[1,5]

[1]Atomic Physics and Astrophysics, UMONS, Mons, Belgium
[2]Institute of Astronomy and Astrophysics, ULB, Brussels, Belgium
[3]SQUARES, ULB, Brussels, Belgium
[4]GSI Helmholtz Center, Darmstadt, Germany
[5]IPNAS, ULiège, Liège, Belgium

The production of elements heavier than iron in the Universe still remains an unsolved mystery. About half of them are thought to be produced by the astrophysical r-process (rapid neutron-capture process) [1], for which one of the most promising production sites are neutron star mergers (NSMs) [2]. In August 2017, gravitational waves produced by a NSM were detected for the first time by the LIGO detectors (event GW170817) [3], and the observation of its electromagnetic counterpart, the kilonova (KN) AT2017gfo, suggested the presence of heavy elements in the KN ejecta [4]. The luminosity and spectra of such KN emission depend significantly on the ejecta opacity, which is thought to be dominated by millions of lines from the heavy elements produced by the r-process, in particular f-shell elements, *i.e.* lanthanides and actinides [5]. Atomic data and opacities for these elements are thus sorely needed to model and interpret KN light curves and spectra.

In this context, the present work focusses on large-scale atomic data and opacity computations for all heavy elements with $Z \geq 20$, with a special effort on lanthanides and actinides, for a grid of typical KN ejecta conditions (temperature, density and time post-merger) between one day and one week after the merger (corresponding to the LTE photospheric phase of the KN ejecta). In order to do so, we used the pseudo-relativistic Hartree-Fock (HFR) method as implemented in the Cowan's codes [6], in which the choice of the configuration interaction model is of crucial importance [7]. In this contribution, HFR atomic data and opacities for all lanthanides and actinides will be presented, as well as some comparisons with previous works. Besides, we will also discuss the contribution of each element to the total KN ejecta opacity for several NSM models [8], depending on their Planck mean opacities and elemental abundances deduced from NSM simulations. The impact of considering such atomic-physics based opacity data instead of typical crude approximation formulae [5] for the determination of the total KN ejecta opacity on KN light curves will also be evaluated.

References

[1] J.J. Cowan, C. Sneden, J.E. Lawler *et al.*, Reviews of Modern Physics **93**, 015002 (2021).
[2] B.D. Metzger, G. Martinez-Pinedo, S. Darbha *et al.*, MNRAS **406**, 2650 (2010).
[3] B.P. Abbott, R. Abbott, T.D. Abbott *et al.*, Phys. Rev. Lett. **119**, 161101 (2017).
[4] D. Kasen, B. Metzger, J. Barnes *et al.*, Nature **551**, 80 (2017).
[5] O. Just, I. Kullmann, S. Goriely *et al.*, MNRAS **510,** 2820 (2022).
[6] R.D. Cowan, The Theory of Atomic Structure and Spectra, California University Press, Berkeley (1981).
[7] A. Flörs, R.F. Silva, J. Deprince *et al.*, MNRAS **524**(2), 3083 (2023).
[8] O. Just, V. Vijayan, Z. Xiong *et al.*, ApJL **951**, L12 (2023).

* E-mail: jerome.deprince@umons.ac.be

Opacity measurements of hot expanded metallic plasma wires

F. Gilleron[1*], S. Bastiani[2], P. Audebert[2], C. Reverdin[1], B. Vauzour[1], J.C. Pain[1], R. Piron[1], C. Esnault[1], T. Blenski[3], M. Poirier[3]

[1]CEA/DAM/DIF, F-91297 Arpajon, France
[2]LULI, Ecole Polytechnique, CNRS/CEA/UPMC, 91128 Palaiseau cedex, France
[3]Laboratoire "Interactions, Dynamiques et Lasers", UMR 9222, CEA/CNRS/Université Paris-Saclay, France

The purpose of this experiment is to characterize the expansion and absorption of hot plasmas in cylindrical geometry, in homogeneous temperature and density conditions ($T \approx 20$ eV and $\rho \approx 10^{-3}$-10^{-2} g/cm^3) and close to local thermodynamic equilibrium (LTE). In the proposed experimental set up [1], a thick 100 microns diameter metallic wire is heated symmetrically by the blackbody radiation of two gold Hohlraums irradiated by laser (squared pulses of 1 ns@2ω, 500 J). The hot plasma is then probed with a delay (from 1 to 5 ns) by a secondary X-ray source created by focusing a short pulse (500 ps@2ω, 20 J) on a thick gold foil. A « point-projection » spectrometer based on a cylindrically curved TlAP crystal (R=100 mm) coupled to an Image Plate detector is used to perform a spectral and spatial imaging of the plasma. The spectral range is 700-1500 eV (resolution of 2 eV) to study the L-shell transitions of mid-Z elements (Cu, Zn, Fe) or K-shell lines of Mg. The spatial resolution is about 20 µm (dimension of the focal spot of the backlighter). The duration of temporal integration is 500 ps (backlighter duration). Compared to thin foils, that we employed in past absorption experiments [2-8], the use of thick wires has its own advantages and disadvantages. They are cheap, easy to produce and can be handled without special precautions. However, the wire is not heated in volume: it forms a superficial plasma which expands cylindrically with large gradients of temperature and density. A « point-projection » spectrometer is needed to record a frequency- and space-resolved image of the backlighter transmitted through the plasma. The optical depth of the plasma can then be reconstructed as a function of its radius and of the photon frequency of the source by applying the Abel transform on the measured signal. The processed signal is thus free (in theory) of temperature and density gradients since the method resolves them. It is also possible to infer a radial density profile of the plasma. The main drawback is a much greater sensitivity to noise (the Abel transform involve the derivative of the signal), which must be taken into account in the experimental set up (filters, shields) and in the numerical analysis, the need for a point-like source (in space and time) and a relevant radiography diagnostics. We will present preliminary results of the campaign.

References

[1] F. Gilleron, S. Bastiani, C. Reverdin, JC. Pain, R. Piron, C. Esnault, T. Blenski, M. Poirier, Internal Report CEA/DAM/DIF/19/24/DO.

[2] F. Thais, S. Bastiani, T. Blenski, C. Chenais-Popovics, K. Eidman, W. Fölsner, J.C. Gauthier, F. Gilleron, and M. Poirier, J. Quant. Spectrosc. Radiat. Transf., 81(1):473-485 (2003).

[3] G. Loisel, P. Arnault, S. Bastiani-Ceccotti, T. Blenski, T. Caillaud, J. Fariaut, W. Foelsner, F. Gilleron, J C Pain, M. Poirier, C. Reverdin, V. Silvert, F. Thais, S. Turck-Chieze, B. Villette, HEDP 5(3):173 (2009).

[4] C. Reverdin, F. Thais, G. Loisel, M. Busquet, S. Bastiani-Ceccotti, T. Blenski, T. Caillaud, J. E. Ducret, W. Foelsner, D. Gilles, F. Gilleron, J. C. Pain, M. Poirier, F. Serres, V. Silvert, G. Soullie, S. Turck-Chieze, and B. Villette, Rev. Sci. Instrum., 83, 10E134 (2012).

[5] M. Dozieres, F. Thais, S. Bastiani-Ceccotti, T. Blenski, M. Comet, F. Condamine, J. Fariaut, F. Gilleron, D. Gilles, J. C. Pain, M. Poirier, C. Reverdin, F. Rosmej, V Silvert, G. Soullie, and B. Villette, HEDP 31:83-91 (2019)

[*] E-mail: franck.gilleron@cea.fr

Effect of Interatomic Interactions on Opacity in Hot Dense Plasmas

J. M. Kasper[1]*, C. E. Starrett[1], and C. J. Fontes[1]

[1] Computational Physics Division, Los Alamos National Laboratory, Los Alamos, NM 87545, USA

Recent opacity experiments at Sandia's Z machine and the National Ignition Facility (NIF) at Livermore have seen disagreement with theory. Of particular note is the iron experiment, which seeks to replicate the conditions present in the solar interior [1]. Although a variety of possible modifications to opacity models have already been examined, none have provided a good explanation to resolve the conflict [2]. In this work we examine the possible role of interatomic interactions between the iron and magnesium ions. If iron and magnesium interact differently than do the analogous chromium–magnesium and nickel–magnesium systems, this could shed light on the discrepancy. Calculations using multiple scattering theory [3] are used to calculate the opacity of mixed metal–magnesium systems generated from snapshots of pseudo-atom molecular dynamics [4] run at the experimental densities and temperatures. While the interatomic interactions included in these calculations do change the positions and intensities of some of the lines, the effect is small and does not meaningfully impact the opacity enough to account for the differences in theory and experiment. This is not particularly surprising at these densities where the average interatomic distance is approximately 3× that of solid density where chemical bonding and interatomic interaction is significant.

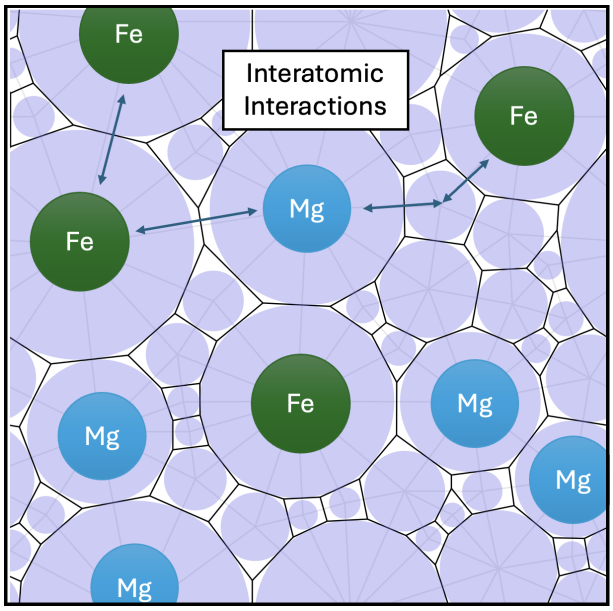

Figure 1. Multiple scattering includes self-consistent corrections to the potential in each cell from its neighbors, capturing interatomic interactions in the electronic structure of each ion.

References

[1] J. E. Bailey, et al., Nature **517**, 56 (2015).

[2] T. Nagayama, et al. Phys. Rev. Lett. **122**, 235001 (2019).

[3] C. E. Starrett and N. Shaffer, Phys. Rev. E. **102**, 043211 (2020).

[4] C. E. Starrett, J. Daligault, and D. Saumon, Phys. Rev. E. **91**, 013104 (2015).

*E-mail: jkasper@lanl.gov

Comparison between ab initio and semi-empirical calculated bound-bound opacities of Tm ions

A. Meftah[1,2], E. Bokamba Motoumba[3,2], C. Balança[2], M. Sabri[1], D. Deghiche[1] and W.-Ü L. Tchang-Brillet[2]

[1]LPCQ, University Mouloud Mammeri, BP17 RP, Tizi-Ouzou, 15000 Algeria
[2]Observatoire de Paris-Meudon-PSL, Sorbonne Université, CNRS, LERMA, F-92195 Meudon, France
[3]Faculté des Sciences et Technique, Université Marien Ngouabi, Brazzaville, BP 69, Congo

Heavy element ions such as lanthanides and actinides are formed in neutron star mergers through neutron capture r-process and greatly contribute to the opacities of the ejecta [1]. The bound-bound part of opacity can be derived from the calculations of transition probabilities of radiative transitions of an ion, taking into account typical conditions in a kilonova.

Here we present the case of triply ionized thulium Tm^{3+} (Tm IV). A recent extended analysis [2] of the high-resolution ultraviolet emission spectrum of the ion increased by ~150 the number of known energy levels previously reported for the four lowest configurations [3]. Based on these energy levels, a semi-empirical approach was adopted by performing parametric calculations using the Cowan codes [4, 5]. Then the Tm IV contribution to opacity is derived from reliable transition probabilities. It is compared to the one derived from calculations applying a fully relativistic ab initio multiconfiguration Dirac-Hartree-Fock (MCDHF) method using the code GRASP2018 [6].

The bound-bound opacity of Tm V from parametric calculations, based on newly determined energy levels will also be presented.

References

[1] D. Kasen, N. Badnell and J. Barnes, The Astrophysical Journal 774, 25 (2013)

[2] M. Sabri, A. Meftah, C. Balança, E. Bokamba Motoumba, C. Champion, C. Blaess and W-Ü L. Tchang-Brillet, poster presentation at the ICAMDATA 2024 conference, Lanzhou, September 22-26, 2024.

[3] A. Meftah, J.-F. Wyart, N. Champion and W.-Ü L.Tchang-Brillet, Eur. Phys. J. D 44, 35 (2007).

[4] R.D. Cowan, The Theory of Atomic Structure and Spectra (University of California Press, Berkeley, 1981)

[5] A. Kramida, A suite of atomic structure codes originally developped by R D Cowan adapted for Windows based on personnal computers, NIST MIDAS site (2018).

[6] C. Froese Fischer, G. Gaigalas, P. Jönsson, et al, Comput. Phys. Commun. **237**, 184 (2019)

* E-mail: ali.meftah@obspm.fr

Platform-dependent advantages and challenges of laboratory stellar-opacity measurements

Taisuke Nagayama[1*], Jim Bailey[1], Greg Dunham[1], Eric Dutra[4], Bob Heeter[2], Matthias Hohenberger[2], Heather Johns[3], Guillaume Loisel[1], Dan Mayes[1], Kathy Opachich[2], Ted Perry[3], Matthew Wallace[2]

[1]Sandia National Laboratories
[2]Lawrence Livermore National Laboratory
[3]Los Alamos National Laboratory
[4]Nevada National Security Site

The accuracy of iron and oxygen opacity calculations is crucial for solar and stellar modeling, as well as numerous high-energy-density (HED) plasma simulations. The lack of benchmark opacity experiments introduces uncertainties into these simulations. The first iron opacity measurement at solar interior temperatures, conducted at the Z-machine at Sandia National Laboratories [1,2], revealed a larger-than-expected discrepancy between measured and modeled iron opacities. While this finding could help resolve discrepancies between solar models and observations, it also sparked controversy within the HED community. An alternative experimental method developed at the National Ignition Facility (NIF) [3,4] aims to independently verify these findings. The Z-machine uses an area backlight approach, whereas NIF employs point-projection. Each method offers unique advantages and challenges due to platform-specific characteristics. This poster summarizes how these approaches complement each other, and how they, when combined, provide unbiased experimental constraints for testing the accuracy of iron and oxygen opacity models.

SNL is managed and operated by NTESS under DOE NNSA contract DE-NA0003525.

References

[1] J. E. Bailey, *et al.*, Nature **517**, 56 (2015).

[2] T. Nagayama, *et al.*, PRL **122**, 235001 (2019).

[3] T. S. Perry, *et al.*, HEDP **23**, 223 (2017)

[4] R. Heeter, *et al.*, Atoms **6**, 57 (2018)

* E-mail: tnnagay@sandia.gov

HRXS – a new High Resolution X-ray Spectrometer of LMJ

C. Reverdin[1], B. Vauzour[1], Q. Alexandre[1], P. Prunet[2], S. Rovillon[2], S. Diop[1], M. Sozet[2], T. Fonseca[2], C. Baccou[1], D. Bernardino[1], C. Blancard[1], M. Bonneau[1], C. Bowen[1], M. Briat[1], A. Chaleil[1], F. Chermette[1], T. Chirac[1], O. Dubos[1], S. Ferré[1], F. Gilleron[1], D. Gontier[1], P. Gruning[1], A. Lejars[1], L. Jacquet[1], J.C. Pain[1], M. Prat[1], P. Rathouit[1], P. Renaudin[1], A. Rousseau[1], G. Soullie[1], B. Villette[2]

[1]CEA DAM, DIF, F-91297, ArpajonFrance
[2]CEA DAM, CESTA, F-33116 Le Barp, France

HRXS (High Resolution X-ray Spectrometer) is a new crystal spectrometer recently implemented on the LMJ facility. Its spectral range is from one keV to twenty keV. It is dedicated to atomic physics and more specifically to NLTE spectroscopy and opacity measurements.

This diagnostic consists in ten measurement channels implemented in three different boxes. The central box contains four measurement channels associated to a framing camera for time-resolved spectra. Each of the two lateral boxes contains a set of three channels and a CCD camera to record time-integrated spectra.

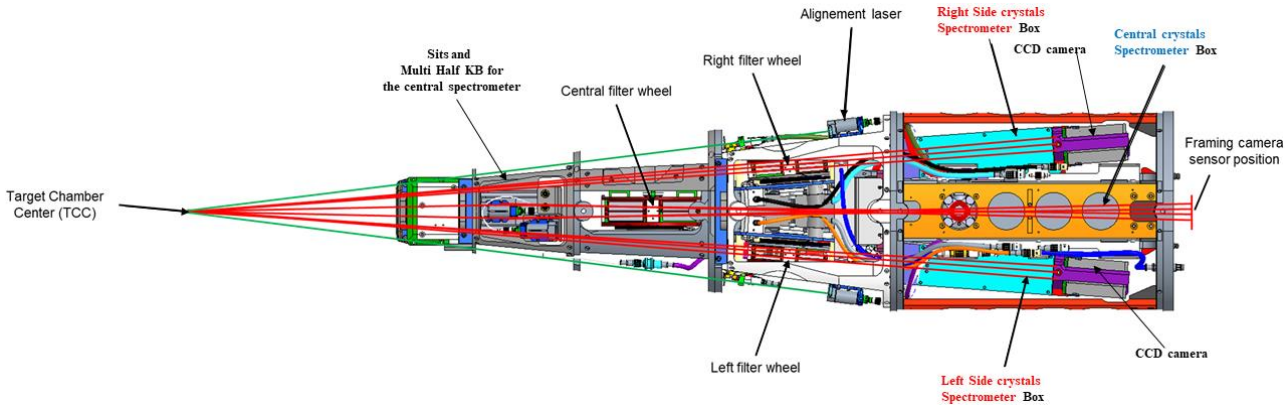

Figure 1. Layout of the ten channels of HRXS, the new x-ray crystal spectrometer of LMJ

Each channel is equipped with a cylindrical Bragg crystal in either reflection or transmission geometry, an adjustable shot-to-shot filter (thanks to a four-position filter wheel), and a slit for spatial resolution and is dedicated to a specific spectral range. The channels are fully customizable, allowing both spectral range and spectral resolution to be adapted to experimental needs. The slits positions can also be easily changed between experimental campaigns to adjust the magnification and thus the field of view along the spatial dimension.

Opacity measurements can be performed by combining each of the four central channels with a grazing incidence spherical mirror (half-KB). This allows the beam to be angularly split and to record on two channels the direct signal and on the two other channels the signal transmitted through the sample on the detector.

HRXS is also equipped with a tungsten alloy collimator at the front end and a debris shield consisting of three successive rolls of aluminized Mylar filters to protect the crystals and detectors.

The first HRXS qualification campaigns took place at the end of last year. Initial results are very promising for future experiments.

* E-mail: charles.reverdin@cea.fr

Efficient computation of low frequency opacity in WDM regime

Mikael Tacu [1,2]*, Jean-Christophe Pain[1,2], and Christophe Blancard[1,2]

[1]CEA, DAM, DIF, F-91297 Arpajon, France
[2]Université Paris-Saclay, CEA, LMCE, F-91680 Bruyères-le-Châtel, France

In investigating the frequency-dependent opacities in plasmas, various approaches are available. They range from experiments to theoretical methods, such as Density Functional Theory based Molecular Dynamics (DFT-MD), or many-body expansion of the grand canonical partition function. As for MD simulations, they are quite demanding in terms of numerical resources, so, for sufficiently hot plasmas, the average-atom approximation is used [1]. Although this significantly speeds up the calculation, a well-known problem inherent to this approximation is the divergence of the free-free opacity at low frequencies in the Kubo-Greenwood formalism. Ziman's approach makes it possible to correct this problem, at the cost of having to calculate the energy-dependent transport cross-section [2]. The phase shifts that enter this cross section may be tricky to correctly compute over large energy and angular number domains. They also greatly vary from element to element.

Here we present a robust method for calculating these phase shifts based on the Calogero [3] equation. This allows us to compute the frequency-dependent opacity, which we compare with ab-initio simulations for various elements. We also explore different approximations in order to speed up the calculations.

References

[1] D. A. Liberman, *Inferno: A better model of atoms in dense plasmas*, J. Quant. Spectrosc. Radiat. Transfer **27**, 335-339 (1982).

[2] W. R. Johnson, *Low-frequency conductivity in the average-atom approximation*, High Energy Density Phys. **5**, 61-67 (2009).

[3] F. Calogero, *Variable Phase Approach to Potential Scattering*, Academic Press, New York, 1967.

*E-mail: mikael.tacu@cea.fr

POSTERS/SLS

Stark line shapes in a constant magnetic field and a periodic electric field

R. Stamm[1 *], I. Hannachi[1,2], J. Rosato[1] and Y. Marandet[1]

[1]Aix-Marseille Univ. and CNRS, PIIM, 13397 Marseille, France
[2]University of Batna 1, PRIMALAB, Department of Physics, Batna, Algeria

Periodic electric fields can change the radiative properties of plasmas, e.g. with changes in the line shape. Such fields may be generated by an external source, as a microwave generator or laser radiation, with the aim of diagnosing or heating the plasma. They may also be created inside the plasma, resulting from a nonthermal effect driven by a plasma instability. For this case a current interest is the diagnostic of energetic particle beams in tokamak edge plasmas, with the potential use of line shape changes due to the generated waves [1]. The effect of oscillating fields on spectral line shapes has been studied since several decades by using approaches based on kinetic theory and retaining the quantum effects of the emitting particles [2-3]. We study here the simultaneous effect of ion dynamics and oscillating electric fields on hydrogen Stark profiles. Ion dynamics is well known to affect the central region of the first Lyman and Balmer lines for plasma densities of 10^{19} to 10^{23} m^{-3} and temperatures of the order of the eV or larger, corresponding to many laboratory, fusion and astrophysical plasmas. Reliable models for ion dynamics are based on computer simulation coupled to a numerical integration of the Schrödinger equation for the emitter evolution operator. We show here some calculations of line shape obtained by a simulation code for hydrogen emitters in a static magnetic field, a plasma microfield, and an oscillating electric field.

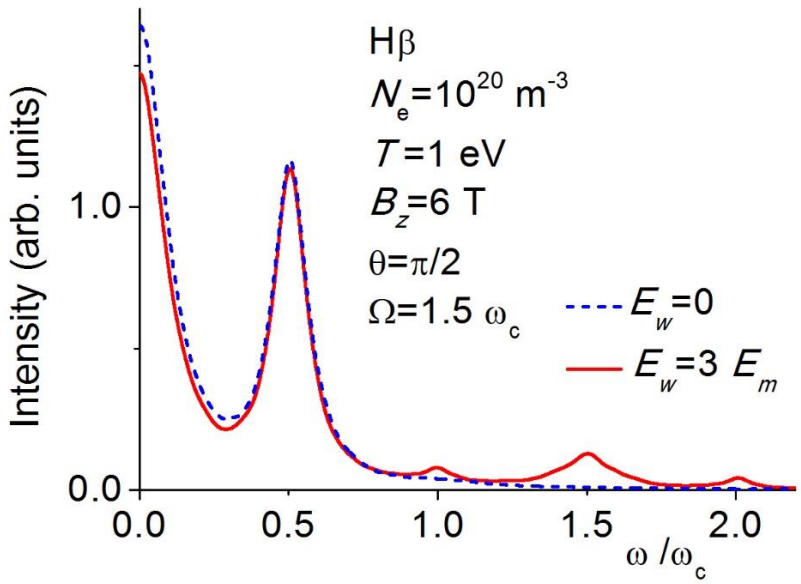

Figure 1. Hβ line observed perpendicular to the magnetic field, for a wave magnitude equal to three time the average plasma microfield and an oscillation frequency equal to 1.5 the cyclotronic frequency.

References

[1] W. Bin et al., Phys. Rev. Lett. **129**, 045002 (2022).

[2] V. Lisitsa, *Atoms in plasmas* (Springer, Berlin, 1994).

[3] E. Oks, *Plasma Spectroscopy* (Springer, Berlin, 1995).

* E-mail: roland.stamm@univ-amu.fr

Pseudoatom Molecular Dynamics Plasma Microfields

J. R. White[*1,2], C. J. Fontes[2], M. C. Zammit[2], T. A. Gomez[1,3,4], C. E. Starrett[2]

[1]Department of Astronomy, University of Texas at Austin, Austin TX, USA
[2]Los Alamos National Laboratory, Los Alamos NM, USA
[3]Astrophysical and Planetary Scienes, University of Colorado Boulder, Boulder CO, USA
[4]National Solar Observatory, University of Colorado Boulder, Boulder CO, USA

Spectral line profiles are powerful diagnostic tools for both laboratory and astrophysical plasmas, as their shape is sensitive to the plasma environment. The low-frequency component of the electric microfield is an important input for analytic line broadening codes. In this poster we present a new method of calculating plasma microfields using configuration-resolved pseudoatom molecular dynamics. This approach accounts for both quantum atomic structure and N-body effects, similar to density functional theory molecular dynamics, but with less computational cost. We present pseudoatom microfields at conditions relevant for recent laboratory experiments. Compared to established microfield codes we find moderate deviations at solid density conditions and strong agreement at lower plasma densities.

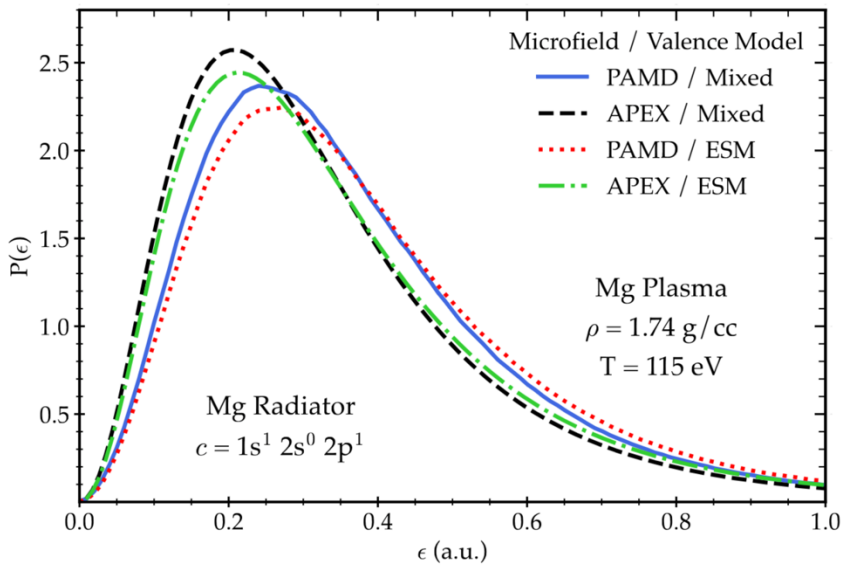

Figure 1. Microfields in a solid-density Mg plasma for an excited He-like Mg atom [1]. The PAMD results (this work) are compared to the APEX code [2]. Different treatments of the valence shell, one following the Excited State Model [3] (ESM) and one following a mixing procedure are compared.

References

[1] J. R. White, C. J. Fontes, M. C. Zammit et al., https://arxiv.org/abs/2407.14455

[2] C. A. Iglesias, F. J. Rogers, R. Shepherd et al., JQSRT **65**, 303–315 (2000)

[3] C. E. Starrett, T. Q. Thelen, C. J. Fontes et al., PRE **109**, 035201 (2024)

[*] E-mail: jacksonw@lanl.gov

POSTERS/SPECTRO

Generation of high-energy-density plasma using Compound Parabolic Concentrator and high-contrast laser

Y. Karaki[1,2]*, Y. Mori[3], E. Ebisawa[4,2], Y. Inubushi[5], S. Kojima[6], K. Yamanoi[2], Y. Abe[4], R. Akematsu[1,2], R. Omura[1,2], H. Matsubara[1,2], H. Xiao[1,2], R. Takizawa[2], K. F. F. Law[1,2], E. Miura[7], Y. Arikawa[2], K. Shigemori[2], A. Iwamoto[8], K. Ishii[3], R. Hanayama[3], Y. Kitagawa[3], H. Sawada[9], T. Sano[2], N. Iwata[2], Y. Sentoku[2], A. Sunahara[2], T. Johzaki[10,2], K. Nagaoka[8], S. Fujioka[2,8]

[1]Graduate School of Science, Osaka University, Osaka, Japan
[2]Institute of Laser Engineering, Osaka University, Osaka, Japan
[3]Graduate School for the creation of New Photonics Industries, Shizuoka, Japan
[4]Graduate School of Engineering, Osaka University, Osaka, Japan
[5]Japan Synchrotron Radiation Research Institute, Hyogo, Japan
[6]Kansai Photon Science Institute, National Institutes for Quantum and Radiological Science and Technology, Kyoto, Japan
[7]National Institute of Advanced Industrial Science and Technology, Ibaraki, Japan
[8]National Institute for Fusion Science, Gifu, Japan
[9]Department of Physics, University of Nevada, Reno, USA
[10]Graduate School of Advanced Science and Engineering, Hiroshima University, Hiroshima, Japan

In the fast ignition approach, a fusion plasma is heated by energetic electrons generated through the interaction between a high-intensity laser pulse and the plasma. Using a cone-attached target has improved plasma heating efficiency [1, 2]. The cone guides the high-intensity pulse to a high-density region of the fusion plasma, surrounded by a long-scale, over-critical-density plasma. A high-contrast laser pulse has revealed that the cone structure also plays a crucial role in suppressing the spatial spread of energetic electrons, further enhancing plasma heating. Our recent study demonstrates the enhancement of plasma heating by irradiating a petawatt-class high-contrast laser onto a target attached with a compound parabolic concentrator (CPC) [3]. With its parabolic-shaped wall, the CPC is designed to focus the incident laser light at the tip by reflecting it by the inner walls, thereby concentrating the energy. To maximize the CPC's focusing effect, minimizing plasma expansion along the inner walls is essential. Our experiments employed a CPC attached to a multi-layer target irradiated by a high-intensity laser with a two-order-of-magnitude improved pulse contrast achieved using a plasma mirror. The multi-layer target consisted of sequential plastic, copper, plastic, titanium, and plastic layers. Resonance X-rays from the copper and titanium layers were measured using X-ray spectrometers and X-ray monochrome imagers [4], as well as an electron spectrometer [5] was used to assess the energy distribution of energetic electrons. The thermal electron temperature of the plasma was inferred by comparing the experimental X-ray spectrum with simulated one calculate with a collisional-radiative spectral code (PrismSPECT). Analysis of the X-ray spectrum from the titanium layer, located 7-μm-depth from the target surface, indicates that the plasma was heated to at least 500 eV. These findings suggest that the interaction between the high-contrast, high-intensity laser and the CPC significantly improves plasma heating efficiency.

References

[1] Norreys,P.A. et al., Phys.Plasmas **7**, 3721 - 3726 (2000).

[2] Kodama,R. et al., Nature **412**, 798 - 802 (2001).

[3] A.G.MacPhee. et al., Optica **7**, 129 (2020).

[4] S. Sakata et al., Nature Comm.**9** 3937 (2018).

[5] Ozaki,T. et al., Review of Scientific Instruments **85**, 11E113 (2014).

*E-mail: u062621d@ecs.osaka-u.ac.jp

POSTERS/XFEL

Hybrid Collisional-Radiative/Molecular-Dynamics Studies of Anisotropic Melting of Ice Induced by Ultrafast Non-thermal Heating

I. Dawod[1,2], K. Patra[1], S. Cardoch[1], O. H. Jönsson[3], J. A. Sellberg[3], A. V. Martin[4], J. Binns[4], O. Grånäs[1], A. P. Mancuso[2,5,6], C. Caleman[1,7]*, and N. Timneanu[1,2]

[1]Department of Physics and Astronomy, Uppsala University, Box 516, SE-75120 Uppsala, Sweden
[2]European XFEL, Holzkoppel 4, DE-22869 Schenefeld, Germany
[3]Department of Applied Physics, KTH Royal Institute of Technology, SE-106 91 Stockholm, Sweden
[4]School of Science, RMIT University, Melbourne, Victoria 3000, Australia
[5]Diamond Light Source, Harwell Science and Innovation Campus, Didcot OX11 0DE, U.K.
[6]Department of Chemistry and Physics, La Trobe Institute for Molecular Science, La Trobe University, Melbourne, Victoria 3086, Australia
[7]Center for Free-Electron Laser Science, Deutsches Elektronen-Synchrotron, Notkestraße 85 D-22607 Hamburg, Germany

Water and ice are routinely studied with X-rays to reveal their diverse structures and anomalous properties. We developed a hybrid collisional-radiative/molecular-dynamics code, MolDstruct [1], to explore how femtosecond X-ray pulses interact with hexagonal ice. We find that ice makes a phase transition into a crystalline plasma where its initial structure is maintained up to tens of femtoseconds. The ultrafast melting process occurs anisotropically, where different geometric configurations of the structure melt on different time scales. The transient state and anisotropic melting of crystals can be captured by X-ray diffraction, which impacts any study of crystalline structures probed by femtosecond X-ray lasers [2].

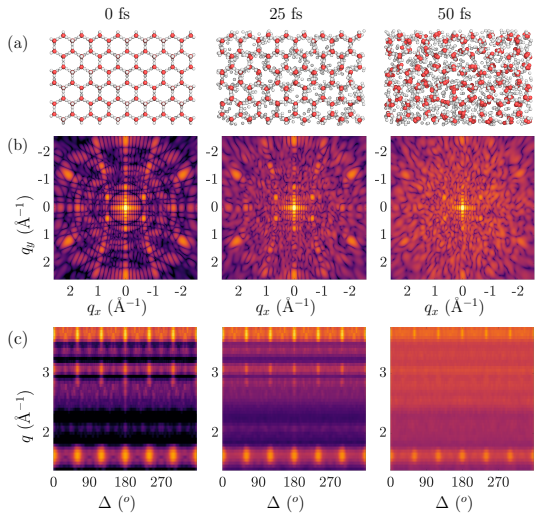

Figure 1. Dynamics of hexagonal ice investigated with an intense 50 fs long X-ray pulse, with 8 keV photons and intensity of 10^{18} Wcm^{-2}. (a) Snapshots of the structures from the hybrid CR/MD simulation of ice at 3 different time points. (b) Diffraction patterns of ice at corresponding time points, with sample to detector distance of 70 mm. (c) Angular correlation of the intensity in the diffraction patterns as a function of angle and momentum transfer.

References

[1] I. Dawod et al. J. Chem. Phys. **160**, 184112 (2024).

[2] I. Dawod et al. , ACS Phys. Chem. Au **6**, 385?392 (2024).

*E-mail: carl.caleman@desy.de

POSTERS/XRS

Characterization of high brightness and multi-keV x-ray sources at the LMJ facility

C. Baccou[1 *], G. Boutoux[1], F. Chermette[1], C. Chollet[1], R. De-Mollerat-Du-Jeu[2], V. Denis[2], P. Dupré[2], T. Fonseca[2], J. Gallaire[3], A. Grolleau[1], L. Jacquet[1], M.-A. Lagache[3], L. Le-Deroff[2], P.-E. Masson-Laborde[1], C. Meyer[1], G. Pavloff[1], V. Prévot[1], M. Primout[1], P. Rathouit[1], C. Reverdin[1], G. Soullie[1], M. Sozet[1], V. Trauchessec[1], B. Vauzour[1] and B. Villette[1]

[1]CEA, DAM, DIF, F-91297 Arpajon, France
[2]CEA, DAM, CESTA, F-33114, Le Barp, France
[3]CEA, DAM, VA, F-21120 Is-sur-Tille, France

The Laser MégaJoule Facility (LMJ) currently delivers 270 kJ of UV laser energy on target with 80 beams (20 quads). Regime of hot dense matter can be achieved and very bright multi-keV nanosecond x-ray sources can be generated, for example for studying the x-ray interaction with materials. The characterization of the x-ray emission in terms of spectrum, fluence and power is essential and requires absolutely calibrated time-resolved x-ray diagnostics, sensitive to soft and hard x-rays above 10 keV. At LMJ facility, broadband x-ray spectrometers as DMX [1] or mini-DMX as well as narrowband spectrometer such as HRXS are fully operational. Recently, experiments with xenon [2], krypton and zirconium have been conducted, demonstrating our capability to produce intense x-ray sources between 2 and 30 keV and our capability to measure time-resolved fluences and spectra.

References

[1] J.-L. Bourgade et al., Rev. Sci. Instrum. **72**, 1173 (2001).

[2] M. Primout *et al.*, Phys. Plasmas **29**, 073302 (2022).

* E-mail: claire.baccou@cea.fr

Toward a realistic modeling of the heating and ionization of a solid target irradiated by an ultra-intense laser

T. Huet[1,2], X. Davoine[1,2,*], C. Blancard[1,2], L. Gremillet[1,2], D. Tordeux[1]

[1]CEA, DAM, DIF, F-91297 Arpajon, France
[2]Univ. Paris-Saclay, CEA, LMCE, 91680 Bruyères-le-Châtel, France

Ultrahigh intensity (UHI) lasers interacting with solid targets are widely employed to generate bright X-ray sources and investigate isochoric heating of buried samples in the warm/hot dense matter regime. Such heating arises from the relativistically hot electron population created at the target surface, whose subsequent transport into the target core induces ultrafast ionization and heating processes. Accurate modeling of these phenomena using particle-in-cell (PIC) codes poses significant computational challenges, often necessitating approximations such as preionized targets or reduced target densities. The purpose of this work is to present realistic, fully self-consistent PIC simulations of the interaction of a 30 fs, 2.2×10^{18} W cm^{-2} laser pulse with a 2 μm thick Al target, using the CALDER code.

Our first effort was to quantify and mitigate numerical heating, a common artifact in PIC simulations involving solid-density plasmas and collisional algorithms. We then sought to elucidate the primary mechanisms behind the physical heating of the target core: (i) collisions between the laser-driven relativistic electrons and the much colder bulk electrons; (ii) resistive dissipation of the return current carried by the collisional bulk electrons, which is induced to neutralize the hot-electron current. This latter Joule-type heating is highly sensitive to the treatment of elastic electron-ion collisions. We show that incorporating the screening effect of bound electrons leads to an enhanced ion-electron collision rate, and thus to stronger heating. Additionally, we study the influence of electron-impact ionization coupled with ionization potential depression, and find that while the ionization level is increased, the overall heating is reduced.

* E-mail: xavier.davoine@cea.fr

Author Index

Abdallah J, Jr, 89
Abe Y, 98
Aberg D P, 10, 12, 34
Adler K, 7
Akematsu R, 98
Albertazzi B, 18, 54, 71
Alexandre Q, 21, 95
Andriyash I, 46
Ansia L, 26, 41, 42
Ao T, 47
Appel K, 26, 27
Arikawa Y, 98
Ariyarathna I, 33
Astapenko V A, 65
Atay K, 66
Audebert P, 91
Aybar N, 37, 38

Baccou C, 95, 105
Baehtz C, 27
Bailey J E, 3, 10, 11, 52, 89, 94
Bailly-Grandvaux M, 63
Balança C, 93
Ballance C P, 3
Banjafar M, 49
Bastiani S, 91
Baton S, 16
Baumann T M, 85
Beard J, 18
Beg F, 63
Beg F N, 59
Beiersdorfer P, 29
Ben Nasr S, 90
Benjamin S N, 66
Benkadda S, 14
Benkadoum Y, 18, 54
Benmouna M, 86
Benredjem D, 87
Bernardino D, 95
Binns J, 103
Bitter M, 82
Blancard C, 10, 16, 55, 84, 89, 95, 96, 106
Blenski T, 74, 91
Bokamba Motoumba E, 93
Bonneau M, 21, 95
Bordón A, 63
Bouffetier V, 27
Boutoux G, 105
Bowen C, 21, 95
Bradley P A, 11
Brochier M, 21
Brown C R D, 29
Brown G V, 29, 82
Bruulsema C, 15
Buldgen G, 55
Burian T, 26
Buscho J, 79
Bussman M, 58

Caleman C, 103
Calisti A, 6, 18, 80
Cangi A, 27
Cardoch S, 85, 103
Carvajal Gallego H, 90
Chaleil A, 16, 95
Chalupsky J, 26
Chao P, 52
Chen H, 37, 38
Cheng Z, 82
Chermette F, 95, 105
Chin D, 59
Chirac T, 21, 95
Cho B, 43
Cho P, 70
Chollet C, 105
Chung H K, 26
Ciardi A, 18, 23
Colgan J, 3, 33, 55, 89
Colombo A P, 10
Condamine F, 57
Coppari F, 59
Cordova T, 59
Cossé P, 10, 16, 55, 84, 89
Courtois C, 21
Cowan T, 43, 58
Cunningham E, 57

Döppner T, 30, 59
Darbon S, 79
Davoine X, 106
Dawod I, 103
de la Varga A G, 41
De León Y, 18
De-Mollerat-Du-Jeu R, 105

Dearling A, 18, 54
Debayle A, 80
Debesset S, 21
Deghiche D, 93
Delahaye F, 23
Denis V, 21, 105
Deprince J, 90
Desgranges C, 62
Diop S, 95
Dornheim T, 27
Doron R, 8
Dozieres-Aybar M, 79
du Jeu R, 21
Dubos O, 95
Dun J, 23
Dunham G S, 10, 11, 89, 94
Dupré P, 21, 105
Duthoit L, 16
Dutra E, 94
Dyer G, 31, 57

Ebisawa E, 98
Eckart M E, 82
Edens A D, 10
Efthimion P C, 66
Emig J, 59
Esnault C, 91
Estrela P, 26

Fairchild A J, 82
Fajardo M, 26, 41, 42
Falcone R W, 30
Farmer W A, 38
Faussurier G, 10, 16, 84, 89
Ferré S, 21, 95
Ferri S, 18, 80
Florido R, 63
Folsom E, 15
Fonseca T, 21, 95, 105
Fontes C J, 3, 4, 10, 11, 33, 35, 52, 55, 89, 92, 101
Foord M, 29
Fournier K B, 30
Fujioka S, 23, 98
Fulford K, 47

Göde S, 27
Gallaire J, 105
Galtier E, 31, 57
Gao C, 44, 48, 60
Gao L, 66, 82
Garcia A, 43
Garcia J, 52
Gard P D, 10
Gautier J, 46
Gawne T, 27
Geissel M, 47
Geoffray I, 21
Gericke D O, 68
Gigosos M A, 63
Gilleron F, 10, 55, 89, 91, 95
Goddet J P, 46
Godefroid M, 90
Golovkin I E, 75, 89
Gomez T A, 7, 11, 89, 101
Gong Y, 23
Gontier D, 21, 95
González A, 41
Goriely S, 90
Gournay L, 57
Grånäs O, 103
Grabowski P E, 34
Greenberg M, 57
Gremillet L, 16, 106
Grolleau A, 105
Gruning P, 95
Gu M F, 75, 89
Guerroudj D, 80
Guirlet R, 62
Gutt C, 49

Höppner H, 43
Hajkova V, 26
Hanano M, 54
Hanayama R, 98
Hannachi I, 19, 100
Hansen S B, 7, 10, 11, 52, 59, 82, 89
Harding E C, 10
Heeter R F, 11, 12, 70, 94
Heimann P, 57
Hell N, 82
Hill K W, 82
Hill M, 29
Hinkel D E, 37, 38
Hoarty D, 29
Hobbs B A, 11
Hobbs L, 29
Hohenberger M S, 11, 12, 70, 94
Hollinger R C, 66
Hou Y, 60
Huang L, 43, 49
Huebl A, 58
Huegel I, 52
Huet T, 106
Humphries O S, 27, 43
Huntington C M, 30

Hussain M, 26

Iglesias C A, 22, 34, 89
Inal M K, 86
Inubushi Y, 98
Ishii K, 98
Iwamoto A, 98
Iwata N, 98

Jönsson O H, 103
Jacquet L, 21, 95, 105
Johns H M, 11, 12, 70, 94
Johzaki T, 98
Juha L, 26
Just O, 90

Kaa J, 26
Kabacinski A, 46
Kallman T, 52
Karaki Y, 23, 98
Kasper J M, 92
Katz J, 15
Kelley R L, 82
Khaghani D, 31, 57
Khieu S, 21
Kilbourne C A, 82
Kilcrease D P, 89
Kimmel M, 10
King J, 66
Kitagawa Y, 98
Klein S R, 30
Kluge T, 43, 49, 58
Koenig M, 18, 23, 54, 71
Kojima S, 98
Koliyadu J C P, 26
Konôpková Z, 27
Konopkova Z, 26
Koubiti M, 14
Kozlova M, 46
Krauland C M, 79
Kraus B F, 66
Kraus D, 43
Kriz E, 66
Kroupp E, 43
Kruse M K G, 59
Kruse V A, 22
Kujala N, 26
Kuranz C C, 30, 59

Lötzsch R, 43
Lagache M-A, 105
Lake P, 79
Lake P W, 89
Landen O L, 37, 38
Law K F F, 23, 98
Lazicki A, 39
Le H, 29
Le-Deroff L, 21, 105
Lecherbourg L, 16
Lee H J, 31, 57
Lefevre F, 71
Leiding J A, 33
Lejars A, 79, 95
Li C, 54
Li C K, 71
Li Y, 44
Li Y J, 48
Li Y Q, 48
Liedahl D A, 37, 38
Lisitsa V S, 65
Liu J, 48
Loisel G P, 10, 11, 52, 89, 94
London R A, 29, 39, 59, 70
Looker Q, 10
Loupias B, 16
Luo Q, 60

Ma K H, 30
MacDonald M J, 29, 30, 59
MacFarlane J J, 75, 89
MacLaren S A, 38
Maeda K, 54
Magee E, 29
Maison L, 72, 76
Makita M, 26, 27, 49
Malko S, 66
Mancini R C, 52, 63, 70, 89
Mancuso A P, 103
Mandelbaum P, 62
Marandet Y, 19, 100
Marley E V, 15, 30, 59
Maron Y, 8
Marquès J R, 18
Marques J R, 71
Marré B E, 58
Martin A V, 103
Martin M, 29
Masson-La-borde P-E, 105
Matsubara H, 23, 98
Mayes D C, 11, 52, 89, 94
McGuffey C, 63
McKelvey A, 57
McPoyle S P, 66
Meftah A, 93
Meyer C, 21, 105

Michel T, 71
Millot M, 59
Mishchenko M, 27, 43
Miura E, 98
Miyanishi K, 49
Moldabekov Z A, 27
Moody J D, 38
More R, 89
Mori Y, 98

Nagaoka K, 98
Nagayama T, 3, 10, 11, 52, 89, 94
Nagler B, 57
Nahar S N, 89
Nakatsutsumi M, 26, 27, 43, 49
Neukirch A J, 33
Neumayer P B, 31, 43
Nilsen J, 39
Nilson P, 59
Nishiuchi M, 49
Noels A, 55

Oezturk O, 49
Oliva E, 46
Omura R, 98
Opachich K, 94
Opachich Y P, 11, 12, 70
Oportus D, 54, 71
Orban C, 89
Orlando S, 54, 71
Ota M, 49
Ozaki N, 18, 54

Pérez-Callejo G, 63
Pablant N A, 82
Pain J C, 10, 16, 21, 55, 87, 89, 91, 95, 96
Palmer C A J, 71
Palmeri P, 72, 76, 90
Parker P, 79
Patel M, 29
Patra K, 103
Pavloff G, 105
Perez F, 16
Perks C, 82
Perry T, 94
Perry T S, 11, 12, 70
Peterson A, 70
Peyrusse O, 62
Pikuz T, 23
Ping W, 89
Piron R, 74, 77, 91
Pitt S, 29
Poirier M, 91
Porter F S, 82
Porter J L, 10
Poujade O, 16
Prévot V, 21, 105
Pradhan A K, 2, 55, 89
Prat M, 95
Prencipe I, 43
Preston T R, 26, 27, 49
Primout M, 105
Prunet P, 21, 95

Quinet P, 72, 76, 90

Rahul S V, 49
Ralchenko Yu, 51, 57
Ramakrishna K, 27
Rambo P, 47
Randolph L, 27, 49
Rathouit P, 95, 105
Renaudin P, 16, 18, 95
Renner O, 57
Reverdin C, 21, 79, 91, 95, 105
Rice J, 82
Rigon G, 54, 71
Rocca J J, 66
Rochau G A, 10, 89
Rogers S, 38
Rosato J, 19, 80, 100
Rosen M D, 38
Roskopf N, 38
Rosmej F B, 57, 65
Rosmej O, 31
Ross J S, 37, 38
Rousseau A, 95
Rovillon S, 95
Rowland J J, 70
Rubensson J E, 85

Sabri M, 93
Sakawa Y, 54
Sano T, 98
Santos J J, 63
Saret J, 63
Saunders A M, 30
Saura N, 14, 62
Sawada H, 98
Schneider M B, 37, 38, 79
Schramm U, 58
Schwalbe S, 27
Schwinkendorf J P, 49
Schwob J L, 62
Scott H A, 26, 29, 30, 38, 59
Sebban S, 46

Seely J, 57
Sekkal-Haddouche A F, 86
Sellberg J A, 103
Sentoku Y, 98
Shepherd R J, 29, 57
Sherril M, 89
Shigemori K, 98
Shlyaptsev V N, 66
Smid M, 43, 67
Son S K, 85
Soullie G, 21, 95, 105
Sozet M, 21, 95, 105
Speas R, 10
Springstead M P, 30, 59
Stahoviak J, 10
Stambulchik E, 8, 43
Stamm R, 19, 100
Starrett C E, 3, 4, 35, 92, 101
Sterne P A, 30, 59
Stoupin S, 79
Sunahara A, 98
Suzuki Y, 54
Suzuki-Vidal F, 63
Swadling G, 15, 38
Swift D, 39

Tacu M, 77, 96
Takizawa R, 23, 98
Tchang-Brillet W-Ü L, 93
Thaury C, 46
Thompson N B, 79
Tieulent R, 82
Timmermans E, 33
Timneanu N, 103, 85
Tissandier F, 46
Toncian T, 43
Tordeux D, 106
Toto E R, 15
Tran Tan H B, 35
Trantham M R, 30
Trauchessec V, 105
Triantafyllidis A, 18, 71

Uschmann I, 43

Vagovic P, 26
Vanderloo N, 71
Vauzour B, 21, 79, 91, 95, 105
Velarde P, 26, 41, 42
Vezinet D, 82
Villette B, 21, 95, 105
Vlachos C, 63
Vonhof S, 38
Vorberger J, 27
Vozda V, 26

Wagle G, 90
Wallace M, 94
Walsh C A, 63
Wang S, 66
Webster L, 79
Whitaker W, 33
White J R, 101
Widera R, 58
Williams G O, 26, 41, 42
Wilson B G, 30, 34, 89
Wollenweber L, 27
Woods D T, 38
Woods T, 37
Wu M, 79

Xiao H, 98

Yabuuchi T, 49
Yakura S, 54
Yamanoi K, 98
Yamazaki R, 54
Yang C, 47
Yuan J, 44, 48, 60

Zahedpour Anaraki S, 66
Zammit M C, 33, 101
Zastrau U, 26, 27, 43
Zeitoun P, 46
Zeng J, 48
Ziaja B, 25